ELSEVIER

Physics Reports 302 (1998) 211–293

PHYSICS REPORTS

Quantum theory of resonances: calculating energies, widths and cross-sections by complex scaling

Nimrod Moiseyev

Department of Chemistry and Minerva Center for Non-linear Physics of Complex Systems, Technion – Israel Institute of Technology, Haifa 32000, Israel

Received September 1997; editor: A. Schwimmer

Contents

PII S0370-1573(98)00002-7

QUANTUM THEORY OF RESONANCES: CALCULATING ENERGIES, WIDTHS AND CROSS-SECTIONS BY COMPLEX SCALING

Nimrod MOISEYEV

Department of Chemistry and Minerva Center for Non-linear Physics of Complex Systems, Technion – Israel Institute of Technology, Haifa 32000, Israel

ELSEVIER

AMSTERDAM – LAUSANNE – NEW YORK – OXFORD – SHANNON – TOKYO

Abstract

Complex scaling enables one to associate the resonance phenomenon, as it appears in atomic, molecular, nuclear physics and in chemical reactions, with a *single* square integrable eigenfunction of the complex-scaled Hamiltonian, rather than with a collection of continuum eigenstates of the unscaled hermitian Hamiltonian. In this report, we illustrate the complex-scaling method by giving examples of simple analytically soluble models. We describe the computational algorithms which enable the use of complex scaling for the calculations of the energy positions lifetimes and partial widths of atomic and molecular autoionization resonance states, of small polyatomic molecules and van der Waals molecules in predissociation resonance states, of atoms and molecules which are temporarily trapped on a solid surface and of atoms and molecules which ionized/dissociate when they are exposed to high intensity laser field. We focus on the properties of the complex scaled Hamiltonian and on the extension of theorems and principles, which were originally proved in quantum mechanics for hermitian operators to non-hermitian operators and also on the development of the complex coordinate scattering theory.

PACS: 31.15. −p

Preface

In his book on scattering theory Taylor considered the resonances as the "most striking phenomenon in the whole range of scattering experiments". Resonances are associated with metastable states of a system which has sufficient energy to break up into two or more subsystems.

Complex scaling (known also as the complex-coordinate method or as the complex-rotational method) enables one to associate the resonance phenomenon, as it appears in atomic, molecular, nuclear physics and in chemical reactions, with a SINGLE square integrable eigenfunction of the complex-scaled Hamiltonian, rather than with a collection of continuum eigenstates of the unscaled hermitian Hamiltonian.

For excellent reviews of the method see Reinhard [23]; Junker [24] and Ho [25]. An updated bibliography is given at the end of the present report.

In this report we will illustrate the complex-scaling method by giving examples of simple analytically soluble models which describe scattering of an electron from a negative ion and transition from reactants to products through a potential barrier in three atomic collinear chemical reactions. We will focus on the properties of the complex scaled Hamiltonian and on the extension of theorems and principles, which were originally proved in quantum mechanics for hermitian operators to non-hermitian operators. We will focus also on the development of the complex coordinate scattering theory and on computational algorithms which enable the use of complex scaling for the calculations of the energy positions lifetimes and partial widths of atomic and molecular autoionization resonance states, of small polyatomic molecules and van der Waals molecules in predissociation resonance states, of atoms and molecules which are temporarily trapped on a solid surface and of atoms and molecules which ionized/dissociate when they are exposed to high intensity laser field. The computational algorithms which will be discussed here enabled also the calculations of the rotational vibrational distribution of diatoms obtained in the photodissociation process; for the calculations of specular and non-specular transition probabilities that are obtained in scattering of atoms and molecules from flat and corrugated surfaces; for calculating above-threshold-ionization (ATI), above-threshold-dissociation (ATD) and harmonic generation (HG) spectra of atoms and molecules which interact with a strong laser field. The complex-scaling theory and computational algorithms described in this report also enable the calculations of energies and lifetimes of transition state resonances in reactive scattering collision experiments, cumulative reaction probabilities, and quantum mechanical thermal rate constants for chemical reactions.

1. Resonances – Why complex scaling?

1.1. Resonances in full collision experiments

Let us consider an experiment in which a "particle" is scattered from a "target". The "particle" can be, for example, an electron, an elementary particle, an atom or a molecule and the "target" can be a nucleus, an atom, a molecule, a flat or a corrugated solid surface. In an *elastic* scattering experiment the energy of the "particle" is conserved. In a *non-elastic* scattering experiment there is an energy exchange between the "particle" and intrinsic degrees of freedom of the "target", and the

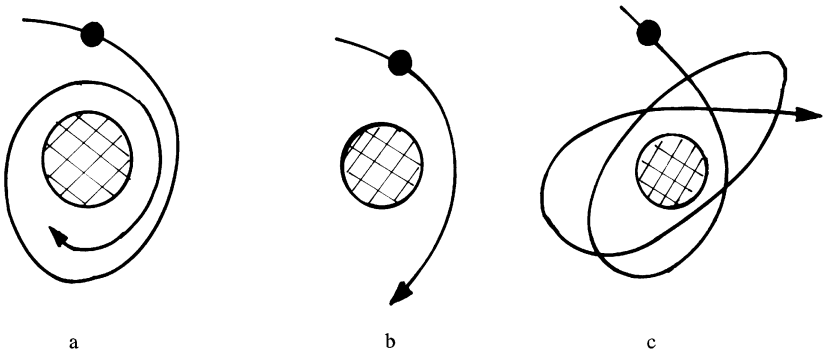

Fig. 1. Three different possible scattering orbits.

final energy of the "particle" in its "out" asymptote limit can be smaller or larger than the initial energy of the "particle" in its in asymptote limit. In a *reactive scattering* experiment the "particle" and the "target" undergo a change during the rearrangement collision and become different species. Even in the simple case of elastic scattering three possibilities may be considered [1].

The first possibility, presented in Fig. 1a, is that of a particle which comes in from infinity, gets trapped by the target and never emerges out of the attractive potential well. As time passes the potential energy of the trapped particle drops down to $-\infty$ whereas the kinetic energy increases to $+\infty$. This "black hole" phenomenon is avoided when the interaction potential at the origin is less attractive than $V(r) = -r^{-2}$. In order to obtain a free particle in the "in" and "out" asymptotes, $V(r)$ should fall off quicker than r^{-3} at infinity. A direct scattering event is illustrated in Fig. 1b. In Fig. 1c we illustrate the third possibility, where, due to multiple-scattering events, the particle is temporarily trapped by the target. When the lifetime of the particle–target system in the region of interaction is larger than the collision time in a direct collision process we call the phenomenon a resonance phenomenon. *A resonance state is defined as a long-lived state of a system which has sufficient energy to break-up into two or more subsystems.* In elastic and inelastic scattering experiments the subsystems are associated with the scattering particle and the target.

1.2. Lifetime of shape and Feshbach-type resonances from motion of wavepacket calculations

Probably the most well-known spherically symmetric potential which supports resonances, $V(r)$, is the potential describing decay of radioactive nuclei or of unstable particles [2]. Naturally, we shall refer to the nucleus as the target in this case. An illustrative plot of $V(r)$ in that case is given in Fig. 2 where r is, for example, the distance between an α particle and the nucleus. E_0 and E_1 represent bound and resonance energies, respectively.

The lifetimes of the resonance states, $|E_1\rangle$, (also known as Gamow or Siegert states) can vary from a few seconds to millions of years (4.5×10^9 y for the decay of the $^{238}\mathcal{U}$ isotope to Thorium). A very similar potential can describe both the molecular interaction in a diatom for which the total angular momentum, j, is much larger than zero and gives rise to a centrifugal potential barrier [3], and the scattering of an electron from a neutral diatom [4]. In such cases, the lifetime of the metastable resonance states (i.e. predissociation states of rotationally excited diatoms which are

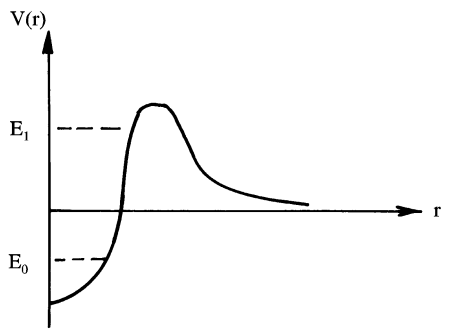

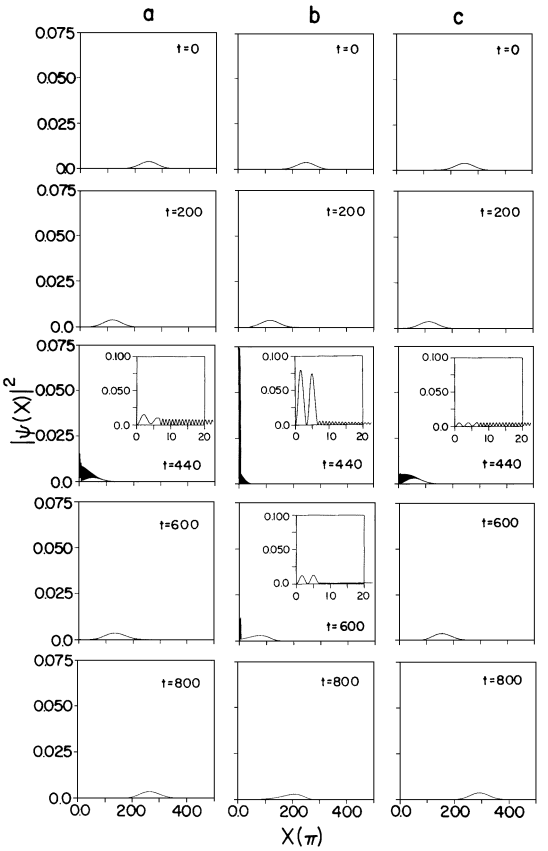

Fig. 2. Schematic representation of the interaction potential between an α particle and the nucleus.

Fig. 3. Gaussian wave packet scattering from a potential barrier. ($v(x) = 0$ if $x < 6.7\pi$, $v = \infty$ if $x < 0$, $v = 1$ if $x \geq 6.7\pi$). (a) the mean energy of the wave packet is below the resonance energy; (b) the mean energy of the wave packet is equal to the resonance energy; (c) the mean energy of the wave packet is above the resonance energy.

formed by the temporary trapping of the two atoms inside the potential well in the scattering experiment, and autoionization states of the negative charged molecular ion) can vary from milliseconds to femtoseconds (about 10^{-15} s for the autoionization of H_2^- in its ground state). In all these cases the temporarily trapping of the "particle" inside the potential well is a quantum phenomenon which is known as the tunneling phenomenon. The quantum equations of motion are reduced to the classical one as $\hbar \to 0$. While $\hbar$ is taken to zero, the penetration probability of the quantum particle through the potential barrier (into the well or out of it) is reduced and in the limit of $\hbar = 0$ *no* resonance states will be observed. These kinds of resonances are known in the literature as *shape-type resonances*. The temporarily trapping of the particle inside the potential well can occur also when the energy of the particle is larger than the height of the potential barrier or even in the absence of a potential barrier (one example is of a Gaussian wave packet scattered from a finite square well for example). In Fig. 3 we show the results obtained for a scattering of a Gaussian wave packet from a potential barrier [5].

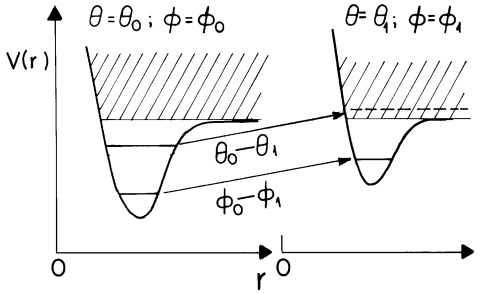

Fig. 4. Schematic representation of two coupled adiabatic potentials.

As one can see from Fig. 3b, unlike the cases where the mean energy of the packet is off resonance, when the mean energy of the Gaussian wave packet is equal to the resonance energy then the wave packet is trapped above the potential barrier for a long period of time $\tau = 56.8$ s. Any small variation in the resonance energy will reduce the lifetime τ.

Let us consider a special case where the internal modes of the scattered particle and the internal modes of the target are not coupled to the relative motion between the particle and the target. In this case, when the interaction potential between the "particle" and the "target" is *not* spherical symmetric it may happen that a bound state of the particle–target system in a fixed orientation (i.e. a square integrable eigenfunction of the one-dimensional time-independent Schrödinger equation $H(r, \theta_0, \phi_0)$ where θ_0 and ϕ_0 are the polar coordinates of the particle relative to the target which are held fixed) is embedded in the continuum of the system in another orientation when $\theta = \theta_1$ and $\phi = \phi_1$. The two adiabatic potentials are schematically presented in Fig. 4.

Due to the coupling of the r-coordinate with the angles θ and ϕ the bound state which is "pushed" up into the continuum becomes a resonance state. These kind of resonances are known as *Feshbach-type resonances* and can also be obtained in classical calculations. Unlike the shape-type resonances, the lifetime of the Feshbach metastable states get *finite values* as $\hbar$ is taken to the limit of $\hbar = 0$. A simple illustrative example is of a rigid rotor (stands for a non-vibrating diatomic molecule) scattered from a flat solid surface [6]. The interaction potential between the scattered "particle" (the diatom) and the "target" (the solid surface) depends on the angle, α, between the molecular axis and the normal to the surface and on the distance of the center of mass of the diatom from the surface. If the potential energy terms which couple α and z are neglected then the bound vibrational states of the free-rotor (diatom with the rotational kinetic energy $B_{\text{rot}}(j + 1)$) are embedded in the continuum of the non-rotating diatom which vibrates above the surface. The potential coupling terms "mix" the bound states of the rotating diatom with the continuum states of the non-rotating molecule and predissociation, which is associated with the resonance phenomenon, takes place.

In Fig. 5 the results obtained for a Gaussian wave packet, representing an HD molecule scattered from an Ag(111) surface, are shown [7]. In the off-resonance case, the initially unrotated ($j = 0$) diatom is excited to its first rotational state, $j = 1$, due to the collision with the flat silver surface. In the resonance case, one can see from Fig. 5b that the HD molecule spends about 0.5 ps close to the Ag(111) surface and as time passes desorption occurs. In the out asymptote limit the probability to observe HD in the $j = 1$ and $j = 0$ rotational states is almost equal.

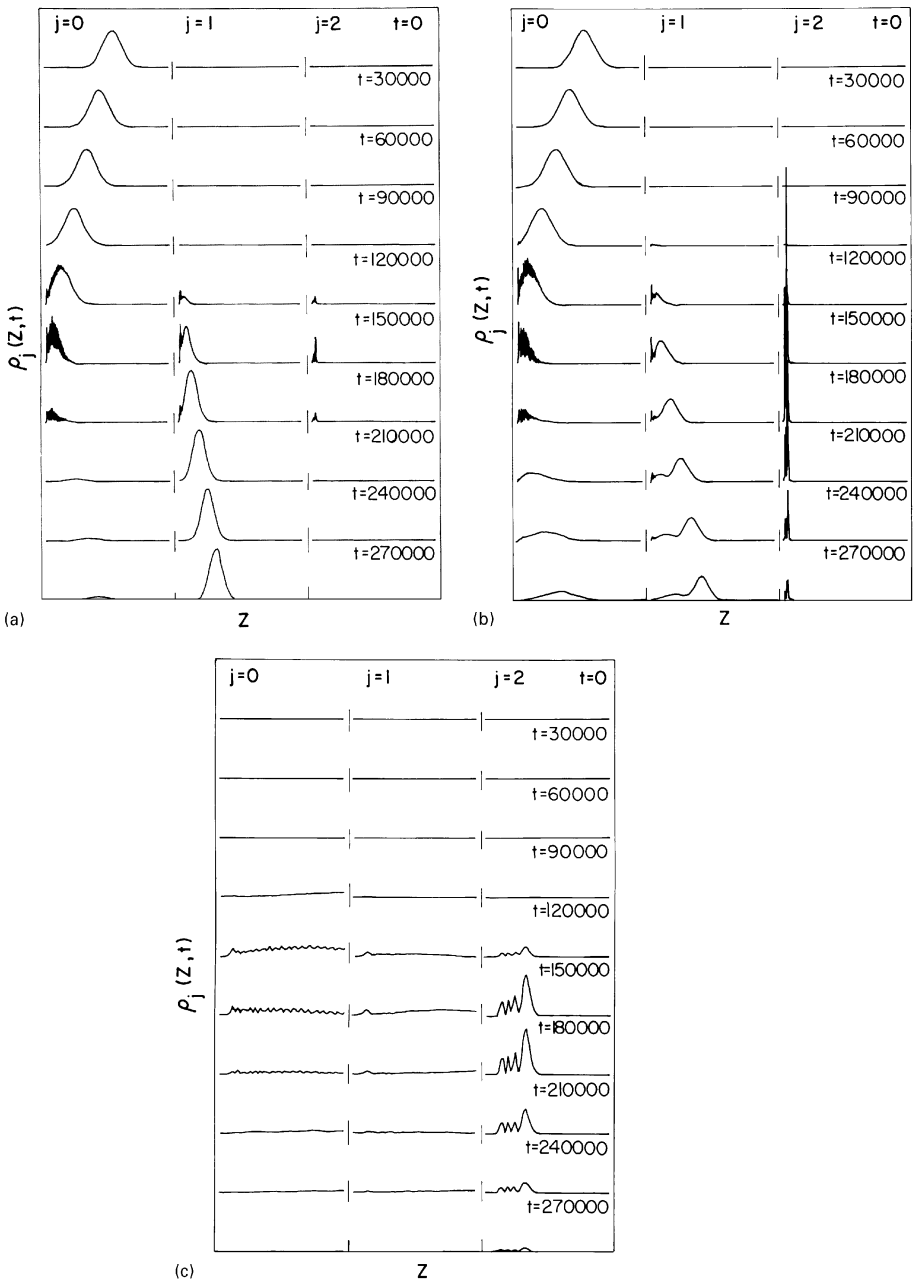

Fig. 5. Scattering of Gaussian wave packet which represents an HD molecule from a flat Ag(111) surface: The rotational probability densities $\rho_j(z,t)$ as a function of z ($-3 < z < 142$ a.u.) are shown, where j is the rotational quantum number. Each row corresponds to a specific time which is marked on the top right corner (in a.u.). The left column represents $\rho_0(z,t)$ (non-rotating HD molecule); the middle column represents $\rho_1(z,t)$; and the right column represents $\rho_2(z,t)$. (a) Direct scattering. The initial scattering energy is 18.97 meV. (b) Resonance scattering. The initial scattering energy is 22.69 meV shows very strong trapping at $j = 2$). (c) as in (b) for $-3 < z < 15$.

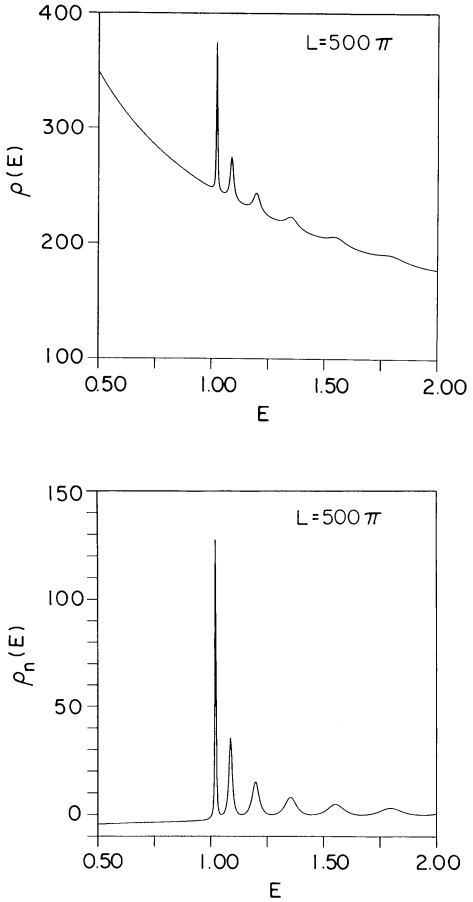

Fig. 6. The density of states $\rho(E)$ as function of the energy E. $\rho_N(E)$ stands for the box normalized density of states where $\rho_N = \rho(E) - L/2\sqrt{E}$ and L is the box size.

1.3. Resonance lifetime from time-independent calculations of density of states

In the above analysis, the lifetime of a resonance state was obtained from time-dependent calculations. It is possible, however, to estimate the resonance lifetime from time-independent calculations. By solving the time-independent Schrödinger equation for the potential barrier described in the caption of Fig. 3 the density of states, ρ, was calculated (note that, when box normalization is used the density of states is obtained by counting number of states with energies between E to $E + \mathrm{d}E$)[8]. The results of the time-dependent calculations are presented in Fig. 6.

In Fig. 6b the background of the density of states, $1/\sqrt{E}$, which results from the use of box normalization condition is removed. The local maxima in the density of states are associated with the resonances. The widths of these Lorenzian peaks, $\Gamma_n = \Delta E_n$; $n = 1, 2, \ldots$, are the inverse lifetimes of the resonances states. That is,

$$\Gamma_n = \hbar/\tau_n \,. \tag{1.3.1}$$

The value of τ_n obtained from Fig. 6b using Eq. (1.3.1) is in a good agreement with the estimate of τ_n which was obtained from the time-dependent calculations presented in Fig. 6b. That is $\Gamma_2 = 1/\tau_2 = 0.0176$ a.u.

1.4. Association of the resonance phenomena with the complex poles of the scattering matrix

We will show now that the widths of the shape and Feshbach-type resonance peaks, Γ_n, in the plots of density of states given in Fig. 6, are associated with the poles of the S-matrix. For the sake of simplicity let us assume that V is a short-range potential and $V \to 0$ (i.e. the threshold energy $E_t = 0$) as the "reaction" coordinate $r \to \infty$. In such a case an eigenfunction of the time-independent Schrödinger equation at $r \to \infty$ is given by

$$\phi(r \to \infty) = A(k)e^{-ikr} + B(k)e^{+ikr} \simeq e^{-ikr} + S(k)e^{+ikr}, \quad E = (\hbar k)^2/2\mu\,, \tag{1.4.1}$$

The S-matrix is defined as the ratio between the amplitude of the out-going plane wave and the in-coming wave. The S-matrix has a pole in two cases:

(1) In the first case when $B(k)$ has a pole. These are "false" poles which are not associated with the resonance phenomenon. "False" poles are independent of the potential, $V = \lambda v(r)$, and exist even when λ approaches zero[9].

(2) When the amplitude, $A(k)$, of the in-coming wave vanishes. When these poles are concentrated on the positive imaginary axis of k they are associated with bound states, which are *not* relevant to the dynamics in a scattering process. As will be shown, the poles which are embedded in the fourth-quarter of the *complex* k-plane (i.e. $\mathrm{Re}(k) > 0$, $\mathrm{Im}(k) < 0$) are associated with the resonance phenomenon. Near the nth simple isolated pole $S(k)$ can be written as [10,11]

$$S(k) \propto 1/(k - k_n) \tag{1.4.2}$$

and

$$d\ln S(k)/dk = -1/(k - k_n)\,, \tag{1.4.3}$$

where k_n is a complex pole such that

$$\mathrm{Re}(k_n) > 0, \qquad \mathrm{Im}(k_n) < 0\,. \tag{1.4.4}$$

Considering a closed contour of integration, C, in the complex k-plane then following the residue theorem

$$N = \frac{1}{2\pi i}\oint_{\mathscr{C}} \frac{\partial \ln S(k)}{\partial k}\,dk\,, \tag{1.4.5}$$

where N is the number of poles in the fourth-quarter of the complex k-plane. When all the poles of $S(k)$ are embedded in a bounded region in the complex k-plane (i.e. all of them are in a finite distance from the real k-axis as shown in Fig. 7) the closed contour of integration C can be replaced by a contour along the real k-axis (k varies from 0 to ∞) and, consequently, $\partial N/\partial k$ is defined as

$$\partial N/\partial k = \partial \ln S(k)/2\pi i \partial k\,. \tag{1.4.6}$$

Since the density of states ρ is given by

$$\rho \equiv dN/dE = \partial N/\partial k\, \partial k/\partial E\,,$$

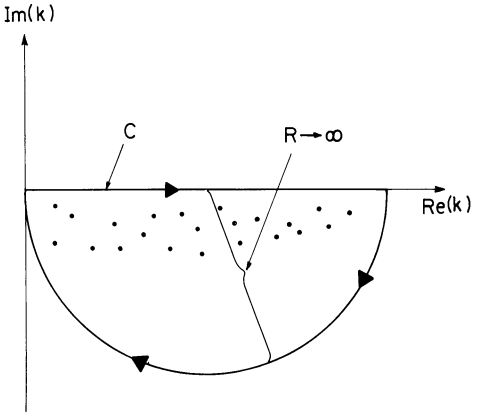

Fig. 7. Schematic representation of a closed contour of integration C in the complex k-plane where "x" denotes the complex poles of the S-matrix.

then

$$\rho = \frac{\mu}{2\pi i\hbar^2 k}\frac{\partial \ln S(k)}{\partial k} = \frac{1}{2\pi i}\frac{\partial \ln S(E)}{\partial E}. \tag{1.4.7}$$

By substituting Eq. (1.4.3) into Eq. (1.4.7), one can see that when $k = \mathrm{Re}(k_n)$, the local maxima of the density of states is obtained for the value of $\rho = \rho_{\max}$, where

$$\rho_{\max}(k = \mathrm{Re}(k_n)) = (\mu/2\pi\hbar^2)[-\mathrm{Re}(k_n)\mathrm{Im}(k_n)]^{-1} = [-2\pi\,\mathrm{Im}(E_n)]^{-1} \tag{1.4.8}$$

and the complex "energy" is given by

$$E_n - E_t = (\hbar k_n)^2/2\mu \tag{1.4.9}$$

with E_t being the threshold energy. The peaks in the density of states presented in Fig. 6 have a Lorenzian shape. The full-width half-maximum of the nth Lorenzian peak, Γ_n, is given by

$$\Gamma_n = 1/\pi\rho_{\max}. \tag{1.4.10}$$

By substituting Eq. (1.4.8) into Eq. (1.4.10), the connection between the widths of the peaks in $\rho(E)$, Γ_n, and the imaginary part of the complex poles of the S-matrix is established, such that,

$$\Gamma_n = -2\mathrm{Im}(E_n). \tag{1.4.11}$$

From this analysis, one can see that the resonance phenomenon as obtained in a scattering experiment is mainly controlled by poles of the scattering matrix. As it will be shown in Section 1.5 the resonance poles are complex eigenvalues of the Hamiltonian,

$$\hat{H}(r)\phi_n^{\mathrm{res}}(r) = E_n\phi_n^{\mathrm{res}}(r), \qquad E_n = \varepsilon_n - (i/2)\Gamma_n, \tag{1.4.12}$$

where ε_n is the resonance position above the threshold, Γ_n is the width (inverse lifetime) as defined in Eqs. (1.4.9) and (1.4.11) and the eigenfunction $\phi_n^{\mathrm{res}}(r \to \infty)$ as given in Eq. (1.4.1) is reduced to

$\exp(ikn)$ since $S(k_n) = \infty$ as one can see from Eq. (1.4.2). Eq. (1.4.12) is the basic equation in the resonance theory for time-independent Hamiltonians. The resonances are associated with complex eigenvalues of the (unscaled !) Hamiltonian which describes the physical system. Usually, one may expect that the Hamiltonian should be hermitian. That is, in the one-dimensional case

$$\int_{-\infty}^{\infty} f(x)\hat{H}(x)g(x)\,dx = \int_{-\infty}^{\infty} g(x)\hat{H}^*(x)f(x)\,dx\,. \tag{1.4.13}$$

By carrying out integration by parts one can see that this equation is satisfied provided

$$g(x)\left|\frac{df(x)}{dx}\right|_{-\infty}^{\infty} - f(x)\left|\frac{dg(x)}{dx}\right|_{-\infty}^{\infty} = 0\,. \tag{1.4.14}$$

Consequently, the hermitian property of $\hat{H}(x)$ depends on the boundary condition of $f(x)$ and $g(x)$. When, for example, $f(x)$ and $g(x)$ are in the Hilbert space, then $f(\pm\infty) = 0$, $g(\pm\infty) = 0$. Consequently, Eq. (1.4.14) is satisfied and $\hat{H}(x)$ is an hermitian operator. In the more general case, Eq. (1.4.14) is satisfied and $\hat{H}(x)$ is hermitian when $f(x)$ and $g(x)$ are bounded functions (NOT necessarily bound states). When $f(x)$ and $g(x)$ are bounded functions then $|f(x)| < C_1$ and $|g(x)| < C_2$ where C_1 and C_2 are two finite valued constants (such as the continuum-type functions for example). When $f(x)$ or $g(x)$ exponentially diverges as ϕ_n^{res} does, Eq. (1.4.14) is not satisfied and $\hat{H}(x)$ is not hermitian!

1.5. The role of complex scaling in the calculations of the resonance poles of the scattering matrix

Let us now consider the properties of the eigenfunctions associated with these complex eigenvalues of the Hamiltonian. The physical Hamiltonians are hermitian only when they operate on bounded functions (not necessarily square integrable) or, when box normalization is used, on a functional space of all possible square integrable functions (i.e. Hilbert space). Therefore, it is obvious that ϕ^{res} which are associated with *complex* eigenvalues are *not* in the hermitian domain of the Hamiltonian (i.e. not in the Hilbert space). For finite range potentials it is clear from Eqs. (1.4.9) and (1.4.12) that the complex wave vector is given by $k_n = |k_n|e^{-i\varphi_n}$, where

$$\varphi_n = \arctan(\Gamma_n/[2(\varepsilon_n - E_t)]) \tag{1.5.1}$$

with E_t being the threshold energy. By substituting Eq. (1.4.13) into Eq. (1.4.1), one can see that the resonance eigenfunctions (associated with the poles of the S-matrix) diverge exponentially,

$$\phi_n^{\mathrm{res}}(r \to \infty) = B(k_n)e^{+i|k_n|e^{-i\varphi_n}r} = B(k_n)e^{ia_n r}e^{+b_n r} \to \infty\,, \tag{1.5.2}$$

where

$$a_n = (2\mu)^{1/2}(\varepsilon_n^2 + (\Gamma_n/2)^2)^{1/4}\cos\varphi_n/\hbar\,,$$

$$b_n = a_n \tan\varepsilon_n > 0\,,$$

$$\varphi_n = \arctan(\Gamma_n/2\varepsilon_n)\,.$$

The physical interpretation of the divergence property of ϕ_{res} is that at $r = \infty$ one observes the "particles" (subsystems as defined above) which were formed an infinitely long time ago [12].

As usual, the solutions of the time-dependent Schrödinger equation for time-independent Hamiltonian are given by

$$\psi_n^{\mathrm{res}}(r,t) = \phi_n^{\mathrm{res}}(r)\mathrm{e}^{-\mathrm{i}E_n t/\hbar} \tag{1.5.3}$$

and, therefore, the probability density

$$|\psi_n^{\mathrm{res}}(r,t)|^2 = |\phi_n^{\mathrm{res}}(r)|^2\mathrm{e}^{-\Gamma_n t/\hbar} \tag{1.5.4}$$

decays to zero as time passes at a constant r. Therefore, the "particles" disappear from any given point in the coordinate space. Due to the exponential divergence of ϕ^{res} the number of particles is conserved *only* when *both* the reaction coordinate, r, and the time, t, approach the limit of infinity.

Most of the computational algorithms in quantum mechanics have been developed for hermitian operators (as discussed above, the physical Hamiltonians are hermitian only when they operate on bounded functions which get finite values as any point in the coordinate space). For example, variational methods which were successfully used to solve many-body problems in physics and chemistry are not applicable and cannot be used to solve Eq. (1.4.12) even for the one-dimensional case. As we will show, here, an extension of the variational principle and of other well-known theorems in quantum mechanics to non-hermitian operators can be made by carrying out similarity transformations $\hat{S}$ which make the resonance functions, ϕ^{res}, square integrable functions. That is,

$$(\hat{S}\hat{H}\hat{S}^{-1})(\hat{S}\phi_n^{\mathrm{res}}) = (\varepsilon_n - (\mathrm{i}/2)\Gamma_n)(\hat{S}\phi_n^{\mathrm{res}}) \tag{1.5.5}$$

such that

$$\hat{S}\phi_n^{\mathrm{res}} \to 0 \quad \text{as } r \to \infty \tag{1.5.6}$$

and $\hat{S}\phi_n^{\mathrm{res}}$ are in the Hilbert space although ϕ^{res} are not. The complex-scaling operator to be defined below is only one example of a possible similarity transformation for which Eq. (1.5.6) is satisfied [13].

The complex-scaling operator is given by

$$\hat{S} = \mathrm{e}^{\mathrm{i}\theta r\,\partial/\partial r} \tag{1.5.7}$$

such that

$$\hat{S}f(r) = f(r\mathrm{e}^{\mathrm{i}\theta}) \tag{1.5.8}$$

for any analytical function $f(r)$. By substituting Eqs. (1.5.7) and (1.5.2) into Eq. (1.5.6) (this is equivalent to scaling r by $\exp(\mathrm{i}\theta)$ in Eq. (1.5.2)), one obtains

$$\hat{S}\psi_n^{\mathrm{res}}(r\to\infty) = B(k_n)\mathrm{e}^{+\mathrm{i}|k_n|\exp(\mathrm{i}(\theta-\varphi_n)r)} = B(k_n)\mathrm{e}^{\mathrm{i}\alpha_n r}\mathrm{e}^{-\beta_n r}\,, \tag{1.5.9}$$

where

$$k_n = |k_n|\mathrm{e}^{-\mathrm{i}\varphi_n}\,,$$

$$\alpha_n = a_n(\cos\theta - \tan\varphi_n \sin\theta)\,,$$

$$\beta_n = a_n(\sin\theta - \tan\varphi_n \cos\theta)\,,$$

$$\varphi_n = \arctan(\Gamma_n/2\varepsilon_n)\,.$$

One immediately sees from Eq. (1.5.9) that for a sufficiently large value of the rotational angle θ the exponential factor β_n gets a positive value and thereby the scaled resonance wave function becomes square integrable. In other words, when

$$\theta \geq \theta_c \,, \tag{1.5.10}$$

where the critical angle θ_c is given by [14,15]

$$\theta_c = \varphi_n \equiv \arctan \Gamma_n/2(\varepsilon_n - E_t) \tag{1.5.11}$$

with ε_n, Γ_n and E_t being, respectively, the real and imaginary part of the complex energy and the threshold energy (E_t was taken to be zero in our studied example) then,

$$\hat{S}\phi_n^{res}(r \to \infty) \to 0 \,. \tag{1.5.12}$$

Note, by passing, that the bound states of the unscaled Hamiltonian are a special case of Eq. (1.5.9) where $\gamma = 0$ (i.e. $\Gamma_n = 0$) and $a_n = \mathrm{i}|a_n|$. Therefore, the critical angle θ_c for the bound state is $\theta_c = 0$.

Here we proved that by scaling the "reaction" coordinate the resonance wave function becomes square integrable and, consequently, the number of particles in coordinate space is conserved. Therefore, complex scaling has the advantage of associating the resonance phenomenon with the discrete part of the spectrum of the complex-scaled Hamiltonian. Moreover, the resonance state is associated with a SINGLE square integrable function, rather than with a collection of continuum eigenstates (see the peaks in the density of states presented in Fig. 6) of the unscaled hermitian Hamiltonian. Complex scaling may be viewed as a procedure which "compresses" information about the evolution of a resonance state at infinity into a small well-defined part of space. The tail in spatial space of a single, time-independent, square integrable resonance wave function contains all the information about the system, including information on partial width and on the way in which the system evolves as the separation between the "particle" and the "target" increases to infinity. The complex eigenvalues of the complex-scaled Hamiltonian (see Eq. (1.5.5)) which are associated with the resonance phenomenon are θ-independent. The imaginary part of the resonance complex eigenvalues has been shown to be the widths of the Lorentzian peaks, Γ_n, in plots of the probability density of states vs. the energy, and through Eq. (1.3.1) one can associate Γ_n with the rate of decay and with the inverse lifetime of the "particle–target" system. The resonance complex-scaled eigenfunctions are, however, θ-dependent. We may interpret θ as a control parameter which "brings" the information of the decay process from infinity to a finite region in space whose size depends on the value of θ. As θ is increased, the information about the decay process is compressed into a smaller part of the coordinate space. However, θ cannot exceed a critical value as it will be discussed in Section 2.

1.6. Complex scaling and resonances in half collision experiments

The resonance wave function which becomes square integrable upon complex scaling can be regarded as the dominant intermediate state in the scattering process. This statement can be explained as follows. The transition probability to get from the in-asymptote to the out-asymptote,

which are denoted by φ_i and φ_f respectively, is given by

$$P(E) = |\langle\varphi_f|\hat{T}(E)|\varphi_i\rangle|^2 , \tag{1.6.1}$$

where E is the total energy of the particle–target system; the T-matrix is defined as usual by

$$T = V(x,y,z) + V(x',y',z')G_E(x',y',z';x,y,z)V(x,y,z)$$

and the Green operator $G_E = (E-H)^{-1}$, provides the probability amplitude to get from (x,y,z) to (x',y',z') at a given energy E. V is the interaction potential between the free particle and the target. The $\langle\varphi_f|V|\varphi_i\rangle$ term in Eq. (1.6.1) describes the direct scattering events whereas the $\langle\varphi_f|VGV|\varphi_f\rangle$ term describes the multiple scattering events. The spectral representation of the Green operator is given by

$$G_E = \sum_i \frac{|\phi_i\rangle\langle\phi_i|}{E-E_i} , \tag{1.6.2}$$

where the intermediate states, $|\phi_i\rangle$, are the eigenfunctions of the Hamiltonian, H, which describes the particle–target system. The energy spectrum is discrete due to the use of box normalization. By rotating the contour of integration from the real axis into the complex plane, the intermediate states and energies are replaced by the eigenfunctions and complex eigenvalues of the complex-scaled Hamiltonian, respectively. For an isolated resonance $E_n = \varepsilon_n - \frac{1}{2}\Gamma_n$, which is sufficiently narrow, i.e. very small Γ_n, there is a single dominant term in the series expansion of the Green operator given in Eq. (1.6.2) when $E = \varepsilon_n$. We shall show that a resonance is considered as sufficiently narrow when $\Gamma_n \ll -\mathrm{Im}[\varepsilon_n \exp(-2\mathrm{i}\theta)]$. Consequently, when the total energy of the particle–target system is about equal to the position of a narrow resonance, Eq. (1.6.1) – the transition probability to get from "reactants" to "products" – is reduced to a Breit–Wigner-type expression [1,16],

$$P(E) = \frac{|\langle\varphi_f|V|\phi_n^{\mathrm{res}}\rangle\langle\phi_n^{\mathrm{res}}|V|\varphi_i\rangle|^2}{(E-\varepsilon_n)^2 + (\Gamma_n/2)^2} \propto \frac{(\Gamma_n/2)}{(E-\varepsilon_n)^2 + (\Gamma_n/2)^2} . \tag{1.6.3}$$

The main conclusion from Eq. (1.6.3) is that when the lifetime of the "particle–target" system is sufficiently large we may say that the "particle" is trapped by the "target" at a single resonance state, ϕ_n^{res}. In such a case, we can distinguish between the mechanism which brings the system to the resonance state, and the decay process from the metastable resonance state to the products ("out" asymptote in the scattering experiment). The decay process can be considered as a *half collision process*. A typical half collision process is the decay of an excited state $|E_1\rangle$ following a laser excitation of a bound state, $|E_0\rangle$, to a r esonance state, $|E_1\rangle$, (see, for example, Fig. 2). One such example is the infra red excitation of a highly rotational excited diatomic molecule from its vibrational ground state to a vibrational state laying just below the top of the centrifugal potential barrier. An example for a Feshbach-type resonance obtained in a half collision experiment is the predissociation of van der Waals complexes [17]. Let us consider, for instance, the predissociation of the van der Waals complex NeICl. The NeICl complex in the B electronic excited state is stable. When the ICl vibration is excited the complex NeICl (B, $v = 2$) gets into a metastable resonance state [18,19]. The lifetime of an excited NeICl molecule is about 2.5 ns and as time passes free ICl

molecules, in the first excited vibrational state and in rotational states which vary from $j = 0$ to about $j = 32$, are obtained.[1]

Another example is the autoionization of the helium atom [20] are the two electrons were excited from the doubly occupied $1s$ orbital to the $2s$ orbital. The energy of $He(2s)^2$ is smaller than the energy of $He^+(2s)$ but greater than the energy of $He^+(1s)$. The $(2s)^2$ state is embedded in the continuum of the $He^+(1s)$ ion.[2] Due to the electronic correlation one electron moves from the $2s$ orbital to the $1s$ ground state orbital and thereby proves the energy which is required for the ionization of the second electron: $He(2s)^2 \rightarrow He^+(1s) + e^{-2}$. The kinetic energy of the free Auger electron [21] is about equal to the position of the resonance state above the 1st threshold energy (the real part of the complex resonance eigenvalue), and the rate of decay (inverse lifetime) is the resonance width (the imaginary part of the complex resonance energy).

1.7. Resonances in multiphoton ionization/dissociation experiments by complex scaling

In Section 1.5 we proved that the complex-scaled resonance eigenfunctions are square integrable (see also Ref. [22]). The proof based on the assumption that the asymptote of the Siegert resonance wave function is an outgoing plane wave. This assumption holds for finite range potentials for which the cut-off approximation is taken into consideration (i.e. $V = 0$ for $r > r_0$). Balslev and Combes [14] and Simon [15] have shown that also for the infinite range, Coulombic potential the complex-scaled resonance wavefunctions are square integrable (see also the reviews of Reinhardt [23], Junker [24] and Ho [25]). It is entirely clear that the cut-off potential argument cannot be taken into consideration when the interaction between "scattered particle" and the "target" does not vanish as $r \rightarrow \infty$. This is exactly the case when the "scattered particle" is an atom/molecule and the "target" is an electromagnetic field. In this case, the interaction potential is proportional to the dipole moment operator $\hat{\mu}$. In the interaction of an atom with an dc field the time-independent Hamiltonian is given by

$$\hat{H}(\boldsymbol{r}) = \hat{H}_0(r) + \varepsilon_0 ez\,, \tag{1.7.1}$$

where ε_0 is the field intensity, $\hat{H}_0$ is the atomic field-free Hamiltonian and $\hat{\mu} = \hat{z}$. In the interaction of atom/molecule with a high intense ac field (where the perturbational methods break down and cannot be used) the time-dependent Hamiltonian is given by

$$H(r,t) = H_0(r) + \varepsilon_0 \mu(\boldsymbol{r}) f(t) \tag{1.7.2}$$

when, for example, a monochromatic electromagnetic field is used, then $f(t) = \cos wt$ where w is the frequency of the cw laser.

---

[1] The predissociation of NeICl when ICl is in its $v = 2$ vibrational excited state is considered as a Feshbach-type resonance phenomenon since the energy of NeICl ($v = 2$) is *smaller* than the energy of ICl ($v = 2, j = 0$) and hence dissociation due to the shape type resonance mechanism does not occur, i.e., NeICl ($v = 2$)$\nrightarrow$Ne + ICl ($v = 2, j = 0$). However, since the energy of NeICl ($v = 2$) is higher than the energy of ICl ($v = 1; j = 0, 1, 2, \ldots, 32$ the dissociation occurs due to the coupling between the internal modes of NeICl.

[2] The ionization due to the Shape-type resonance mechanism, does not occur, $He(2s)^2 \nrightarrow He^+(2s) + e^-$, since the energy of $He(2s)^2$ is smaller than the energy of $He^+(2s)$. The autoionization due to the Feshbach-type resonance mechanism is an example of the electron correlation effect.

Reinhardt, Chu and coworkers studied extensively this problem, and showed numerically that even in these cases, when $\mu \to \infty$ as $x \to \infty$, the complex-scaled resonance wave functions are square integrable [26]. Here we shall prove that upon complex scaling of a general time-dependent Hamiltonian (given in the length gauge representation)

$$\hat{H} = (\hat{p}_x)^2/2m + V(x) + \mu(x)f(t)\,, \tag{1.7.3}$$

where

$$V(x) \to 0 \quad \text{as } x \to \infty \tag{1.7.4}$$

and

$$\lim_{x\to\infty} \mu(x) = \varepsilon_0 x\,, \tag{1.7.5}$$

the resonances are isolated from the other states in the continuum and are associated with square integrable functions. The proof will be given in three steps:

(I) Transformation of the Hamiltonian from the length-gauge to the momentum gauge
By substituting Eq. (1.7.3) into the time-dependent Schrödinger equation

$$\hat{H}\psi = \mathrm{i}\hbar\,\partial\psi/\partial t \tag{1.7.6}$$

where

$$\psi = \mathrm{e}^{-\mathrm{i}\mu(x)\int f(t)\,\mathrm{d}t/\hbar}\phi(x,t)\,, \tag{1.7.7}$$

one can get that

$$\left[\frac{(\hat{p}_x - \mu'(x)\int f(t)\,\mathrm{d}t)^2}{2m} + V(x)\right]\phi(x,t) = \mathrm{i}\hbar\frac{\partial\phi(x,t)}{\partial t}\,, \tag{1.7.8}$$

where

$$\mu'(x) \equiv \partial\mu(x)/\partial x\,. \tag{1.7.9}$$

Using the condition given in Eq. (1.3.1) it is clear that

$$\mu'(x) \to \varepsilon_0 \tag{1.7.10}$$

as $x \to \infty$.

(II) Transformation of the Hamiltonian from the momentum gauge to the acceleration gauge
Following Kramers–Henneberger transformation [27] the complex-scaled wave function $\phi(x,t)$,

$$\begin{aligned}\phi(x,t) &= \mathrm{e}^{-\mathrm{i}b(t)}\tilde{\phi}(x,t)\,,\\ \tilde{\phi}(x,t) &= \mathrm{e}^{\mathrm{i}a(t)\hat{p}_x}\chi(x,t)\,,\end{aligned} \tag{1.7.11}$$

where

$$b(t) = \frac{\varepsilon_0^2}{2m\hbar}\int F^2(t)\,\mathrm{d}t\,,$$
$$a(t) = \frac{\varepsilon_0}{m\hbar}\int F(t)\,\mathrm{d}t\,, \tag{1.7.12}$$
$$F(t) = \int f(t)\,\mathrm{d}t$$

is substituted into Eq. (1.7.8). Since we are interested here in the property of the resonance wave functions in its asymptotic limit, we shall assume that $\mu'(x) = \varepsilon_0$ for any value of x. The conclusion obtained on the basis of this assumption holds in the more general case where $\lim_{x\to\infty}\mu'(x) = \varepsilon_0$. As a result one gets that

$$\left[\frac{(\hat{p}_x)^2}{2m} + \tilde{V}(x,t)\right]\chi(x,t) = \mathrm{i}\hbar\frac{\partial\chi(x,t)}{\partial t}\,, \tag{1.7.13}$$

where

$$\tilde{V}(x,t) = \mathrm{e}^{-\mathrm{i}\hat{p}a(t)}V(x)\mathrm{e}^{+\mathrm{i}\hat{p}a(t)}\,. \tag{1.7.14}$$

By noticing that

$$\mathrm{e}^{+\mathrm{i}\hat{p}a}\chi(x,t) = \chi(x+a,t) \tag{1.7.15}$$
$$\mathrm{e}^{-\mathrm{i}\hat{p}a}[V(x)\chi(x+a,t)] = [V(x-a)\chi(x,t)]\,. \tag{1.7.16}$$

One can get that

$$\tilde{V}(x,t) = V(x-a) \tag{1.7.17}$$

and, therefore,

$$\left[\frac{(\hat{p}_x)^2}{2m} + V\left(x - \frac{\varepsilon_0}{m\hbar}\int\int f(t)\,\mathrm{d}t\right)\right]\chi(x,t) = \mathrm{i}\hbar\frac{\partial\chi(x,t)}{\partial t}\,. \tag{1.7.18}$$

(III) Multiphoton ionization/dissociation resonance wave functions are square integrable

From Eq. (1.7.8) one can see that for any given time t, $\tilde{V} = V(x-a(t)) \to 0$ as $x \to \infty$ consequently, the coupling of between the atomic/molecular Hamiltonian and the ac field vanishes as $x \to \infty$ and as time passes a free particle (an electron or a molecular fragment) will be obtained. For time periodic Hamiltonians, the resonance Floquet quasi-energy state is given by

$$\chi_{\mathrm{res}}(x,t) = \mathrm{e}^{-\mathrm{i}E_{\mathrm{res}}t/\hbar}\Phi_{\mathrm{res}}(x,t) \tag{1.7.19}$$
$$\Phi_{\mathrm{res}}(x,t) = \Phi_{\mathrm{res}}(x,t+2\pi/w) \tag{1.7.20}$$

and the resonance complex quasi-energy, E_{res}, and the time-periodic function $\Phi_{\mathrm{res}}(x,t)$ are, correspondingly, the eigenvalue and eigenfunction of the Floquet Hamiltonian

$$\left(-\mathrm{i}\hbar\frac{\partial}{\partial t} + \frac{(\hat{p}_x)^2}{2m} + V\left(x - \frac{\varepsilon_0}{m\hbar}\int\int f(t)\,\mathrm{d}t\right)\right)\Phi_{\mathrm{res}}(x,t) = E_{\mathrm{res}}\Phi_{\mathrm{res}}(x,t)\,, \tag{1.7.21}$$

where

$$E_{\rm res} = \varepsilon - {\rm i}/2\Gamma\,, \tag{1.7.22}$$

$$\Phi_{\rm res}(x,t) = \sum_{n=-\infty}^{\infty} {\rm e}^{{\rm i}wnt}\varphi_n(x)\,. \tag{1.7.23}$$

For the open Floquet channels, $n<0$, (here we assume that the resonance state is in the $n=0$ Brillouin zone which implies that $-\hbar w<\varepsilon<0$) and within the framework of the cut-off approximation (i.e. $V(x>x_0)=0$)

$$\varphi_{n<0}(|x|>x_0) \to \sqrt{m/\hbar k_n}\,{\rm e}^{{\rm i}k_n x} \tag{1.7.24}$$

$$(\hbar k_n)^2/2m = \varepsilon - ({\rm i}/2)\Gamma - \hbar w n \tag{1.7.25}$$

provided n gets a sufficiently large value such that Real $(\hbar k_n)^2>0$. φ_n becomes square integrable when

$$x = x'{\rm e}^{{\rm i}\theta} \tag{1.7.26}$$

and x' is a real variable (for a detailed discussion see Section 1.5). For long-range potential such as the coulombic potential, $v(x-a(t))$, the complex-scaled resonances are square integrable functions following the Balslev–Combes theorem.

From Eqs. (1.7.7), (1.7.11), (1.7.19), (1.7.23), (1.7.24) and (1.7.25) one can see that since the resonance state $\chi(x,t)$ is a square-integrable function then $\phi(x,t)$ and, therefore, $\psi(x,t)$ are the complex-scaled square-integrable resonance wave function.

We can summarize the discussion by saying that here we prove that the complex-scaled resonance wave function calculated either in the length-gauge; momentum-gauge, or acceleration-gauge representation of the Hamiltonian are square-integrable functions regardless of the fact that $\mu(x)$ may get an infinite large value as $x\to\infty$. The proof holds provided that $\mu(x)/x$ approaches a constant value as $x\to\infty$. The proof can be extended to time-dependent Hamiltonians which are not necessarily time periodic (this is the case when short pulse high intense lasers are used) by the (t,t') method recently introduced by Peskin and Moiseyev [28].

2. From complex-scaled Hamiltonians to resonance positions and widths

As was discussed in Section 1, the long-lived states of a system which has sufficient energy to break-up into two or more subsystems are associated with the complex poles of the S-matrix. The resonance positions and widths are, respectively, associated with the real and imaginary part of the complex eigenvalues of the time-independent non-scaled [13] Hamiltonian (see Eq. (1.4.12)). The resonance eigenfunctions diverge exponentially as it is shown in Eq. (1.4.13) and therefore they cannot be in the hermitian domain of the Hamiltonian. Consequently, the corresponding resonance eigenfunctions are definitely NOT in the Hilbert space. As it is well known the eigenvalues of hermitian Hamiltonians are real and cannot get complex values. The hermitian property is not only a property of the operator but also of the functions on which the operator is acting (see Section 1.4). As we discussed in Section 1, the resonance eigenfunctions can be taken into the Hilbert space (which contains all possible square integrable functions) by carrying out a "proper"

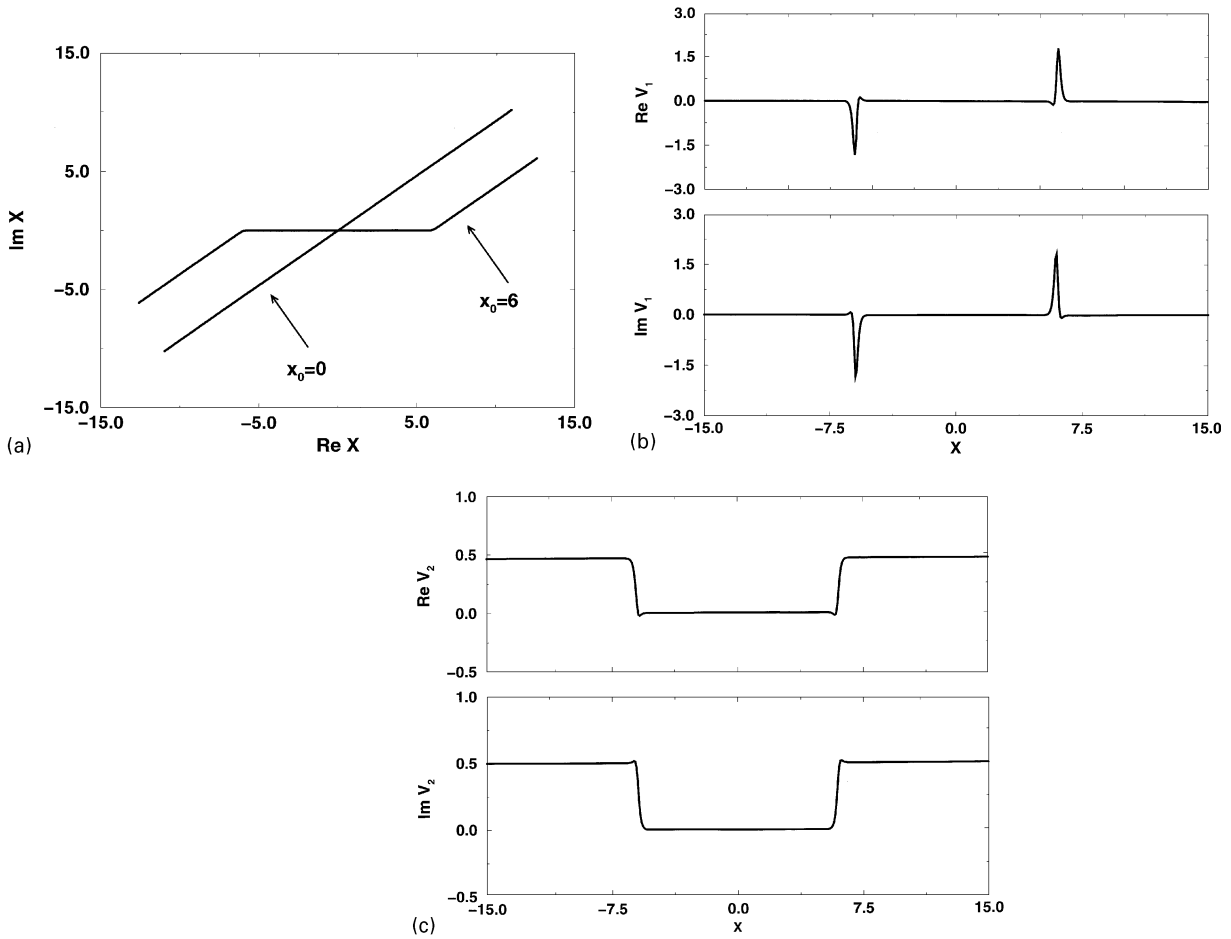

Fig. 8. (a) Two possible integration paths, $F(x)$, in the complex coordinate plane (see Eq. (2.1.30) in the text). For $\lambda =$ the conventional complex path is obtained, for $\lambda = 5$ and $x_0 = 6$ a.u. a smooth-exterior-scaling path is obtained. In both two cases $\theta = 0.75$ rad. (b) The complex $V_1(x)$ local extremely short-range potential (see Eq. (2.1.21) in the text) which is the coordinate dependent linear factor of the flux-type term in $\hat{V}_{\mathrm{CAP}}$ (see Eq. (2.1.20)). The path in the complex coordinate plane is $F(x)$ as shown in Fig. 8 for $\lambda = 5$. (c) The complex $V_2(x)$ potential which vanishes when the physical potential gets non-zero values (see Eq. (2.1.22) in the text) which is the coordinate dependent linear factor of the diffusion-like term in $\hat{V}_{\mathrm{CAP}}$ (see Eq. (2.1.20)). The path in the complex coordinate plane is $F(x)$ as shown in Fig. 8(a) for $\lambda = 5$.

similarity transformation of the Hamiltonian (see Eqs. (1.5.5), (1.5.6), (1.5.7), (1.5.8), (1.5.9), (1.5.10), (1.5.11) and (1.5.12)). Moiseyev and Hirschfelder [13] suggested the following as "proper" similarity transformations:

$$\hat{S} \sim \exp[-\theta f^{1/2}(r)(\partial/\partial r) f^{1/2}(r)]\,, \tag{2.0.1}$$

where $f(r)$ can be any function for which $f(r)/r \to 1$ as $r \to \infty$. In the conventional complex scaling, as first proposed by Hartree during the Second World War [29] and more recently by Balslev and Combes [14] and by Simon [15], $f(r) = r$. In Fig. 8a we represent several illustrative contours, $\hat{S}r$, in the complex coordinate space.

The exterior complex scaling [30–32]

$$\hat{S} = \begin{cases} 1 & \text{if } r < r_0 \,, \\ \exp[-\theta(r - r_0)\partial/\partial r & \text{if } r \geq r_0 \end{cases} \tag{2.0.2}$$

was suggested by Simon [32] to avoid the intrinsic non-analyticities of the potential, **V**, by passing on the right-hand side of the singularity points of **V**. We shall represent here several properties of the complex-scaled Hamiltonians.

2.1. The complex scaled Hamiltonian

2.1.1. "*Conventional*" *complex scaling*

For the sake of clarity, and without loss of generality, let us describe the one-dimensional complex-scaled Hamiltonian. When the potential is dilution analytic, the complex-scaled Hamiltonian (in dimensionless units)

$$H_\theta = S^{-1}(\theta)\hat{H}\hat{S}(\theta) \tag{2.1.1}$$

(where $\hat{S}$ is the complex scaling operator as defined in Eq. (1.5.7)) is given by

$$H_\theta = -\frac{e^{-2i\theta}}{2}\frac{\partial^2}{\partial x'^2} + V(x\,e^{i\theta}) \tag{2.1.2}$$

where

$$-\infty \leq x' \leq \infty \tag{2.1.3}$$

and the complex rotational coordinate x (shown in Fig. 8a) is given by

$$x = x' e^{i\theta} \,. \tag{2.1.4}$$

If $V(x')$ gets a minimal value at $x' = x_0$, one may wish (to achieve a rapid numerical convergence in the solution of the time-independent Schrödinger equation) to define x as

$$x = (x' - x_0)e^{i\theta} + x_0 \,. \tag{2.1.5}$$

2.1.2. "*Exterior*" *complex scaling*

For non-dilution analytical potential one may use the exterior complex-scaling operator which is defined in Eq. (2.0.2). The complex rotational coordinate x (shown in Fig. 8a) in this case is given by

$$x = \begin{cases} x' & \text{if } x' < x_0 \,, \\ e^{i\theta}x' & \text{if } x' \geq x_0 \,. \end{cases} \tag{2.1.6}$$

Consequently,

$$\partial/\partial x = g(x')\partial/\partial x' \,, \tag{2.1.7}$$

where

$$g(x') \equiv \frac{\partial x'}{\partial x} = \begin{cases} 1, & x' < x_0\,, \\ \mathrm{e}^{-\mathrm{i}\theta}, & x' \geq x_0\,. \end{cases} \tag{2.1.8}$$

Therefore,

$$g' \equiv \partial g/\partial x = (\mathrm{e}^{-\mathrm{i}\theta} - 1)\delta(x' - x_0) \tag{2.1.9}$$

and

$$\begin{aligned} \partial^2/\partial x^2 &= g^2\,\partial^2/\partial x'^2 + g\cdot g'\,\partial/\partial x' \\ &= g^2(x')\partial^2/\partial x'^2 + \mathrm{e}^{-\mathrm{i}\theta}(\mathrm{e}^{-\mathrm{i}\theta} - 1)\delta(x' - x_0)\partial/\partial x'\,. \end{aligned} \tag{2.1.10}$$

From Eqs. (2.1.6), (2.1.7), (2.1.8), (2.1.9) and (2.1.10) one can see that the complex exterior-scaled Hamiltonian is given by

$$H_\theta = -\frac{[g(x')]^2}{2}\frac{\partial^2}{\partial x'^2} - \left(\frac{\mathrm{e}^{-2\mathrm{i}\theta} - \mathrm{e}^{-\mathrm{i}\theta}}{2}\right)\delta(x' - x_0)\frac{\partial}{\partial x'} + V(x)\,, \tag{2.1.11}$$

where $g(x')$ and x are defined above.

By carrying out integration by parts it has been shown by Rom and Moiseyev [33] that the complex exterior-scaled kinetic matrix is given by

$$\begin{aligned} -\frac{1}{2}\left\langle \phi_i\left|\frac{\partial^2}{\partial x^2}\right|\phi_j\right\rangle &= \frac{1}{2}\int_0^{x_0}\left(\frac{\mathrm{d}\phi_i}{\partial x'}\right)\left(\frac{\mathrm{d}\phi_j}{\mathrm{d}x'}\right)\mathrm{d}x' \\ &+ \frac{\mathrm{e}^{-2\mathrm{i}\theta}}{2}\int_{x_0}^{\infty}\left(\frac{\mathrm{d}\phi_i}{\mathrm{d}x_i'}\right)\left(\frac{\mathrm{d}\phi_j}{\mathrm{d}x'}\right)\mathrm{d}x' - \frac{1}{2}\phi_i(x_0)\left.\frac{\mathrm{d}\phi_j(x')}{\mathrm{d}x'}\right|_{x'=x_0}\cdot(1 - \mathrm{e}^{-\mathrm{i}\theta}) \end{aligned} \tag{2.1.12}$$

when $\phi_i(x')$ and $\phi_j(x')$ are real square integrable basis functions.

2.1.3. "Smooth-exterior" complex scaling

The Moiseyev–Hirschfelder [13] generalization of the complex coordinate method associated the resonance-poles of the S-matrix, $E = E_r - \mathrm{i}E_i$, with the θ-independent complex eigenvalues of $\hat{\mathscr{H}}$:

$$\hat{\mathscr{H}}\Psi = E\Psi\,, \tag{2.1.13}$$

where

$$\hat{\mathscr{H}} = -\hbar^2/2M\,\partial^2/\partial z^2 + V(z) \tag{2.1.14}$$

and $z = F(x)$ is a path in the complex coordinate plane such that

$$z = F(x) \to x\exp(\mathrm{i}\theta) \quad \text{as } x \to \infty\,. \tag{2.1.15}$$

In the spirit of Simon's proposition to avoid the need to carry out analytical continuation of the potential term in the Hamiltonian into the complex coordinate plane [30–32] Rom, Engdahl and Moiseyev first proposed to define a smooth-exterior-scaling path which is defined as [34]

$$f(x) = \partial F/\partial x = 1 + (\exp(\mathrm{i}\theta) - 1)g(x)\,, \tag{2.1.16}$$

where $g(x)$ is varied from 0 to 1 value around the point $x = x_0$. If $V(x \geq x_0) = 0$ one can use the unscaled potential $V(x)$ rather than using the complex potential $V(z)$. Note however, that the path which defined in Eq. (2.1.16) is very general and is not necessarily limited to the case where $V(z) = V(x)$ or when $V(z) \sim V(x)$.

It is easy to see that since

$$\partial/\partial z = f^{-1}(x)\,\partial/\partial x\,, \tag{2.1.17}$$

then

$$\partial^2/\partial z^2 = -f^{-3}(x)\,\partial f(x)/\partial x\,\partial/\partial x + f^{-2}(x)\partial^2/\partial x^2\,. \tag{2.1.18}$$

Consequently, the smooth-exterior-scaled Hamiltonian as derived by Moiseyev is given by [35]

$$\hat{\mathscr{H}} = -\hbar^2/2M\,\partial^2/\partial x^2 + V[F(x)] + \hat{V}_{\mathrm{CAP}}\,, \tag{2.1.19}$$

where

$$\hat{V}_{\mathrm{CAP}} = \tfrac{1}{2}V_1(x)\,\partial/\partial x + V_2(x)\partial^2/\partial x^2 \tag{2.1.20}$$

and

$$V_1(x) = \hbar^2/Mf^3(x)\,\partial f(x)/\partial x\,, \tag{2.1.21}$$

$$V_2(x) = (\hbar^2/2M)(1 - f^{-2}(x))\,. \tag{2.1.22}$$

The volume element is given by

$$\mathrm{d}z = f(x)\,\mathrm{d}x\,. \tag{2.1.23}$$

As usual one can transform the Hamiltonian in order to simplify the expression of the volume element to be equal to $\mathrm{d}z = \mathrm{d}x$ by defining a new function Φ,

$$\Psi(x) = f^{-1/2}\Phi(x)\,. \tag{2.1.24}$$

Such that

$$\hat{\mathscr{H}}_f = -(\hbar^2/2M)\nabla_f^2 + V[F(x)]\,, \tag{2.1.25}$$

where

$$\nabla_f^2 = f^{+1/2}(x)(\partial^2/\partial z^2)f^{-1/2}(x)\,.$$

After some algebraic derivations one gets that $\Phi(x)$ is an eigenfunction of $\hat{\mathscr{H}}_f$,

$$\hat{\mathscr{H}}_f = -\hbar^2/2M\,\partial^2/\partial^2 x + V[F(x)] + \hat{V}_{\mathrm{CAP}}^{(f)}\,, \tag{2.1.26}$$

where

$$\hat{V}_{\mathrm{CAP}}^{(f)} = V_0(x) + V_1(x)\partial/\partial x + V_2(x)\partial^2/\partial x^2\,. \tag{2.1.27}$$

The functions $V_1(x)$ and $V_2(x)$ are as defined in Eq. (2.1.21) and Eq. (2.1.22) where $V_0(x)$ is given by

$$V_0(x) = \hbar^2/4Mf^{-3}(x)\partial^2 f/\partial x^2 - (5\hbar^2/8M)f^{-4}(x)(\partial f/\partial x)^2\,. \tag{2.1.28}$$

As one can see the price one pays for the simplification of the expression of the volume element is in the inclusion of an extra term V_0 in the complex absorbing potential (CAP) and in doubling the weight of the flux-type term.

Without loss of generality, let us define a specific family of integration paths in the complex coordinate plane by defining $g(x)$ in Eq. (2.1.16) as [144]

$$g(x) = 1 + 0.5(\tanh(\lambda(x - x_0)) - \tanh(\lambda(x + x_0))) . \tag{2.1.29}$$

By carrying out integration over $g(x)$ the complex paths, $F(x)$, are obtained,

$$F(x) = x + (\exp(i\theta) - 1)[x - x_0 + (1/2\lambda)\ln(1 + \exp(-2\lambda(x - x_0)))] - \ln(1 + \exp(-2\lambda(x + x_0))) . \tag{2.1.30}$$

Illustrative examples for different possible integration paths are given in Fig. 8a for $\lambda = 0, 3, 5$ and $x_0 = 6$. For $\lambda = 0$, the usual complex coordinate path, $z = x\exp(i\theta)$, is obtained. For large values of λ the smooth-exterior-scaling path is obtained. At the limit of $\lambda \to \infty$ the exterior scaling path [32] is obtained and

$$z = \begin{cases} x & \text{if } -x_0 \le x \le x_0 \\ (x - x_0)e^{i\theta} + x_0 & \text{if } x > x_0 \\ (x + x_0)e^{i\theta} - x_0 & \text{if } x < -x_0 \end{cases} . \tag{2.1.31}$$

The CAP terms can be calculated using the above expression for $g(x)$ and the following analytical expressions for the first and second derivatives of $f(x)$:

$$\partial f/\partial x = 0.5\,\lambda(\exp(i\theta) - 1)\,(\cosh^2(\lambda(x + x_0)) - \cosh^2(\lambda(x - x_0))) \tag{2.1.32}$$

and

$$\partial^2 f/\partial x^2 = \lambda^2(\exp(i\theta) - 1)(\tanh(\lambda(x + x_0))(1 - \tanh^2(\lambda(x + x_0))) - \tanh(\lambda(x - x_0))(1 - \tanh^2(\lambda(x - x_0))^2)) . \tag{2.1.33}$$

In Fig. 8b, c illustrative examples for V_1 and $V_2(x)$ are given for $\lambda = 5$. As one can see from Fig. 8b $V_1(x)$ is an extremely short-range potential for the chosen value of λ. Since $V_1(x)$ looks like a delta function and since the flux operator is defined as $i\delta(x - x_0)\partial/\partial x$ we refer to the corresponding first term in the CAP which is defined in Eq. (2.1.20) as a flux-type operator. The second term is a kinetic-type operator which describes the diffusion at $x \sim x_0$. As one can see from Fig. 8c $V_2(x)$ vanishes when $-x_0 < x < x_0$. The value of x_0 can be chosen such that only within this interval of x the physical potential gets non-zero values and vanishes elsewhere. It should be stressed that in the calculations the potential $V(x)$ can remain unscaled due to the properties of the chosen integration path, $F(x)$, (see Fig. 8a for $\lambda = 5$).

We can summarize it by saying that the use of the universal Flux-diffusion-type CAP which is constructed from the V_1 and V_2 functions which are presented in Fig. 8b, c, enables us to obtain in a very high accuracy many resonances (regardless to their widths and being isolated or overlapping resonances) from a single diagonalization of a complex non-symmetric matrix. Exactly as in the conventional complex scaling. The use of the fact that for some cases we can choose a path in the complex coordinate plane that leaves the physical potential unscaled, i.e. $V(F(x)) = V(x)$, enables

one to construct the unscaled Hamiltonian matrix elements by conventional computational algorithms and by using available program packages (for example, the Gaussian code by which the neutral and ionize polyatomic molecular Hamiltonians can be constructed). The complex smooth-exterior scaling Hamiltonian is obtained by adding to the unscaled Hamiltonian matrix a matrix which represents the universal $\hat{V}_{\mathrm{CAP}}$ (using the same basis set which has been used to represent $\hat{H}$).

2.1.4. Comment on the "smooth-exterior" complex scaling and other approaches using "complex-absorbing-potentials"

In multi-channel problems, one can define an non-local, energy-dependent operator, the so-called optical potential, that enables the calculation of cross sections for a subset of channels. All effects caused by the excluded channels are accounted for by the optical potential. "Optical potentials" has been used in nuclear physics a long time ago [36].

This type of optical potentials should be distinguished from negative-imaginary-short-range potentials that are added to the Hamiltonian in order to impose absorbing boundary conditions which provide outgoing waves in the asymptotic limit. In the literature this type of potentials are sometimes also called optical potentials [37]. To avoid confusion we do not use the term optical potential here but adopt the more suitable expression CAPs, complex-absorbing-potentials, as proposed by Riss and Meyer [38] in order to name the artificial potentials introduced to impose absorbing boundary conditions. In molecular physics the use of CAPS avoids artificial reflections which result from the use of the finite basis/grid approximation [39] and allows simulations of large scale strongly coupled scattering problems (such as in four-center reactions) involving millions of basis functions [40].

In optical simulations the Maxwell equation is solved by using CAPs (see, for example, Refs. [16, 41]) to design wave guides which have specific properties. More recently, Neuhauser presented a new highly accurate and anomaly free time-independent approach to reactive scattering based on the use of very short-range imaginary potentials [42]. In a one-dimensional simulation the CAPs covered only two grid points!

Unlike other methods such as the complex-coordinate method which stays on a solid mathematical ground given by Balslev and Combes [14] and Simon [15], the use of CAPs was based on intuition and numerical experience. It has been proved that poles of the scattering matrix are also the eigenvalues of the complex-scaled Hamiltonian, but it has not been proved that they are the eigenvalues of the Hamiltonian which is perturbed by a CAP. Rom et al. [43] have shown that the use of a CAP is similar to the use of the exterior scaling and more precise to the use of the smooth-exterior-scaling method which was formulated by Rom et al. [34]. Riss and Meyer [38] addressed themselves also to the question of under what conditions the resonances obtained by the use of CAPs are indeed the poles of the scattering matrix. Their strategy and derivation was as follows: the CAPs would provide the exact poles of the S-matrix if they would be reflection-free potentials. The reflection can be made smaller than any given limit, if the CAP is made weak and long enough; moreover, they showed that one may minimize the reflections of a short-range CAP by adding specific energy-dependent terms to the effective Hamiltonian which includes the CAP; from the requirement that the CAP in the free-reflection modified Hamiltonian will be energy linearly dependent they obtained a new effective Hamiltonian which consists of smooth-exterior-scaled kinetic operator and a potential term which is vanished (unlike the usual used CAPs) when the potential of interaction, V, is vanished as well; Their so-called TCAP-method [44] is, in fact,

very similar to the smooth exterior complex scaling [34] except that they add an extra local complex potential which is problem-dependent.

The strategy by Moiseyev [35] is in reversed to the one by Reiss and Meyer. Reiss and Meyer started from the Hamiltonian perturbed by a CAP and end up with a complex-scaled-type operator. We get out from the Moiseyev–Hirschfelder generalized representation of the complex coordinate method and end up with the non-scaled Hamiltonian perturbed by a CAP which is problem independent. As we show above this *universal energy-independent* CAP is a linear combination of Flux- and diffusion-type operators. In order to avoid confusion we should stress that the Flux CAP derived here is not related to the use of reactive flux and CAPs made recently by Jäkel and Meyer in the formulation of a new modified flux operator formalism for the calculations of state-to-state transition probabilities [45]. It is also different from the Bloch flux-type CAP derived by Lipkin, Brändas and Moiseyev [46] from the exterior complex scaling approach [32]. The main difference between the Bloch-type CAP derived by Lipkin and coworkers and the CAP operator derived here, is in the fact that the Bloch operator is energy-dependent whereas the CAP presented below (see Eq. (2.1.20)) is energy-independent. Therefore, the use of the Bloch-type CAP enables the calculations of the resonances one by one and by the use of an iterative numerical procedure [8], whereas the use of the CAP derived here enables one to get at once many resonances from a single diagonalization of a complex non-hermitian matrix.

2.2. The complex "energy" spectrum – Resonance positions, widths and rotating continua

2.2.1. General discussion

Following the Balslev–Combes theorem [14], the complex eigenvalues (defined as the complex "energy" spectrum) of the complex scaled Hamiltonian, $\hat{S}(\theta)\hat{H}(x)\hat{S}^{-1}(\theta)$, which are associated with BOUNDED not necessarily square integrable eigenfunctions are given in Fig. 9.

We have already shown in Section 1 that bound states and resonance states are associated with the discrete part of the energy spectrum. Both the bound states and the resonance states are associated with square integrable functions and consequently belong to the Hilbert space. For a simple proof see Eqs. (1.5.7), (1.5.8), (1.5.9), (1.5.10), (1.5.11) and (1.5.12). The continuum, unlike the bound and resonance states, is affected by the value of the rotational angle θ. Following the Balslev and Combes theorem, the scattering states are rotated into the lower-half of the complex energy plane by the angle 2θ. It is easy to prove this theorem for short-range potentials. In such cases, the scattering states have the asymptotic behavior given by

$$\phi^{\mathrm{scatt}}(r \to \infty) = A(k)\mathrm{e}^{-\mathrm{i}kr} + B(k)\mathrm{e}^{+\mathrm{i}kr} \tag{2.2.1}$$

where

$$E = (\hbar k)^2/2m\,. \tag{2.2.2}$$

The energy gets any real positive value (provided that the threshold energy is taken as zero). The complex-scaled scattering states are given by

$$\phi^{\mathrm{scatt}}(r'\mathrm{e}^{\mathrm{i}\theta}) \underset{r'\to\infty}{\to} A(k)\mathrm{e}^{-\mathrm{i}k\mathrm{e}^{\mathrm{i}\theta}r'} + B(k)\mathrm{e}^{+\mathrm{i}k\mathrm{e}^{\mathrm{i}\theta}r'}\,. \tag{2.2.3}$$

From Eq. (2.2.3) one can see that for real values of k (i.e. real positive eigenvalues **E**) ϕ^{scatt} diverges as $r' \to \infty$ and $\theta < \pi$ since the real part of the exponential factor is positive. That is,

$$\mathrm{Re}(-ike^{i\theta}) = k\sin\theta > 0\,. \tag{2.2.4}$$

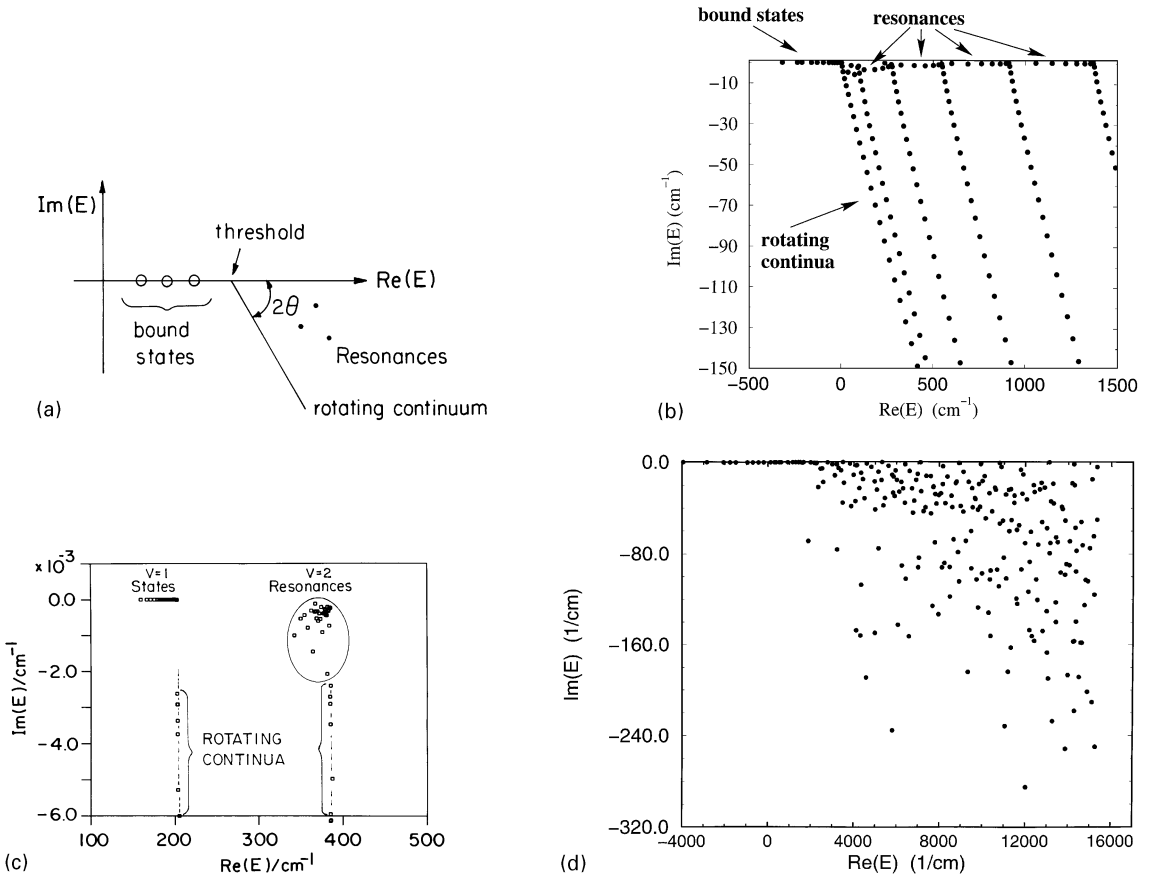

Fig. 9. (a) Schematic representation of the eigenvalues (i.e. "energy spectrum") of the complex coordinate plane scaled Hamiltonian, H_θ, according to the theorem of Balslev and Combes. (b) The complex eigenvalues of the complex-scaled Hamiltonian which describes the interaction of helium atom with the corrugated Cu(117) surface as calculated by Engdahl et al. [138]. The first three full circles below the first threshold stand for the vibrational bound states of helium adsorbed on the surface. The other full circles stands for the selective adsorption resonances. (c) The complex eigenvalues of the complex scaled Hamiltonian which describes the reaction, $\mathrm{NeICl}(B, v = 2) \to \mathrm{Ne} + \mathrm{ICl}(B, v = 1)$ as calculated by Lipkin et al. [19,139]. (d) The complex eigenvalues of the complex-scaled DVR (discrete variable representation) $\mathrm{HCO}(J = 0)$ Hamiltonian which are associated with the HCO molecular predissociation resonances as calculated by Ryaboy and Moiseyev [94]. (e) The eigenvalues of the complex-scaled Hamiltonian HD/Ag(111) which are associated with square integrable and continuum-type bounded eigenfunctions (Peskin and Moiseyev in Refs. [6,108]). (f) The complex eigenvalues of the complex-scaled Floquet operator, $-i\hbar\partial^2/\partial t^2 - \frac{1}{2}\partial^2/\partial x^2 + V(x,t)$, were $V(x,t)$ is a time periodic driven Rosen–Morse potential, as calculated by Moiseyev and Korsch [128]. The full circles which are laying close to the real axis are the quasi-energy resonances which are defined modulo of $\hbar\omega$, where $\omega = 1$ is taken as the laser frequency.

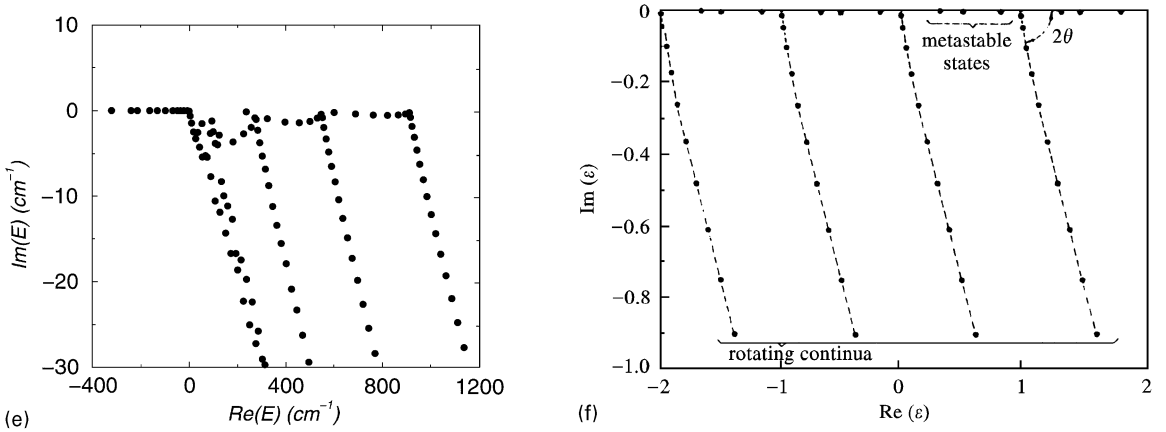

Fig. 9. Continued

The ONLY bounded non-divergent (not square integrable) functions are obtained when k gets complex values,

$$k = |k|e^{-i\theta} \tag{2.2.5}$$

and therefore (when the threshold is taken as the zero reference energy)

$$E_{\text{scatt}}(\theta) = |E|e^{-2i\theta}; \quad |E|\varepsilon[0, \infty] \tag{2.2.6}$$

where E is defined in Eq. (2.2.2).

Consequently, the complex-scaled scattering eigenfunctions have exactly the SAME asymptotical behavior as the unscaled states, but are associated, however, with a continuum which is rotated into the lower-half part of the complex energy plane by the angle 2θ. The rotating one-dimensional continuum is a "white" continuum in the sense that its density of states is varied monotonously as the energy, $|E_{\text{scatt}}(\theta)|$, is increased. When the continuum-type wave functions are box normalized, the density of states of the rotating one-dimensional continuum is expected to be proportional to $|E_{\text{scatt}}(\theta)|^{-1/2}$. The deviation from this behavior due to the use of a finite box size in the normalization procedure has been discussed by Alon and Moiseyev [8].

The schematic representation of the eigenvalues of the complex-scaled Hamiltonian given in Fig. 9a describes the "energy" spectrum of potentials which support shape-type resonances (see, for example, Fig. 2). In the case of potentials that support Feshbach-type resonances (see, for example, Fig. 4) the continuum spectrum splits into several branches which come out of the threshold energies. See, for example, the eigenvalues spectrum of the complex scaled Hamiltonian, presented in Fig. 9b–f, which describes the interaction of helium with Cu(117); dissociation of van der Waals complex NeICl and of HCO; interaction of HD molecules with Ag(111) surface and multiphoton ionization/dissociation of a model Hamiltonian.

The threshold energies are the bound state energies of the "subsystems" (e.g. the rotational energy levels of the free HD molecule) which are obtained due to the decay process (e.g.

predesorption in our illustrative example) of the system (e.g. HD adsorbed on Ag(111)) which was prepared in a metastable (resonance) state.

In the case of 3D potential energy surfaces it is sufficient to scale only the reaction coordinate. We (Lipkin, Ryaboy and Moiseyev) developed a code that enables the calculations of the predissociation resonances of any three atomic molecular system by complex scaling the distance of the dissociative atom from the center of mass of the diatom. In Fig. 9d we show, for example, thousands of HCO resonances (HCO $\rightarrow$ H + CO) which were all obtained from a single diagonalization of the complex-scaled Hamiltonian.

2.2.2. *Resonance transition states for analytical models*

By using complex-scaling arguments, the θ-independent complex eigenvalues which are associated with shape-type resonances can be immediately obtained from the bound state spectrum of analytically solvable model Hamiltonians. Let us assume that for a given system an analytical expression of the bound state discrete spectrum $E(n,\lambda)$, as a function of the quantum energy level n and as a function of the potential strength parameter λ $\mathbf{V}(r)=\lambda v(r)$ is known. For positive values of λ, $V(r)$ has a potential well which supports the bound states. There are two cases where complex energy spectrum can be immediately obtained from the known analytical expression of the discrete bound state spectrum. In the first case, a finite number of bound states associated with real eigenvalues are obtained when $n<n_0$. By substituting values for n which are larger than n_0, $E(n>n_0,\lambda)$ gets complex values which are associated with the resonance states. In the second class of potentials there are either finite or infinite number of bound states (i.e. $n_0=\infty$). By making the transformation of $\lambda\rightarrow -\lambda$ the up-side-down potential $-V(r)$ has a potential barrier. If the new potential $-V(r)$ supports resonance states then $E(n,-\lambda)$ would be a COMPLEX function of the quantum number n. The real and the imaginary parts of $E(n,-\lambda)$ are, respectively, the resonance positions and widths. Here we used indirectly the fact that upon complex scaling the resonance eigenfunctions become square integrable. Let us denote by $\phi(E,\lambda,r)$ a solution of the time-independent Schrödinger equation with the original potential well $V(r)$. The eigenfunction ϕ reduces to a square integrable function if we let the eigenvalue E get only discrete values assigned by the quantum number n, $E_n=E(n,\lambda)$, $n=1,2,\ldots,n_0$. In the first case mentioned above, the $\phi(E,+\lambda,r)$ solutions reduce to square integrable functions when E gets only discrete COMPLEX values, $E_n=E(n,+\lambda)$, $n=n_0+1,n_0+2,\ldots$, by taking a complex contour $r=|r|\exp(\mathrm{i}\theta)$ in the coordinate space. In the second case, the $\phi(E,-\lambda,r)$ solutions reduces to a product of an exponential decaying function and a polynomial (and thereby to a square integrable function) when E gets only discrete COMPLEX values, $E_n=E(n,-\lambda)$ by taking the inverse sign of λ and by choosing a complex contour $r=|r|\exp(\mathrm{i}\theta)$ in the coordinate space.

The main conclusion from this analysis is that there is a SINGLE expression for the discrete energy spectrum of a given model Hamiltonian. By varying either the quantum number n or one of the REAL potential parameters (λ in our above discussion), the REAL energies (associated with bound states) and the COMPLEX "energies" (ONLY when resonance states do exist in the studied class of potentials) are obtained. To illustrate this use of the complex coordinate method we shall look at several simple analytically solvable model Hamiltonians.

We will show here for several model Hamiltonians that the expressions of the resonance positions and widths obtained from the requirement that the resonance complex scaled solutions

are square integrable are identical to the expressions obtained from the bound state energy spectra when the simple procedures proposed above are used.

2.2.2.1. The parabolic potential barrier. The eigenfunctions of the well-known harmonic oscillator potential $V(x) = kx^2/2$ are product of an exponential decaying function and the Kummer functions, $M(E/(\alpha/4 - 2E/(4\hbar\sqrt{k/m}), \alpha/2, \hbar\sqrt{k/m}x^2)$, where $\alpha = 1$ for even functions and to $\alpha = 3$ for odd functions. The Kummer functions reduce to Hermit polynomials when

$$\alpha/4 - E/(2\hbar\sqrt{k/m}) = -n\,. \tag{2.2.7}$$

A parabolic potential barrier is obtained when $k \to -k$. When x is scaled by the complex factor $\exp(i\theta)$ and from the requirement that $M(E/(\alpha/4 - 2E/(4\hbar\sqrt{-k/m}), \alpha/2, \hbar\sqrt{-k/m}x^2\exp(2i\theta)/\hbar)$ would be an n-degree finite polynomial, we get that complex-scaled square integrable eigenfunctions of the complex-scaled Hamiltonian,

$$\hat{H} = -e^{-2i\theta}\hbar^2/2m\,d^2/dx^2 - e^{+2i\theta}(k/2)x^2 \tag{2.2.8}$$

are associated with the negative "purely" imaginary eigenvalues given by

$$\alpha/4 - (E_n/2\hbar)(-k/m)^{1/2} = -n\,, \tag{2.2.9}$$

where for $k > 0$

$$(-k/m)^{+1/2} = -i(k/m)^{+1/2} = i\omega\,. \tag{2.2.10}$$

Consequently,

$$E_n = -i\hbar\omega((4n + \alpha)/2)$$

or

$$E_n = -i\hbar\omega(n + 1/2), \quad n = 0, 1, 2, \ldots\,. \tag{2.2.11}$$

Using the terminology given in Section 1 we can say that in this case the resonance positions (i.e. $\mathrm{Re}(E_n)$) are all equal to zero, (note that the top of the barrier is located at $V = 0$) whereas the resonance widths are given by

$$\Gamma_n = 2\hbar\omega(n + 1/2), \quad n = 0, 1, 2\ldots\,. \tag{2.2.12}$$

For a detailed study of this problem see Atabek et al. [47]. In chemical reactions the potential barrier between the reactants and products is often described by a parabolic potential barrier. In such cases, the resonances are transition states associated with complex-scaled square integrable wavefunctions which are located inside the potential barrier. The lifetime, τ, of these transition states is associated with the inverse resonance widths,

$$\tau(\text{transition states}) = [2\omega(n + 1/2)]^{-1}\,. \tag{2.2.13}$$

2.2.2.2. A model Hamiltonian of an electron scattering from a negative ion. One of the examples which were given by Landau and Lifshitz [48] for analytically soluble problems is of a particle moving in a central symmetric field with potential energy $V(r) = \lambda(\gamma/r^2 - 1/r)$. The solution of the time-independent Schrödinger equation is given by

$$\psi = R(r)Y_{lm}(\theta, \phi)\,, \tag{2.2.14}$$

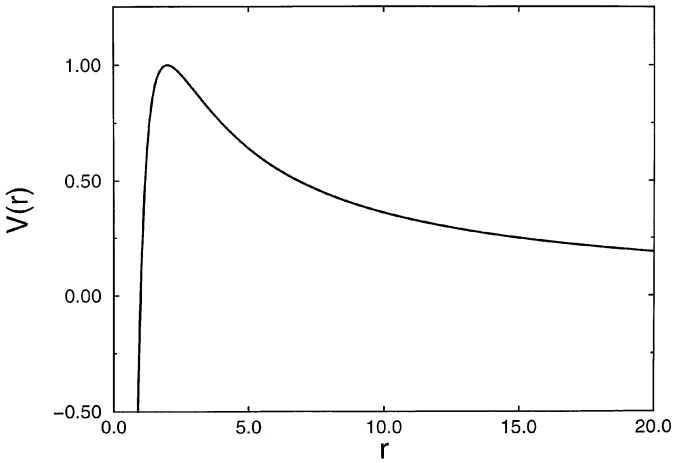

Fig. 10. The potential $V(r) = \ell^2/r - \gamma/r^2$ as function of the radius r.

where $Y_{lm}(\theta, \phi)$ are the spherical harmonics and $R(r)$ is obtained by solving the following radial Schrödinger equation,

$$\left[\frac{\mathrm{d}^2R(r)}{\mathrm{d}r} + \frac{2}{r}\frac{\mathrm{d}R(r)}{\mathrm{d}r} + \frac{2\mu}{\hbar^2}\left(E - \frac{\hbar^2}{2\mu r^2}\ell(\ell+1)\right) - V(r)\right]R(r) = 0\,. \tag{2.2.15}$$

The solution which is associated with negative energy levels and is finite for $r = 0$ is given by

$$R(r) = r^s \exp([-2\mu E]^{1/2} r/\hbar) F(s+1-\lambda[\mu/(-2E)]^{1/2}/\hbar, 2s+2, 2(-2\mu E)^{1/2} r/\hbar)\,, \tag{2.2.16}$$

where

$$s(s+1) = \ell(\ell+1) + 2\mu\lambda\gamma/\hbar^2 \tag{2.2.17}$$

The confluent hypergeometric function F reduces to a polynomial of degree n (i.e. square integrable function) when n obeys the equation

$$n = \lambda\sqrt{(\mu/-2E)/\hbar} - s - 1 \tag{2.2.18}$$

and gets positive integer (or zero) value. Consequently, the bound states energy spectrum is given by

$$E_n = -(2\lambda^2 m/\hbar^2)[2n+1+\{(2\ell+1)^2 + 8m\lambda\gamma/\hbar^2\}^{1/2}]^{-2}\,. \tag{2.2.19}$$

By making the transformation of

$$\lambda \to -\lambda \tag{2.2.20}$$

we get the up-side-down potential which is presented in Fig. 10.

This potential is a model for an electron approaching a negative ion (such as H^- for example). Resonances and bound states are associated with the complex-scaled square integrable eigenfunctions $R(r)$. Therefore by scaling the r coordinate by a complex factor $\exp(\mathrm{i}\theta)$ the confluent

hypergeometric function F,

$$F(s+1+\lambda\sqrt{(\mu/-2E)/\hbar}, 2s+2, 2\sqrt{(-2\mu E)r\mathrm{e}^{\mathrm{i}\theta}/\hbar}) \tag{2.2.21}$$

reduces to a polynomial of degree $n = 0, 1, 2, 3 \ldots$ when

$$n = -\lambda\sqrt{(\mu/-2E)/\hbar - s - 1} \tag{2.2.22}$$

and s is defined as in Eq. (2.2.17). Note that Eq. (2.2.22) is obtained also from Eq. (2.2.18) by making the transformation $\lambda \to -\lambda$.

The corresponding θ-independent resonances and bound states discrete spectrum is obtained by substituting Eq. (2.2.17) into Eq. (2.2.22) or by replacing λ by $-\lambda$ in Eq. (2.2.19). For $\lambda = 1$ we obtain the complex energy levels which are given by

$$\begin{aligned} E_n &= +\frac{2\lambda^2 m}{\hbar^2}[(2n+1) + \mathrm{i}\{8m\gamma/\hbar^2 - (2\ell+1)^2\}^{1/2}]^{-2} \\ &= \frac{2\lambda^2 m}{\hbar^2}\frac{(2n+1)^2 - \Delta - 2\mathrm{i}(1n+1)\Delta^{1/2}}{[(2n+1)^2 - \Delta]^2 + 4(1n+1)^2\Delta}, \end{aligned} \tag{2.2.23}$$

where

$$\Delta \equiv 8m\gamma/\hbar^2 - (2\ell+1)^2 .$$

From Eq. (2.2.23), one can see that shape-type resonances are obtained (i.e. $\mathrm{Im}(E_n) < 0$) when the attractive part of the potential is strong enough such that $\Gamma > 0$ and

$$\gamma > \hbar^2(l+1/2)^2/2m, \quad l = 0, 1, 2 . \tag{2.2.24}$$

The resonance eigenvalues and eigenfunctions for the special case of $l = 0$ were first introduced by Doolen [49], and for the more generalized case where $l \neq 0$ by Junker [24].

Note by passing that in a very similar way the resonance energies of a barrier potential given by $V(r) = \pm A/r^2 - Br^2$ can be obtained by making the transformation $A \to -A$ and $B \to -B$ in the analytical expression of the bound spectrum of $-V(r)$ given by Landau and Lifshitz [48].

2.2.2.3. The Eckart potential – a model for A + BC reactive system. The transition from reactants to products in an elementary chemical reaction characterized by the presence of a potential barrier. The symmetric potential barrier presented in Fig. 11 describes the potential energy of $H + H_2$ (within the framework of the Born–Oppenheimer approximation) as a function of the reaction coordinate x. The reaction coordinate is defined as the minimum energy path from the reactants' "valley" to that of the products. For non-homonuclear chemical reactions the potential barrier is non-symmetric.

The Eckart potential is probably the most commonly used model for the description of a chemical reaction potential barrier. It has been shown on the basis of semiclassical transition theory formulated by Miller [50] that the cumulative reaction probability as a function of the translational energy, $N(E)$, can be calculated only from the contributions of the Siegert poles of the scattering matrix even when $N(E)$ is structureless [50,51]. Following the strategy to obtain analytical expressions for the resonance positions and widths (i.e. complex Siegert eigenvalues of

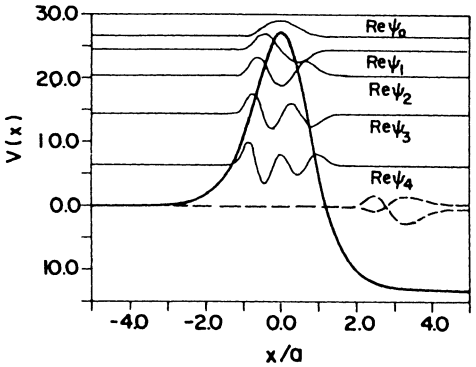

Fig. 11. Non-symmetric Eckart potential energy curve.

the complex-scaled Hamiltonian) described above, Ryaboy and Moiseyev [52] obtained the resonance energy levels of a particle moving in the symmetric and non-symmetric Eckart potential barrier.

(a) Symmetric potential barrier

Here we follow Landau and Lifshitz [53] solution for the Rosen–Morse model Hamiltonian [54] which supports bound states. Note that V(Rosen–Morse) $= -$ V(Eckart). The Rosen–Morse model Hamiltonian is given by

$$\hat{H}(x) = -\hbar^2/2m\,\mathrm{d}^2/\mathrm{d}x^2 + V_0/[\cosh^2(x/a)]\,. \tag{2.2.25}$$

By making the transformation $V_0 \to -V_0$ we get the up-side-down Rosen–Morse potential which is the symmetric Eckart potential barrier. By choosing in Eq. (2.2.25), a complex contour, $x = x'\exp(\mathrm{i}\theta)$, where $x' \in (-\infty, +\infty)$, and sufficiently large value of θ, the resonance eigenfunctions become square integrable. The wave functions $\psi(x)$ are proportional to hypergeometric functions F,

$$\psi(x) \sim F[\varepsilon - s, \varepsilon + s + 1, \varepsilon + 1, x]\,, \tag{2.2.26}$$

where

$$\varepsilon = (a/\hbar)\sqrt{-2mE} \tag{2.2.27}$$

and

$$s(s+1) = -2mV_0a^2/\hbar^2\,. \tag{2.2.28}$$

In order to get square integrable functions, F should be truncated to a finite order n-degree polynomial by following the requirement of:

$$\varepsilon - s = n = 0, 1, 2, \ldots \tag{2.2.29}$$

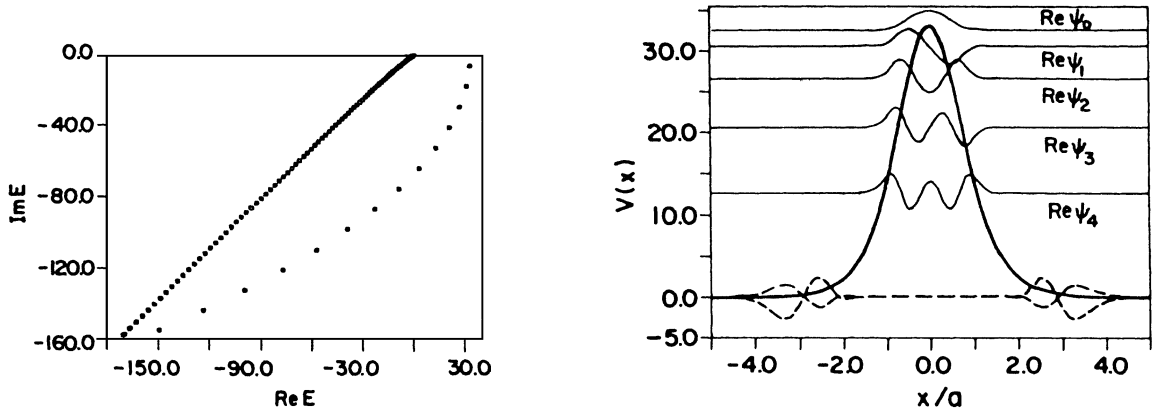

Fig. 12. The Siegert transition-state resonance eigenvalues and 2θ rotated continuum.

Fig. 13. Symmetric Eckart potential $V(x)$ (solid lines) and five Siegert eigenvalues $\mathrm{Re}\,\psi_n(x)$; $n = 0 - 4$. Two states closest to the reaction threshold $E = 0$ continuum eigenfunctions are given by dashed lines for comparison.

Therefore,

$$\begin{aligned} E &= -(\hbar^2/8ma^2)[-(1+2n) + \sqrt{1 - 8mV_0a^2/\hbar^2}]^2 \\ &= (\hbar^2/8ma^2)[(1+2n) - \mathrm{i}\sqrt{8mV_0a^2/\hbar^2 - 1}]^2 . \end{aligned} \tag{2.2.30}$$

Eq. (2.2.30) can be rewritten

$$E_n = 1/\alpha[\omega_s/2 - \mathrm{i}(n + 1/2)]^2 , \tag{2.2.31}$$

where

$$\alpha = 2ma^2/\hbar^2 \quad \text{and} \quad \omega_s = \sqrt{4\alpha V_0 - 1} . \tag{2.2.32}$$

Note that here we choose the positive root of -1, that is, $\sqrt{-1} = +\mathrm{i}$. See, for example, the Siegert eigenvalues presented in Fig. 12.

As one can see the Siegert states can be counted by their nodes, in the same way as bound state wave functions. The complex-scaled resonance wave functions are localized within the potential barrier region. The two closest eigenfunctions to the reaction threshold, $E = 0$, continuum are given in Fig. 13 for comparison.

(b) Non-symmetric potential barrier

The non-symmetric Eckart potential is given by

$$V(x) = -V_0 \cosh^2\mu\{\tanh[(x - \mu a)/a] + \tanh(\mu)\}^2 + V_0\,\mathrm{e}^{-2\mu} , \tag{2.2.33}$$

where the potential barrier height is $V_0\,\mathrm{e}^{-2\mu}$ and the two threshold energies are 0 and $-2V_0 \sinh(2\mu)$, respectively. When $\mu = 0$ Eq. (2.2.33) reduces to the symmetric potential barrier that appear in Eq. (2.2.26). Similarly to the derivation of the Siegert eigenvalues for the symmetric

potential we shall follow here the analytical solution presented by Morse and Feshbach [55]:

$$V(\text{Morse} - \text{Feshbach}) = -V(\text{non-symmetric Eckart})$$

and obtain the complex Siegert eigenvalues which are given by

$$E_n = -2\beta_2 + [\beta_1 + \mathrm{i}(n + 1/2)]^2 + \frac{\beta_2^2}{[\beta_1 + \mathrm{i}(n + 1/2)]^2} = (z + -\beta_2/z)^2 , \tag{2.2.34}$$

where

$$\begin{aligned} &\alpha = 2ma^2/\hbar , \\ &\varepsilon = \alpha E , \\ &v = \alpha V_0 , \\ &\beta_1 = (v\cosh^2\mu - 1/4)^{1/2} , \\ &\beta_2 = (v\sinh 2\mu)/2 , \\ &z = +\beta_1 + \mathrm{i}(n + 1/2) . \end{aligned} \tag{2.2.35}$$

2.2.2.4. Resonances of non-dilation-analytical potential by complex translation. This is an example for the case where the complex resonance eigenvalues are obtained by letting the quantum number n in the expression for the discrete bound state spectrum to exceed a certain value n_0. The Natanzon model Hamiltonian [56] is given by

$$\hat{H} = -\mathrm{d}^2/\mathrm{d}x^2 + V(x) , \tag{2.2.36}$$

where

$$\begin{aligned} &V(x) = -\lambda^2 v(v + 1)(1 - y^2) + (1 - y^2)(1 - \lambda^2)[5(1 - \lambda^2)y^4 - (7 - \lambda^2)y^2 + 2]/4 \\ &x = \frac{1}{2\lambda^2}\left[\ln\frac{1 + y}{1 - y} + \mathrm{i}c\ln\left(\frac{\mathrm{i} + cy}{\mathrm{i} - cy}\right)\right] = \mathrm{Re}(x) , \\ &c = (\lambda^2 - 1)^{1/2} , \end{aligned} \tag{2.2.37}$$

and

$$-\infty < x < +\infty \ \text{ as } \ -1 < y < 1 \tag{2.2.38}$$

λ and v are dimensionless parameters describing the shape and number of bound states. The potential shown in Fig. 14 (for the values of $\lambda = 26$, $v = 5.5$) supports six bound states and resonances which result from the tunneling through the two symmetrical potential barriers.

There are four singularities at $y = \pm 1$ and $y = \pm \mathrm{i}/c$. As pointed out by Certain and coworkers [57], these singularities avoid a straightforward use of the complex-scaling procedure.

As discussed in Section 1.5, the resonance eigenfunctions diverge asymptotically but upon scaling the coordinate x by $\exp(\mathrm{i}\theta)$,

$$\psi(x\mathrm{e}^{\mathrm{i}\theta}) \to 0 \quad \text{as } x \to \pm\infty \tag{2.2.39}$$

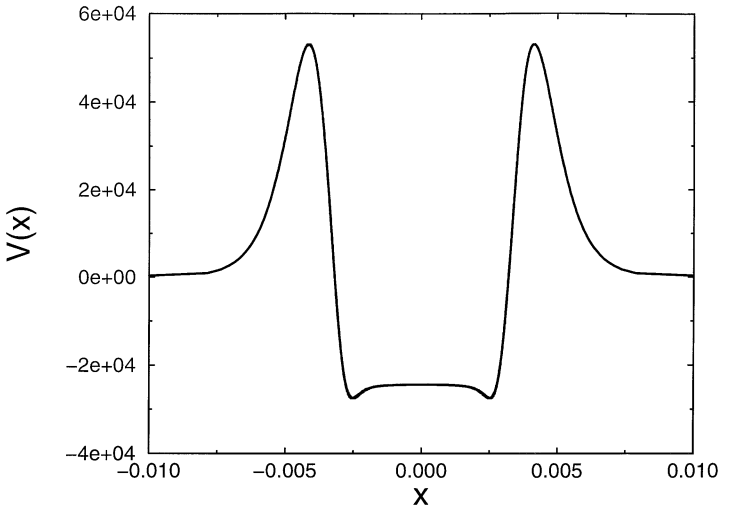

Fig. 14. The Natanzon non-analytical potential.

when $\theta > \theta_c$ and the critical angle θ_c is given by Eq. (1.5.11). Since in the studied case even the critical angle θ_c associated with the longest lived resonance is beyond the angle $\theta = \tan^{-1}(1/c)$ at which the singularity occurs,

$$\theta_c > \tan^{-1}(1/c)\,, \tag{2.2.40}$$

the complex eigenvectors obtained for $\theta > \theta_c$ do not have the characteristic resonance asymptotical behavior of a purely out-going plane wave. In order to avoid singularity points and to obtain the resonance complex eigenvalues by bound state techniques one can use the exterior-scaling procedure described above, or, as it will be shown here, to translate into the complex coordinate plane, rather than dilate, a transformation of the variable y. The transformation of the variable used by Ginnochio [58],

$$\cos\alpha = \lambda y/[1 + (\lambda^2 - 1)y^2]^{1/2} \tag{2.2.41}$$

reduces the original Schrödinger equation for the Natanzon potential to the Gegenbauer equation,

$$\left[-\frac{d^2}{d\alpha^2} + \left(a + \mu + \frac{1}{2}\right)^2 - \left(\frac{\mu^2 - \frac{1}{4}}{\sin^2\alpha}\right)\right] f(\cos\alpha) = 0\,, \tag{2.2.42}$$

where

$$\begin{aligned} &\mu = (-\varepsilon)^{1/2}/\lambda^2\,, \\ &a = [\tfrac{1}{4} + \mu^2(1 - \lambda^2) + \nu(\nu + 1)]^{1/2} - \mu - \tfrac{1}{2} \end{aligned} \tag{2.2.43}$$

and

$$\psi = \left(\frac{\lambda^2 + (1 - \lambda^2)\cos^2\alpha}{\sin^2\alpha}\right)^{1/4} f(\cos\alpha)\,. \tag{2.2.44}$$

The Gegenbauer function $f(\cos(\alpha))$ is square integrable if the parameter defined in Eq. (2.2.43) gets non-negative integer values.

$$a = 0, 1, 2, \ldots, n\,. \tag{2.2.45}$$

From Eqs. (2.2.43) and (2.2.45) we get

$$E_n = -\lambda^2(v+\tfrac{1}{2})^2 + (\lambda^2-2)(n+\tfrac{1}{2})^2 + (2n+1)[\lambda^2(v+\tfrac{1}{2})^2 + (1-\lambda^2)(n+\tfrac{1}{2})^2]^{1/2}\,, \tag{2.2.46}$$

where

$$n \le n_0 \tag{2.2.47}$$

and n_0 is given by

$$n_0 = \lambda(v+\tfrac{1}{2})/(\lambda^2-2)^{1/2} - \tfrac{1}{2}\,. \tag{2.2.48}$$

This is exactly the algebraic form of the eigenenergies obtained by Ginocchio for bound states. However, following the above analysis, this expression is valid for resonances as well when

$$n > n_0\,. \tag{2.2.49}$$

As was shown by Lipkin and Moiseyev [59], the complex translated (not scaled!) eigenfunction $\psi(\alpha + i\theta)$ is a square integrable function when $n > n_0$.

Consequently, the complex resonance eigenvalues are given by

$$E = -\lambda^2(v+\tfrac{1}{2})^2 + (\lambda^2-2)(n+\tfrac{1}{2})^2 - i(2n+1)|\lambda^2(v+\tfrac{1}{2})^2 + (1-\lambda^2)(n+\tfrac{1}{2})^2|^{1/2}, \quad n > n_0\,. \tag{2.2.50}$$

The same analytical expression for the resonances was obtained also by Ginocchio and by Alhassid et al. [60].

2.3. Restrictions on the complex-scaling parameter

As it was pointed out in Section 1, the resonances are associated with square integrable eigenfunctions of the complex-scaled Hamiltonian, provided the rotational angle θ is larger than a critical value, θ_c, given in Eq. (1.5.11), where the complex-scaling parameter is given by $\exp(i\theta)$. The value of the critical angle depend on the ratio between the resonance width and the resonance position. Here we shall address the question of what are the upper bounds to the rotational angle θ. We shall distinguish between two cases. In the first one the exterior scaling procedure is used to avoid complex scaling of the SHORT range potential. That is,

$$H = -\tfrac{1}{2}\mathrm{d}^2/\mathrm{d}r^2 + V(r) \quad \text{when} \quad r < r_0 \tag{2.3.1}$$

and since $V(r > r_0) = 0$, then

$$H = -\frac{\mathrm{e}^{-2i\theta}}{2}\mathrm{d}^2/\mathrm{d}r^2 \quad \text{when} \quad r > r_0\,. \tag{2.3.2}$$

From Eq. (1.5.9), one can see that the scaled resonance function is square integrable when the exponential factor $\beta = |k_n| \sin(\theta - \phi_n)$ is positive. Consequently,

$$0 < (\theta - \phi_n) < \pi \,. \tag{2.3.3}$$

By substituting $\phi_n = \theta_c$ as defined in Eq. (1.5.11), one immediately sees that

$$\theta_c < \theta < \theta_c + \pi \,. \tag{2.3.4}$$

In the second case the "reaction" coordinate is scaled by a complex factor, $\exp(i\theta)$, over the entire available space. Therefore, the upper limit of the rotational angle θ depends on the analytical properties of the potential.

The upper limit of θ results from the inapplicability of the Balslev–Combes theorem to the bound states (rather than to resonances) when θ exceeds a given value which is potential dependent. Namely, when θ gets beyond a critical value the bound states are not associated with real eigenvalues as they should. Following the work of Moiseyev and Katriel [61] let us consider for example the *bound* class of potentials

$$V(x) = x^{2m} \,, \tag{2.3.5}$$

where

$$m = 1, 2, \ldots \,. \tag{2.3.6}$$

The asymptotic behavior of the eigenfunctions of the Hamiltonian

$$-\tfrac{1}{2}\mathrm{d}^2/\mathrm{d}x^2 + V(x) \tag{2.3.7}$$

can be easily shown to be (note that for large values of $x\,v(x) - E \simeq v(x)$ and $H\psi = 0$).

$$\phi_{\pm}(x) \underset{x\to\infty}{\to} x^{-m/2} \exp[\pm 2^{1/2}(m+1)^{-1} x^{m+1}] \,. \tag{2.3.8}$$

Here ϕ_- are square integrable functions but ϕ_+ are not. Note that the square integrable solutions, ϕ_-, are associated with the discrete bound states, whereas the non-square integrable solutions, ϕ_+, are not associated with resonances (which do not exist in this case) and are known in scattering theory as anti-bound or virtual states. Upon complex scaling, $x \to x\exp(i\theta)$, and the scaled, $\phi_+(x\,e^{i\theta})$ or $\phi_-(x\,e^{i\theta})$, are respectively square integrable when

$$\mathrm{Re}\exp[i(m+1)\theta] = \cos[(m+1)\theta] \tag{2.3.9}$$

is negative or positive. The critical angles, for which $\cos[(m+1)\theta] = 0$ and the eigenfunctions "jump" from one type of boundary condition (e.g. $\phi_+ \to 0$) to another type (e.g. $\phi_- \to 0$) are:

$$\theta_c^{(j)} = \pi/(m+1)(j+\tfrac{1}{2}), \quad j = 0, 1, 2, \ldots \,. \tag{2.3.10}$$

Writing the complex-scaled Hamiltonian in the form

$$\hat{H}(\theta) = e^{-2i\theta}\left[-\frac{1}{2}\frac{\mathrm{d}^2}{\mathrm{d}x^2} + e^{2i\theta(m+1)} x^{2m} \right], \tag{2.3.11}$$

we note that for $\exp[2i\theta(m+1)] = 1$, i.e.

$$\theta \equiv \theta_j = \pi j/(m+1), \quad j = 0, 1, \ldots \tag{2.3.12}$$

exists

$$\hat{H}(\theta_j) = e^{-2i\theta_j}\hat{H}(\theta = 0) \tag{2.3.13}$$

and, therefore,

$$E_n^{(j)} = e^{-[2j\pi/(m+1)]i}E_n(\theta = 0), \quad j = 0, 1, 2, \ldots, \tag{2.3.14}$$

where $E_n^{(j)}$ are the eigenvalues of the complex-scaled BOUND Hamiltonian, (i.e. no continuum spectrum), and $E_n(\theta = 0)$ are the eigenvalues of the unscaled Hamiltonian $H(x)$.

Within the range

$$\theta_c^{(j)} < \theta < \theta_c^{(j+1)}, \tag{2.3.15}$$

the spurious complex energy $E_n^{(j)}$ as given by Eq. (2.3.14) is θ-independent. The changes in the phase occur abruptly at the critical angles $\theta_c^{(j)}$. *The energy spectrum of the bound states remain on the real energy axis only when* $\theta < \theta_c^{(0)}$. Atabeck and Lefebvre [62] numerically observed a similar phenomenon. That is, by rotating the coordinate beyond its critical upper limit, complex eigenvalues of exponential BOUND potential were obtained. This numerical observation can be understood on the basis of the analytical results obtained for the x^n (note that here $n = 2m$ and Eq. (2.3.14) is valid also for odd values of n). The dominant term, m, in the expansion of the exponential potential

$$V(x) = Ae^{+\lambda x} = A\sum_{n=0}^{\infty}(\lambda x)^n/n! \tag{2.3.16}$$

in the vicinity of $x = x_0$

$$\frac{\partial \ln[(\lambda x_0)^n/n!]}{\partial n} \simeq \ln(\lambda x_0) - \ln(n) = 0\,. \tag{2.3.17}$$

That is, for $\lambda = 1$

$$n \simeq x_0\,. \tag{2.3.18}$$

Let x_0 be the classical turning point, determined by

$$V(x_0) = Ae^{\lambda x_0} = E\,. \tag{2.3.19}$$

Consequently, at the classical turning point the exponential can be approximately represented as $V(x) = x^{2m}$; $m = x_0/2$. Using Eqs. (2.3.14) and (2.3.15) for $n = x_0$ and $m = n/2$ we get

$$E_n^{(j)} = e^{-(4j\pi/x_0+1)i}\,E_n(\theta = 0), \quad j = 0, 1, 2, \ldots\,. \tag{2.3.20}$$

and

$$\arctan\left(\frac{\mathrm{Im}\,E_n}{\mathrm{Re}\,E_n}\right) \simeq \frac{4\pi j}{x_0 + 1}, \quad j = 0, 1, 2, \ldots \tag{2.3.21}$$

when x is scaled by a complex factor $\exp(i\theta)$,

$$\pi/(x_0+1)(2j+1) < \theta < \pi/(x_0+1)(2j+2)\,. \tag{2.3.22}$$

Therefore the Balslev–Combes theorem is satisfied (*i.e. bound states are associated with real eigenvalues even when the Hamiltonian is complex scaled*) *only with* $\theta < \pi/(x_0+1)$. A similar analysis for estimating the upper limits of the rotational angle for other analytical given potentials can be carried out.

2.4. The generalized inner product for complex-scaled Hamiltonians

2.4.1. The c-product for time-independent Hamiltonians

The inner product is defined in quantum mechanics as the scalar product, that is,

$$\langle f|g\rangle = \int_{\text{all space}} f^* g \, d\tau \tag{2.4.1}$$

where f, g are functions in the Hilbert space.

When f and g are exponentially divergent functions – as the resonance Siegert eigenfunctions of $\hat{H}$ are – they are NOT in the Hilbert space, and they are NOT in the hermitian domain of $\hat{H}$. By scaling the coordinates in the time-independent Schrödinger equation by a complex factor, the exponentially divergent resonance states become square integrable. However, in spite of the fact that the complex-scaled resonance states are in the generalized Hilbert space, they are not associated with an hermitian operator ($\hat{H}(xe^{i\theta})$ is non-hermitian) and as we shall show in this section the scalar hermitian product given in Eq. (2.4.1) should be replaced by a generalized inner product (the so-called c-product). In the c-product, the complex conjugate of the terms in the function which are complex not as a result of the complex scaling are taken. In the c-product first the complex conjugate of the function is taken and only then the coordinates or the momentum are analytically continued into the complex plan. If, for example, $f^* = \exp(-ikx)$ when k is real, then the complex scaled f^* is given by $\exp(-ike^{+i\theta}x)$. Here $e^{i\theta}$ can be interpreted as the scaling factor of x or (when $\theta < 0$), as the analytically continuation of k into the complex plan such that $(\hbar k e^{i\theta})/(2\mu)$ is the complex resonance energy and $\exp(+ike^{i\theta}x)$ is the exponentially diverged Siegert state. The c-product as it is described below facilitates the discussion of theorems for the complex scaled (non-hermitian) operator $H(\theta)$ which are analogous to those for H, and enables the derivation of the complex-coordinate scattering theory for time-independent and for time-dependent Hamiltonians which are discussed in Section 3. Only when the c-product rather than the metric scalar product is used in the calculation of the spectral representation of the Green operator, a remarkable agreement between the theoretical and experimental non-specular scattering intensities of helium atom scattered from corrugated Cu(115) surface were obtained.

Moiseyev, Certain and Weinhold [63] proposed a c-product *where ONLY the complex conjugate of the terms in the "bra" state, which are complex regardless of the use of the complex scaling, should be taken.* This definition is in the spirit of the usual understanding of analytical continuation. *One does not take the complex conjugate of the terms in the wavefunction which become complex only due to the rotating of the coordinate into the complex plane.* If for example, the eigenfunctions of the unscaled Hamiltonian are real and the COMPLEX eigenfunctions of the complex-scaled

Hamiltonian are expanded in terms of REAL functions, then the inner product is given by

$$\langle\langle f|g\rangle\rangle \equiv (f|g) \equiv \langle f^*|g\rangle = \int_{\text{all space}} fg \, d\tau \, . \tag{2.4.2}$$

For different approaches see "The Letropet Symposium View on a Generalized Inner Product" [64]. In order to get a generalized definition of the inner product that should be used, let us represent the differential time-independent Schrödinger equation as a matrix eigenvalue problem,

$$\boldsymbol{H}\boldsymbol{\psi}_i^{\mathrm{R}} = E_i \boldsymbol{\psi}_i^{\mathrm{R}} \, , \tag{2.4.3}$$

where $\boldsymbol{\psi}^{\mathrm{R}}$ is the vector representation of the "ket" state. Without loss of generality, we assume that H is a symmetry adapted Hamiltonian matrix and the eigenvalue spectrum is non-degenerate. The inner product is required to satisfy the conditions,

$$((\boldsymbol{\psi}_i^{\mathrm{L}})^{\mathrm{t}}|\boldsymbol{\psi}_j^{\mathrm{R}}) = \delta_{ij} \, . \tag{2.4.4}$$

Thus, the set of right and left eigenvectors $\{\boldsymbol{\psi}_i^{\mathrm{R}}, \boldsymbol{\psi}_j^{\mathrm{L}}\}$ forms a complete set of orthonormal functions. The right-hand eigenvectors of $\boldsymbol{H}$ are defined as the "ket" states. In order to define the "bra" states the left-hand eigenvectors of the same $\boldsymbol{H}$ should be calculated:

$$(\boldsymbol{\psi}_j^{\mathrm{L}})^{\mathrm{t}}\boldsymbol{H} = \tilde{E}_j (\boldsymbol{\psi}_j^{\mathrm{L}})^{\mathrm{t}} \, . \tag{2.4.5}$$

By taking the transpose of Eq. (2.4.5), one gets

$$\boldsymbol{H}^{\mathrm{t}}\boldsymbol{\psi}_j^{\mathrm{L}} = \tilde{E}_j \boldsymbol{\psi}_j^{\mathrm{L}} \, . \tag{2.4.6}$$

Since the eigenvalues of $\boldsymbol{H}^{\mathrm{t}}$ are the eigenvalues of H,

$$E_j = \tilde{E}_j \tag{2.4.7}$$

then

$$\boldsymbol{H}^{\mathrm{t}}\boldsymbol{\psi}_j^{\mathrm{L}} = E_j \boldsymbol{\psi}_j^{\mathrm{L}} \, . \tag{2.4.8}$$

From Eq. (2.4.8), one can see that $\boldsymbol{\psi}_j^{\mathrm{L}}$ are the right-hand-side eigenvectors of the transposed of the Hamiltonian matrix $\boldsymbol{H}$. Therefore, the inner product is the product of the eigenvectors of the Hamiltonian matrix, $\boldsymbol{H}$, and the eigenvector of its transpose, $\boldsymbol{H}^{\mathrm{t}}$, associated with the same eigenvalue.

When the Hamiltonian matrix is hermitian

$$\boldsymbol{H}^{\mathrm{t}} = \boldsymbol{H}^* \, . \tag{2.4.9}$$

Consequently,

$$\boldsymbol{\psi}_j^{\mathrm{L}} = (\boldsymbol{\psi}_j^{\mathrm{R}})^* \tag{2.4.10}$$

and the inner product is the ordinary metric scalar product.

When the Hamiltonian matrix is complex and symmetric (for example, when the Hamiltonian becomes complex only upon complex scaling, and real basis functions are used to construct the

Hamiltonian matrix), then

$$\boldsymbol{H}^{\mathrm{t}} = \boldsymbol{H} \tag{2.4.11}$$

and therefore the two column vectors are identical

$$\boldsymbol{\psi}_j^{\mathrm{L}} = \boldsymbol{\psi}_j^{\mathrm{R}} . \tag{2.4.12}$$

In the general case, the Hamiltonian matrix is complex because of the use of complex-scaled coordinate, and because of the use of complex functions as a basis set. In such a case, the right-hand side eigenvectors of the Hamiltonian matrix and of its transposed should be calculated. *If ALL the right-hand side eigenvectors of H are known, then the left-hand side eigenvectors* (*i.e. eigenvector matrix of the transposed Hamiltonian*) *are obtained by calculating the transpose of the inverse of the eigenvector matrix of H*,

$$(\boldsymbol{\psi}_1^{\mathrm{L}}, \boldsymbol{\psi}_2^{\mathrm{L}}, \dots) = [(\boldsymbol{\psi}_1^{\mathrm{R}}, \boldsymbol{\psi}_2^{\mathrm{R}}, \dots)^{-1}]^{\mathrm{t}} . \tag{2.4.13}$$

A complex basis function is a natural choice, for example, when the energies and lifetimes of three atomic molecules are calculated. To conserve the total angular momentum J, and its projection M along the laboratory z-axis, the eigenfunction of the complex-scaled Hamiltonian are expanded in terms of the $y_{j,\ell}^{J,M}$ basis functions, given by

$$\mathscr{Y}_{j,\ell}^{J,M}(\gamma) = \sum_{m_\ell=-\ell}^{\ell} \sum_{m_j=-j}^{j} (\ell j m_\ell m_j | \ell j J M) Y_{j,m_j}(\hat{\mathrm{R}}) Y_{\ell,m_\ell}(\hat{\mathrm{r}}) \tag{2.4.14}$$

when $J = M = 0$ then $\ell = j$ and

$$\mathscr{Y}_{j,\ell}^{J,M} = Y_{j,0}(\cos\gamma) \tag{2.4.15}$$

and $\cos\gamma = \hat{R}\cdot\hat{r}$ where R and r are, respectively, defined as the distance from the dissociative atom C to the center of mass of the diatom AB and the internuclear distance of the diatom AB; $(\ell\, j\, m_\ell\, m_j | \ell\, j\, J\, M)$ are the Clebsh–Gordon coefficients and $Y_{j,0}$ is the spherical harmonic. When real basis functions $\varphi_n(R)$ and $\chi_m(r)$ are used, the Hamiltonian matrix elements given by

$$[\boldsymbol{H}(\theta)]_{(n',\,m',\,j',\,\ell'),\,(n,\,m,\,j,\,\ell)} = \langle \varphi_{n'}\chi_{m'}\mathscr{Y}_{j'\ell'}^{JM} | \hat{H}(\mathrm{R}e^{\mathrm{i}\theta}, r, \gamma) | \varphi_n\chi_m\mathscr{Y}_{j,\ell}^{JM} \rangle \tag{2.4.16}$$

are complex even for the case where $\theta = 0$ (i.e. no rotation of the coordinates to the complex plane) and $J \neq 0$. Here the basis functions are defined as

$$\langle \phi_k(\hat{r}, \hat{R}) \equiv |\varphi_n\chi_m\mathscr{Y}_{j,\ell}^{JM}\rangle \tag{2.4.17}$$

when the index k stands for the collective indices $\{n, m, j, \ell\}$. The complex-scaled square-integrable eigenfunctions of $\boldsymbol{H}(\theta)$ are orthonormal,

$$\langle\!\langle \psi_j^{\mathrm{L}} | \psi_i^{\mathrm{R}} \rangle\!\rangle \equiv (\psi_j^{\mathrm{L}} | \psi_i^{\mathrm{R}}) = e^{\mathrm{i}\theta} \int_{\text{all space}} \psi_j^{\mathrm{L}} \psi_i^{\mathrm{R}}\, \mathrm{d}\tau = \delta_{ij} \tag{2.4.18}$$

when ψ_i^{R} is given by

$$\psi_i^{\mathrm{R}} = \sum_k (\boldsymbol{C})_{k,i} \phi_k(\hat{R}, \hat{r}) \tag{2.4.19}$$

and ψ_j^{L} is given by

$$\psi_j^{\mathrm{L}} = \sum_k (\boldsymbol{C}^{-1})_{k,j}^{\mathrm{t}} \phi_k^*(\hat{R}, \hat{r}) , \tag{2.4.20}$$

where $\boldsymbol{C}$ is the eigenvector matrix of the complex-scaled Hamiltonian matrix $H(\theta)$.

A knowledge of the eigenfunctions of the complex-scaled Hamiltonian enables us to calculate the uncertainty in measuring different dynamical quantities. The COMPLEX expectation value of a given quantity is given by expressions bi-linear in ψ^{R} and ψ^{L},

$$\langle\!\langle \psi^{\mathrm{L}}|\hat{O}(\theta)|\psi^{\mathrm{R}} \rangle\!\rangle \equiv (\psi^{\mathrm{L}}|\hat{O}(\theta)|\psi^{\mathrm{R}}) = \frac{\int_{\text{all space}} \psi^{\mathrm{L}}\hat{O}(\theta)\psi^{\mathrm{R}}\,\mathrm{d}\tau}{\int_{\text{all space}}\psi^{\mathrm{L}}\psi^{\mathrm{R}}\,\mathrm{d}\tau} , \tag{2.4.21}$$

where $\hat{O}$ is the COMPLEX-scaled operator associated with the measured dynamical quantity. If $\hat{O}$ is, for example, the complex-scaled Hamiltonian, $H(\theta)$, the expectation value is a complex number, $E = \varepsilon - (\mathrm{i}/2)\Gamma$. The real part of E, ε, is the average measured energy of the system in its metastable state, whereas the imaginary part, Γ is the uncertainty of ε, even when the standard deviation of $H(\theta)$ is zero (i.e. $\langle\!\langle H(\theta)^2 \rangle\!\rangle - \langle\!\langle H(\theta) \rangle\!\rangle^2 = 0$). Similarly, the imaginary part of $(\psi^{\mathrm{L}}|\hat{O}(\theta)|\psi^{\mathrm{R}})$ can be interpreted as the uncertainty of measuring the quantity of $\hat{O}$ when the system is prepared in a resonance (i.e. metastable) state.

2.4.2. The c-product for time periodic Hamiltonians

The interaction of atoms and molecules in CW lasers is described by time-periodic Hamiltonians. However, even in short pulse experiments the time periodic behavior of the Hamiltonian may be assumed when the field oscillates more than 50–100 times during the pulse "lifetime" [65].

When the Hamiltonian is time periodic

$$\hat{H}(x,t) = \hat{H}(x, t+T) , \tag{2.4.22}$$

the solutions of the complex-scaled time-dependent Schrödinger equation

$$\hat{H}(x\mathrm{e}^{\mathrm{i}\theta}, t)\psi_\theta(x,t) = \mathrm{i}\hbar\frac{\partial\psi_\theta(x,t)}{\partial t} \tag{2.4.23}$$

for a given initial state $\psi_\theta(x,0)$ can be described as a linear combination of the quasi-energy solutions (known also as the Floquet states). The quasi-energy complex-scaled states are given by

$$\begin{aligned} &\psi_\theta(x,t) \equiv \psi_\alpha^{\mathrm{QE}}(x,t) , \\ &\psi_\alpha^{\mathrm{QE}}(x,t) = \mathrm{e}^{-\mathrm{i}E_\alpha t/\hbar}\phi_\alpha^\theta(x,t) , \end{aligned} \tag{2.4.24}$$

where

$$\phi_\alpha^\theta(x,t) = \phi_\alpha^\theta(x, t+T) \tag{2.4.25}$$

(when box normalization is used then the spectrum is discrete and $\alpha = 1, 2, \ldots$). For dissociative/ionizing systems the quasi-energies get complex values and the resonance quasi-energies, E_α, are θ-independent:

$$E_\alpha = \varepsilon_\alpha - (\mathrm{i}/2)\Gamma_\alpha . \tag{2.4.26}$$

The periodic functions, ϕ_α^θ, and the quasi-energies, E_α, are respectively defined as the eigenfunctions and eigenvalues of the complex-scaled Floquet operator,

$$\hat{\mathscr{H}}_\theta \phi_\alpha^\theta = E_\alpha \phi_\alpha^\theta , \tag{2.4.27}$$

where

$$\hat{\mathscr{H}}_\theta = -\mathrm{i}\hbar\frac{\partial}{\partial t} + \hat{H}(x\mathrm{e}^{\mathrm{i}\theta}, t) . \tag{2.4.28}$$

The complex-scaled time periodic eigenfunctions ϕ_α^θ can be expanded in a Fourier basis set,

$$\phi_\alpha^\theta(x,t) = \sum_{n=-\infty}^{\infty} \varphi_{n,\alpha}^\theta(x)\mathrm{e}^{\mathrm{i}\omega n t} \tag{2.4.29}$$

where $\omega = 2\pi/T$ and $\varphi_{n,\alpha}^\theta$ are the components of *the right* eigenvectors of the Floquet Hamiltonian matrix [66,128],

$$\mathscr{H}^\theta(x)\boldsymbol{\varphi}_\alpha^\theta(x) = E_\alpha \boldsymbol{\varphi}_\alpha^\theta(x) \tag{2.4.30}$$

and

$$\begin{aligned}[\mathscr{H}^\theta(x)]_{n',n} &= \frac{1}{T}\int_0^T \mathrm{e}^{-\mathrm{i}wn't}\left(-\mathrm{i}\hbar\frac{\partial}{\partial t} + H(x\mathrm{e}^{\mathrm{i}\theta}, t)\right)\mathrm{e}^{\mathrm{i}wnt}\,\mathrm{d}t \\ &= \frac{1}{T}\int_0^T \hat{H}(x\mathrm{e}^{\mathrm{i}\theta}, t)\mathrm{e}^{\mathrm{i}w(n-n')t}\,\mathrm{d}t + \hbar\omega\delta_{n,n'} .\end{aligned} \tag{2.4.31}$$

The time-dependent inner product should satisfy the following condition:

$$\begin{aligned}\langle\!\langle \psi_{\alpha'}^{\mathrm{L}}(QE)|\psi_\alpha^{\mathrm{R}}(QE)\rangle\!\rangle &\equiv (\psi_{\alpha'}^{\mathrm{L}}(QE)|\psi_\alpha^{\mathrm{R}}(QE)) \\ &= \frac{1}{T}\int_0^T \mathrm{d}t \int_{\text{all space}} \mathrm{d}x \psi_{\alpha'}^{\mathrm{L,\,QE}}(x\mathrm{e}^{\mathrm{i}\theta}, t)\cdot\psi_\alpha^{\mathrm{R,\,QE}}(x\mathrm{e}^{\mathrm{i}\theta}, t) = \delta_{\alpha,\alpha'}\end{aligned} \tag{2.4.32}$$

Therefore (see Eqs. (2.4.24) and (2.4.29)), the right-hand quasi-energy state is given by

$$\psi_\alpha^{\mathrm{R,\,QE}} \equiv \mathrm{e}^{-\mathrm{i}E_\alpha t/\hbar}\sum_{n=-\infty}^{\infty}\varphi_{n,\alpha}^\theta(x)\mathrm{e}^{+\mathrm{i}wnt}, \quad \alpha = 1,2,\ldots , \tag{2.4.33}$$

whereas the left-hand quasi-energy state is given by

$$\psi_{\alpha'}^{\mathrm{L,\,QE}} = \mathrm{e}^{+\mathrm{i}E_{\alpha'}t/\hbar}\sum_{n=-\infty}^{\infty}\varphi_{n,\alpha'}^{\theta,\mathrm{L}}(x)\mathrm{e}^{-\mathrm{i}wnt}, \quad \alpha' = 1,2,\ldots , \tag{2.4.34}$$

where $\varphi_{n,\alpha}^{\theta,\mathrm{L}}$ are the components of the left eigenvectors of $\mathscr{H}^\theta(x)$. It should be stressed here that one should NOT take the complex conjugate of the complex quasi-energies E_α. Only when real basis functions, $\{\chi_i(x),\ i = 1,\ldots,N\}$ are used to diagonalize the Floquet Hamiltonian matrix $\mathscr{H}^\theta(x)$ and the Hamiltonian has a time reversal symmetry, then $\varphi_{n,\alpha}^{\theta,\mathrm{L}} = \varphi_{n,\alpha}^{\theta}$. The $\varphi_{n,\alpha}^\theta(x)$ functions

(components of the vector $\boldsymbol{\varphi}^{\theta}_{\alpha}$), which are used in Eq. (2.4.33), are given by

$$\varphi^{\theta}_{n,\alpha}(x) = \sum_i C^{\mathrm{R}}_{(n,i),\alpha}(\theta)\chi_i(x)\,, \tag{2.4.35}$$

where $C^{\mathrm{R}}_{(n,i),\alpha}$ are the components of the right eigenvectors of $\mathscr{H}^{\theta}$,

$$\mathscr{H}^{\theta}\boldsymbol{C}^{\mathrm{R}}_{\alpha}(\theta) = E_{\alpha}\boldsymbol{C}^{\mathrm{R}}_{\alpha}(\theta)\,, \tag{2.4.36}$$

where

$$(\mathscr{H})^{\theta}_{k',k} = \int_{\text{all space}} \mathrm{d}\tau\chi^{*}_{i'}(x)[\hat{\mathscr{H}}(x\mathrm{e}^{\mathrm{i}\theta})]_{n',n}\chi_i(x)\,. \tag{2.4.37}$$

The row and column indices, k and k', are associated, respectively, with (n,i) and (n',i'). n defines the nth Fourier basis function and i defines the ith complex basis function $\chi_i(x)$. The $\varphi^{\theta}_{n,\alpha'}(x)$ functions which are used in Eq. (2.4.34) are given by

$$\varphi^{\theta}_{n,\alpha'}(\alpha) = \sum_i C^{\mathrm{L}}_{(n,i),\alpha}(\theta)\chi^{*}_i(x)\,, \tag{2.4.38}$$

where $\{C^{\mathrm{L}}_{(n,i),\alpha}\}$ are the components of the left eigenvectors of $\mathscr{H}^{\theta}$ (as defined in Eq. (2.4.37))

$$(\mathscr{H}^{\theta})^{\mathrm{t}}\boldsymbol{C}^{\mathrm{L}}_{\alpha'}(\theta) = E_{\alpha'}\boldsymbol{C}^{\mathrm{L}}_{\alpha'}(\theta)\,. \tag{2.4.39}$$

For example, in the study of multiphoton processes in time-dependent ionizing/dissociative systems, the use of the inner product as defined in Eqs. (2.4.33), (2.4.34), (2.4.35), (2.4.36), (2.4.37), (2.4.38) and (2.4.39) is the key point in the evaluation of accurate time-independent expressions for the probability to obtain high harmonics [65]. The probability to obtain high harmonics, i.e. radiation with the frequency $\Omega = kw$, is associated with the Fourier transform of the time-dependent dipole moment [67],

$$\sigma(\Omega) \propto \left|\frac{1}{T}\int_0^T \mathrm{e}^{-\mathrm{i}\Omega t}D(t)\,\mathrm{d}t\right|^2. \tag{2.4.40}$$

When the system is "trapped" in a long lived resonance quasi-energy state

$$\psi^{\theta}_{\mathrm{res}} = \mathrm{e}^{-\mathrm{i}E_{\mathrm{res}}t/\hbar}\phi^{\theta}_{\mathrm{res}}(x,t) \tag{2.4.41}$$

and

$$E_{\mathrm{res}} = \varepsilon_{\mathrm{res}} - (i/2)\Gamma_{\mathrm{res}}\,.$$

The complex expectation value of the dipole moment is given by

$$D(t) = \frac{1}{T}\int_0^T \mathrm{d}t\int_{\text{all space}} \psi^{\mathrm{L},\theta}_{\mathrm{res}}(x,t)x\mathrm{e}^{\mathrm{i}\theta}\psi^{\mathrm{R},\theta}_{\mathrm{res}}(x,t)\,\mathrm{d}x\,, \tag{2.4.42}$$

where

$$\frac{1}{T}\int_0^T \mathrm{d}t\int_{\text{all space}} \mathrm{d}x\psi^{\mathrm{L},\theta}_{\mathrm{res}}(x,t)\psi^{\mathrm{R},\theta}_{\mathrm{res}}(x,t) = 1 \tag{2.4.43}$$

Using the c-product as defined above in Eqs. (2.4.33) and (2.4.34) Ben-Tal et al. [65] derived the time-independent expression for the probability of obtaining radiation with the frequency Ω,

$$\sigma(\Omega = kw) = \left| \sum_{n=-\infty}^{\infty} \int \varphi^{\theta,\mathrm{L}}_{n+k,\,\mathrm{res}}(x) x \varphi^{\theta}_{k,\,\mathrm{res}}(x)\,\mathrm{d}x \right|^2 \tag{2.4.44}$$

where $\varphi^{\theta}_{n+k,\,\mathrm{res}}(x)$ and $\varphi^{\theta}_{k,\,\mathrm{res}}(x)$ are the Fourier components of $\phi^{\theta}_{\mathrm{res}}(x,t)$ as defined in Eqs. (2.4.41) and (2.4.38).

2.4.3. The c-product for a general time-dependent Hamiltonian

The solution of the complex-scaled time-dependent Schrödinger equation for *any* time-dependent Hamiltonian (not necessarily a time periodic one) can be obtained as [68]

$$\psi_\theta(x,t) = \psi_\theta(x,t',t)|_{t'=t}\,, \tag{2.4.45}$$

where

$$\psi_\theta(x,t',t) = \mathrm{e}^{-\mathrm{i}/\hbar\,\hat{\mathscr{H}}(\mathrm{e}^{\mathrm{i}\theta}x,\,t')(t-t_0)}\psi_\theta(x,t',t_0) \tag{2.4.46}$$

and

$$\psi_\theta(x,t_0,t_0) \equiv \psi(x\mathrm{e}^{\mathrm{i}\theta},t_0) \tag{2.4.47}$$

is the initial given state, and $\hat{\mathscr{H}}(x\mathrm{e}^{\mathrm{i}\theta},t')$ and $\hat{\mathscr{H}}^{\mathrm{L}}(x\mathrm{e}^{\mathrm{i}\theta},t')$ are the right and left Floquet-type operators

$$\hat{\mathscr{H}}(x\mathrm{e}^{\mathrm{i}\theta},t') = \hat{H}(x\mathrm{e}^{\mathrm{i}\theta},t') - \mathrm{i}\hbar\,\partial/\partial t'\,, \qquad \hat{\mathscr{H}}^{\mathrm{L}}(x\mathrm{e}^{\mathrm{i}\theta} + \mathrm{i}\hbar\,\partial/\partial t') \tag{2.4.48}$$

The time variable t' acts as an additional coordinate in a generalized Hilbert space introduced by Howland [69,70]. This space contains all possible square integrable functions of x and t', where box normalization is used for x and for $t'\,(0 < t' < T)$.

The eigenfunctions of $\mathscr{H}(x\mathrm{e}^{\mathrm{i}\theta},t)$ forms a complete set for the generalized Hilbert space (see the discussion in Section 2.4.4). The inner product in the generalized Hilbert space is defined as

$$\langle\!\langle \phi_i|\phi_j \rangle\!\rangle \equiv (\phi_i|\phi_j) = \frac{1}{T}\int_0^T \mathrm{d}t' \int_{\text{all space}} \mathrm{d}x \phi^{\mathrm{L}}_i(x\mathrm{e}^{\mathrm{i}\theta},t')\phi^{\mathrm{R}}_j(x\mathrm{e}^{\mathrm{i}\theta},t') = \delta_{ij}\,, \tag{2.4.49}$$

where

$$\begin{aligned} &\hat{\mathscr{H}}(x\mathrm{e}^{\mathrm{i}\theta},t')\phi^{\mathrm{R}}_j(\mathrm{e}^{\mathrm{i}\theta}x,t') = E^{\theta}_j\phi^{\mathrm{R}}_j(\mathrm{e}^{\mathrm{i}\theta}x,t')\,,\\ &\hat{\mathscr{H}}^{\mathrm{L}}(x\mathrm{e}^{\mathrm{i}\theta},\,t')\phi^{\mathrm{L}}_i(\mathrm{e}^{\mathrm{i}\theta}x,t') = E^{\theta}_i\phi^{\mathrm{L}}_i(\mathrm{e}^{\mathrm{i}\theta}x,t')\,. \end{aligned} \tag{2.4.50}$$

Assuming that the eigenfunctions of the complex-scaled Floquet Hamiltonian form a complete set, the unit operator is given by

$$\sum_j |\phi^{\mathrm{R}}_j\rangle\!\rangle\langle\!\langle \phi^{\mathrm{L}}_j| = \hat{1}\,. \tag{2.4.51}$$

By substituting Eq. (2.4.51) into Eq. (2.4.46), one gets that the solution of the time-dependent Hamiltonian (which describes ionizing or dissociative systems) for the initial state $\psi(x,t_0)$ is given by

$$\psi_\theta(x,t) = \sum_j \mathrm{e}^{-\mathrm{i}E^{\theta}_j t}\langle\!\langle \phi^{\mathrm{L}}_j|\psi(t_0)\rangle\!\rangle\phi^{\mathrm{R}}_j(x\mathrm{e}^{\mathrm{i}\theta},t)\,, \tag{2.4.52}$$

where

$$\langle\langle \phi_j^{\mathrm{L}} | \psi(t_0) \rangle\rangle = \frac{1}{T}\int_0^T \mathrm{d}t' \int_{\text{all space}} \mathrm{d}x \phi_j^{\mathrm{L}}(x\mathrm{e}^{\mathrm{i}\theta}, t')\psi(x\mathrm{e}^{\mathrm{i}\theta}, t_0)\,. \tag{2.4.53}$$

When complex basis functions $\chi_i(x)$ and Fourier basis set, $\exp(2\pi t\mathrm{i}/T)$, are used to diagonalize $\mathscr{H}(x\mathrm{e}^{\mathrm{i}\theta}, \pm t')$ then ϕ_j^{L} and ϕ_j^{R} are calculated as described in Eqs. (2.4.29), (2.4.35), (2.4.36), (2.4.37), (2.4.38) and (2.4.39).

Two cases may be considered. In the first case, the Hamiltonians are NOT time periodic. In such a case box normalization for x and t' implies that $\psi(x\mathrm{e}^{\mathrm{i}\theta}, t', t)$ is a square integrable function of x and t'. Long time (i.e. t) propagation requires the use of a large box (i.e. T should get sufficient large value). In the second case time periodic boundary conditions are required although the Hamiltonians are NOT time periodic,

$$\psi(x\mathrm{e}^{\mathrm{i}\theta}, t', t) = \psi(x\mathrm{e}^{\mathrm{i}\theta}, t' + T, t)\,,$$

where

$$0 \le t' \le T\,.$$

The physical solution is obtained when

$$t' = t \bmod T\,.$$

Solving the complex-scaled time-dependent Schrödinger equation for time-dependent Hamiltonians by the (t, t') method enables the evaluation of time-independent state-to-state transition probabilities, and the calculation of the time evolution operator as for time-independent Hamiltonians (provided the propagated wave packet remains square integrable for $t \le T$ for ionizing/dissociative systems [55]).

2.4.4. The turn-over rule

If $\hat{H}(\theta = 0)$ is a real and self-adjoint operator, then the complex-scaled Hamiltonian is given by

$$\hat{H}_\theta = \hat{S}^{-1}(\theta)\hat{H}\hat{S}(\theta) \tag{2.4.54}$$

and obeys

$$\hat{H}_\theta^+ = \hat{H}_\theta^*\,. \tag{2.4.55}$$

If f and g are two complex square integrable basis functions (regardless of the fact that $\theta \neq 0$) then,

$$\langle f|\hat{H}_\theta g\rangle = \langle H_\theta^+ f|g\rangle = \langle \hat{H}_\theta^* f|g\rangle = \langle g^*|\hat{H}_\theta f^*\rangle\,. \tag{2.4.56}$$

However, if f and g are complex functions ONLY due to the fact that $\theta \neq 0$ as we shall discuss below (see Section 2.4.1 on the c-product)

$$(f|\hat{H}_\theta g) = \langle f^*|\hat{H}_\theta g\rangle = \langle(\hat{H}_\theta^+ f^*)|g\rangle = \langle(\hat{H}_\theta^* f^*)|g\rangle = (\hat{H}_\theta f|g)\,. \tag{2.4.57}$$

Therefore, $\hat{H}_\theta$ is symmetric and satisfies the turn over rule with respect to the complex product

$$(f|H_\theta g) = (H_\theta f|g) = (g|H_\theta f)\,. \tag{2.4.58}$$

2.5. Do the eigenfunctions of the complex-scaled Hamiltonian matrix form a complete basis set?

On the basis of Motzkin and Taussky results [71], Moiseyev and Friedland [72] proved that for very special values of the complex-scaling parameter, $\eta = \exp(\mathrm{i}\theta)$, (where θ may get complex values) an incomplete spectrum of N-dimensional Hamiltonian matrix is obtained. The spectrum is incomplete in the sense that the eigenfunctions of the complex-scaled Hamiltonian matrix do not form a complete basis set and the number of non-linear independent eigenvectors of the non-hermitian matrix is smaller than N. Note, however, that any infinitesimally small variation in θ will make the spectrum to be a complete one.

Within the framework of the finite basis set approximation the time-independent Schrödinger equation is given by

$$\boldsymbol{H}(\theta)\boldsymbol{\psi}_i^{\mathrm{R}} = E_i\boldsymbol{\psi}_i^{\mathrm{R}} \quad \text{and} \quad \boldsymbol{H}^{\mathrm{t}}(\theta)\boldsymbol{\psi}_i^{\mathrm{L}} = E_i\boldsymbol{\psi}_i^{\mathrm{L}}\,, \tag{2.5.1}$$

where the complex-scaled Hamiltonian matrix is given by

$$(\boldsymbol{H}(\theta))_{ij} = \langle\chi_i|\hat{H}(x\mathrm{e}^{\mathrm{i}\theta})|\chi_j\rangle, \quad (i,j) = 1,2,\ldots,N \tag{2.5.2}$$

and $\{\langle\chi_i\rangle\}$ are square integrable basis functions. In Section 2.4 we assumed that the eigenfunction of $\boldsymbol{H}(\theta)$ forms a complete set. That is, there are N normalizeable independent eigenvectors

$$(\boldsymbol{\psi}_i^{\mathrm{L}}|\boldsymbol{\psi}_j^{\mathrm{R}}) = \delta_{ij}, \quad (i,j) = 1,2,\ldots,N\,. \tag{2.5.3}$$

Since the complex-scaled Hamiltonian matrix is not hermitian and

$$H_{ij}(\theta) \neq H_{ji}^{*}(\theta) \tag{2.5.4}$$

it may happen that the $N \times N$ Hamiltonian matrix $\boldsymbol{H}(\theta)$ has $N-1$ or even less linear independent eige$^{<}$nvectors for special values of θ. In such a case the eigenvectors of $\boldsymbol{H}(\theta)$ do NOT form a complete set for the N-dimensional vectors. For example [72], the complex symmetric 3×3 matrix

$$\boldsymbol{H}(\theta) = \begin{pmatrix} 6 & e^{\mathrm{i}\theta} & -1 \\ \mathrm{e}^{\mathrm{i}\theta} & 5 & 2\mathrm{e}^{i\theta} \\ -1 & 2\mathrm{e}^{\mathrm{i}\theta} & 1 \end{pmatrix} \tag{2.5.5}$$

has only two distinct eigenvectors when $\theta = \pi/2$,

$$E_1 = 6, \quad \boldsymbol{\psi}_1^{\mathrm{R}} = \boldsymbol{\psi}_1^{\mathrm{L}} = \begin{pmatrix} 1 \\ \mathrm{i}/3 \\ -1/3 \end{pmatrix}, \tag{2.5.6}$$

$$E_2 = 3, \quad \boldsymbol{\psi}_2^{\mathrm{L}} = \boldsymbol{\psi}_2^{\mathrm{R}} = \begin{pmatrix} 0 \\ 1 \\ \mathrm{i} \end{pmatrix}. \tag{2.5.7}$$

It should be stressed here that although the 3×3 matrix given in Eq. (2.5.5) has only 2 eigenvalues there is no degeneracies in the spectrum. Degeneracy implies two non-linear-dependent eigenvectors which are associated either with $E = 3$ or with $E = 6$. As one can see from Eq. (2.5.6) and

Eq. (2.5.7) there are no such degenerated states. Since the matrix is complex and symmetric we use here the c-product rather than the usual scalar product.

The fact that for $\theta = \pi/2$ the spectrum of $\boldsymbol{H}(\theta)$ is incomplete is reflected in the fact that the second eigenvector $\boldsymbol{\psi}_2$ is not c-normalizable and

$$(\boldsymbol{\psi}_2^{\mathrm{L}}|\boldsymbol{\psi}_2^{\mathrm{R}}) = 0 \tag{2.5.8}$$

$\boldsymbol{\psi}_2$ and E_2 are considered, respectively, as a defective eigenvector and eigenvalue of the matrix $\boldsymbol{H}$. In such a case E_2 is NOT a simple pole of the resolvent $(\boldsymbol{H} - E\boldsymbol{1})^{-1}$. A defective eigenvalue and eigenvector is obtained at a branch point $\theta_b = \pi/2$, where

$$E_2 \to E_3 \tag{2.5.9}$$

and $\boldsymbol{\psi}_2$ and $\boldsymbol{\psi}_3$ are coalesced,

$$\boldsymbol{\psi}_2 \to \boldsymbol{\psi}_3 \tag{2.5.10}$$

as

$$\theta \to \theta_{\mathrm{b}}\,. \tag{2.5.11}$$

We can summarize it by saying that the eigenvalues $E_i(\theta)$ are analytical in θ except for a finite number of complex values of the rotational angle $\theta_{\mathrm{b}} = \theta_1, \ldots, \theta_q$, which are the branch points for some eigenvalues. Therefore, some $E_i(\theta)$ do not have a Taylor expansion in $\eta = \exp(\mathrm{i}\theta)$ around the branch points $\eta_b = \exp(\mathrm{i}\theta_{\mathrm{b}})$. However, $E_i(\theta)$ does have an expansion in $(\eta - \eta_{\mathrm{b}})^{1/p}$ (known as Puiseux series):

$$E_i(\theta) = \sum_{k=0}^{\infty} a_{ik}(\eta - \eta_{\mathrm{b}})^{k/p} + E_i(\theta_{\mathrm{b}})\,. \tag{2.5.12}$$

Here $N \geq p \geq 2$ is an integer which implies the coalescence of p eigenvectors of $\boldsymbol{H}$ as $\theta \to \theta_{\mathrm{b}}$. Usually, θ_{b} gets complex value and, consequently, the absolute value of the complex scaling factor $\eta = \exp(\mathrm{i}\theta)$ is not equal to unity, i.e. $|\eta| \neq 1$. For a computational method to calculate the branch points θ_{b} for complex-scaled Hamiltonian matrices see Moiseyev and Certain in Ref. [73]. In Fig. 15 the complex eigenvalues of a finite Hamiltonian matrix for ^1S resonance of Helium as a function of the complex-scaling parameter η are presented [72], showing a branch point in the complex "energy" plane at $|\eta_{\mathrm{b}}| = 1.0837$, $\cos|\theta_{\mathrm{b}}| = -0.996432$.

2.6. The complex analog to the variational principle: The c-variational principle

The complex analog to the variational principle provides the *formal justification to the use of computational techniques that originally were developed for bound states* in the calculation of the resonance position and widths by the complex coordinate method.

As discussed in Section 2.6 one can assume that the eigenfunctions of $\hat{H}(\theta)$ form a complete c-normalizable (see Section 2.4) set. In such a case it is easy to verify that the Rayleigh quotient

$$\bar{E}^{\theta} = (\phi|\hat{H}_{\theta}|\phi)/(\phi|\phi) \tag{2.6.1}$$

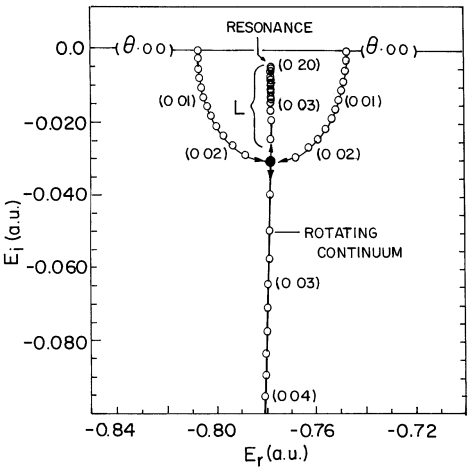

Fig. 15. 0-trajectory energy spectrum of the complex scaled Hamiltonian of helium which was calculated with 36 Hylleeraas-type basis functions. The black dot denotes the branch point in which the spectrum of the 36×36 Hamiltonian matrix is incomplete.

provides a stationary approximation to the true complex eigenvalue E_k^θ when ϕ is a c-normalizable (i.e. $(\phi|\phi) = 1$) approximation that is close to the eigenfunction of $\hat{H}_\theta$, ψ_k; that is,

$$\phi = \psi_k + \eth(\varepsilon) \quad \text{implies} \quad E^\theta = E_k^\theta + \eth(\varepsilon^2)\,. \tag{2.6.2}$$

This complex variational principle [63] is, however, a stationary principle rather than an upper or lower bound for either the real or imaginary part of the complex eigenvalue. As noted above, even this stationary property fails if the eigenfunctions are not c-normalizable (i.e. c-normalization implies that $(\psi_k|\psi_k) \neq 0$ for any value of k).

Linear c-variational calculations. Let us expand the trial functions ϕ by N orthonormal basis functions, $\{\chi_i, i = 1, \ldots, N\}$; that is,

$$\begin{aligned} |\phi\rangle &= \sum_{j=1}^{N} C_j^{\mathrm{R}} \chi_j\,, \\ \langle\phi| &= \sum_{i=1}^{N} C_i^{\mathrm{L}} \chi_i\,. \end{aligned} \tag{2.6.3}$$

By substituting Eq. (2.6.3) into Eq. (2.6.1), one obtains

$$\sum_{i,\,j} C_i^{\mathrm{L}} C_j^{\mathrm{R}} (H_{ij}(\theta) - \bar{E}\delta_{ij}) = 0\,, \tag{2.6.4}$$

where

$$H_{ij}(\theta) = \langle\chi_i|\hat{H}_\theta|\chi_j\rangle\,. \tag{2.6.5}$$

On the basis of the c-variational principle given in Eqs. (2.6.1) and (2.6.2) and proved by Moiseyev et al. [63], we require that

$$\partial\bar{E}/\partial C_i^{\mathrm{L}} = 0 \quad \text{for } i = 1, 2, \ldots, N \,. \tag{2.6.6}$$

Consequently,

$$\sum_{j=1}^{N} C_j^{\mathrm{R}}(H_{ij}(\theta) - \bar{E}\delta_{ij}) = 0 \tag{2.6.7}$$

or

$$\boldsymbol{H}(\theta)\boldsymbol{C}^{\mathrm{R}} = \bar{E}\boldsymbol{C}^{\mathrm{R}} \,. \tag{2.6.8}$$

Here we proved that the solutions of the matrix eigenvalue problem are stationary solutions in the complex variational space, and as $N \to \infty$ the exact solution of the time-independent complex-scaled Schrödinger equation would be obtained. This theorem is the ground for the c-variational calculations by which the autoionization, predissociation and other type resonance positions and widths (inverse lifetimes) were obtained. For the generalized variational theorem (not necessarily linear variational space) see Moiseyev in Ref. [74].

2.7. The complex analog to the hypervirial theorem

From the turn-over rule Eq. (2.5.5) for the complex-scaled Hamiltonian, it follows immediately that commutators of $\hat{H}_\theta$ and any given operator $\hat{\Lambda}$ have vanishing c-expectation values in any eigenstate ψ_k,

$$(\psi_k|[\hat{H}_\theta, \hat{\Lambda}]\psi_k) = 0 \,. \tag{2.7.1}$$

This complex analog to the hypervirial theorem [63] holds for a wide class of operators $\hat{\Lambda}$, whether hermitian or not.

In particular, if $\hat{\Lambda}$ is chosen to be $\boldsymbol{r}\cdot\boldsymbol{V}$ (or a sum of such terms in a many-particle system), and if the potential V is a homogeneous function of coordinates of degree m, Eq. (2.7.1) reduces to the complex *virial theorem* ($\hat{K}_\theta$ is the kinetic energy operator)

$$(\psi_k||T_\theta|\psi_k) = (m/2)(\psi_k|\hat{V}_\theta|\psi_k) \tag{2.7.2}$$

relating the (complex) kinetic and potential "energies". For example, when atomic autoionizing resonances are studied then $m = 1$[40]. For alternative proofs of the complex analog to the virial theorem see Froelich and Brandas [75], Wingler and Yarris [76], and Moiseyev [77].

2.8. Cusps, θ trajectories and complex-analog Hellmann–Feynman theorem

The Hellmann–Feynman theorem [78] can be extended to the complex-scaled non-hermitian Hamiltonians [63]. Suppose Φ depends on a variational parameter C_i (e.g. $\boldsymbol{C}$ can be taken as the linear variational parameters as described in Section 2.6). Variationally optimal values of these parameters must satisfy the relation

$$\partial\bar{E}/\partial C_i = 0, \quad i = 1, 2, \ldots, N \,, \tag{2.8.1}$$

where

$$\bar{E} = \frac{(\phi|\hat{H}_\theta|\phi)}{(\phi|\phi)} \tag{2.8.2}$$

and H_θ contains an embedded parameter ζ,

$$H_\theta = H_\theta(\zeta)\,. \tag{2.8.3}$$

For example, ζ can be the scaling factor, $\eta = \exp(\mathrm{i}\theta)$, or a physical parameter such as a nuclear charge, intramolecular distance in the Born–Oppenheimer Hamiltonian, etc.

However, for c-normalized ϕ (i.e. $(\phi|\phi) = 1$),

$$\frac{\mathrm{d}\bar{E}}{\mathrm{d}\zeta} = \left(\phi\left|\frac{\partial H_\theta}{\partial\zeta}\right|\phi\right) + \sum_{j=1}^{M}\left(\frac{\partial\bar{E}}{\partial C_j}\right)\left(\frac{\partial C_j}{\partial\zeta}\right). \tag{2.8.4}$$

Thus, if ϕ is variationally optimal for any given value of ζ Eqs. (2.3.1) and (2.6.6) is satisfied and therefore Eq. (2.8.4) reduces to

$$\mathrm{d}\bar{E}/\mathrm{d}\zeta = \left(\phi\left|\frac{\partial H_\theta}{\partial\zeta}\right|\phi\right). \tag{2.8.4a}$$

This is the complex form of the Hellmann–Feynman theorem. When $\zeta = \exp(\mathrm{i}\theta)$ the requirement of $\mathrm{d}\bar{E}/\mathrm{d}\theta = 0$ (the resonance solution satisfies this condition following the Balslev–Combes theorem) leads to another derivation of the virial theorem Eq. (2.8.2). Within the framework of the finite basis set approximation ($\boldsymbol{C}$ are the linear variational parameters) the resonance stationary condition

$$\left|\frac{\mathrm{d}\bar{E}}{\mathrm{d}\theta}\right|_{\theta_{\mathrm{opt}}} = 0 \tag{2.8.5}$$

($\zeta \equiv \theta$ in Eq. (2.8.4)) leads to an iterative procedure for calculating the resonances:

$$\boldsymbol{H}_\theta = \mathrm{e}^{-2\mathrm{i}\theta}\boldsymbol{T} + \boldsymbol{V}_\theta, \quad (H_\theta)_{ij} = \langle\chi_i|H(x\mathrm{e}^{\mathrm{i}\theta})|\chi_j\rangle$$

$$\boldsymbol{H}_\theta\boldsymbol{C}_k^{\mathrm{R}} = \bar{E}_k\boldsymbol{C}_k^{\mathrm{R}}, \qquad \boldsymbol{H}_\theta^{\mathrm{t}}\boldsymbol{C}_k^{\mathrm{L}} = \bar{E}_k\boldsymbol{C}_k^{\mathrm{L}}, \tag{2.8.5a}$$

$$\mathrm{e}^{-2\mathrm{i}\theta} = \frac{(\boldsymbol{C}_k^{\mathrm{L}})^{\mathrm{t}}(\partial\boldsymbol{V}_\theta/\partial\theta)\boldsymbol{C}_k^{\mathrm{R}}}{2\mathrm{i}(\boldsymbol{C}_k^{\mathrm{L}})^{\mathrm{t}}\boldsymbol{T}\boldsymbol{C}_k^{\mathrm{R}}}\,. \tag{2.8.6}$$

Note that following the Cauchy–Reimann conditions θ_{opt} for which Eqs. (2.8.5) and (2.8.6) are satisfied will usually get a complex value. Real (θ_{opt}) should satisfy the conditions discussed in Section 2.3. The $\mathrm{Im}(\theta_{\mathrm{opt}})$ can get either negative or positive values, that is, the absolute value of the complex-scaling parameter, $\eta = \exp(\mathrm{i}\theta_{\mathrm{opt}})$, can be either smaller or larger than unity. For atomic coulombic potentials Eq. (2.8.5) reduces to the c-virial theorem. Moiseyev, Certain and Weinhold used this iterative algorithm for calculating the autoionization resonances of Helium [63]. Moiseyev and Corcoran [79] succeeded to avoid numerical difficulties in the first studied molecular autoionization resonances in H_2^- and H_2 due to the fact that $\mathrm{Im}\,\theta_{\mathrm{opt}}$ was found to be negative in their calculations.

Cusps and θ-trajectories. Doolen et al. [80] proposed a graphical method of solving Eq. (2.8.4) (known as θ-trajectory), in which $\bar{E}(\theta)$ is plotted as function of Re(θ), holding Im(θ) fixed. The stationary points along the trajectories which provide the minimal (not necessarily zero value) of $|\mathrm{d}\bar{E}/\mathrm{d}\theta|$ have been assumed to correspond to resonances [81]. Moiseyev et al. [82] proved that the stationary solution where $\mathrm{d}\bar{E}/\mathrm{d}\theta = 0$ at $\theta = \theta_{\mathrm{opt}}$ is associated with a cusp in θ-trajectory plot. The proof is as follows: in the neighborhood of a stationary point the complex energy, $\bar{E}$, can be expanded in powers of $(\eta - \eta_{\mathrm{opt}})$, (Puiseux expansion). Where the first two terms are

$$\bar{E} = E_0 + a(\eta - \eta_{\mathrm{opt}})^{\mu} + \cdots \tag{2.8.8}$$

$$\eta = \mathrm{e}^{\mathrm{i}\theta} = \alpha \mathrm{e}^{\mathrm{i}\theta_{\mathrm{R}}}, \qquad \eta_{\mathrm{opt}} = \mathrm{e}^{\mathrm{i}\theta_{\mathrm{opt}}} = \alpha_{\mathrm{opt}} \mathrm{e}^{\mathrm{i}\theta_{\mathrm{R}}^{(0)}}$$

$$\theta = \theta_{\mathrm{R}} + \mathrm{i}\theta_{\mathrm{I}}, \qquad \theta_{\mathrm{opt}} = \theta_{\mathrm{R}}^{(0)} + \mathrm{i}\theta_{\mathrm{I}}^{(0)} \tag{2.8.9}$$

$$\alpha = \mathrm{e}^{-\theta_{\mathrm{I}}}, \qquad \alpha_{\mathrm{opt}} = \mathrm{e}^{-\theta_{\mathrm{I}}^{(0)}}$$

and μ is a positive rational number.

For small enough $(\eta - \eta_0)$ along the θ-trajectory

$$\eta = \alpha_{\mathrm{opt}} \mathrm{e}^{\mathrm{i}\theta_{\mathrm{R}}} \tag{2.8.10}$$

and, therefore, we can write

$$\eta - \eta_{\mathrm{opt}} = \mathrm{i}\eta_{\mathrm{opt}} x\,, \tag{2.8.11}$$

where

$$x = \theta_{\mathrm{R}} - \theta_{\mathrm{R}}^{(0)}\,. \tag{2.8.12}$$

Consequently, for $x \geq 0$ (i.e. approaching the cusp from "above")

$$\bar{E}_{+} = E_0 + a(\mathrm{i}\eta_{\mathrm{opt}})^{\mu} |x|^{\mu} + \cdots \tag{2.8.13}$$

while, for $x \leq 0$ (i.e. approaching the cusp from "below")

$$x = -|x| = |x| \mathrm{e}^{\mathrm{i}\pi} \tag{2.8.14}$$

and

$$\bar{E}_{-} = E_0 + a(\mathrm{i}\eta_{\mathrm{opt}})^{\mu} |x|^{\mu} \mathrm{e}^{\mathrm{i}\pi\mu} \ldots\,. \tag{2.8.15}$$

One thus sees that a cusp exists between the two branches $\bar{E}_{+}$ and $\bar{E}_{-}$ at the stationary point, $\theta = \theta_{\mathrm{opt}}$, with a cusp angle πμ.

A smooth curve (cusp angle = π) will be observed at the stationary point when μ is an odd integer (3, 5, 7, …).

A schematic representation of such an example is given in Fig. 16a, where it is seen that the θ_{R}-trajectory "slows down" at the stationary point, but yet there is no cusp. It should be remembered, however, that the θ_{R}-trajectories for non optimum $|\eta_{\mathrm{opt}}|$ (i.e. non-optimal value of $\mathrm{Im}(\theta_{\mathrm{opt}})$) are smooth also. This case (i.e. no cusp) has been observed numerically by McCurdy [83] in calculations of shape-type resonances of the $v = r^2 \exp(-0.61r)$ potential.

A zero cusp angle will be observed at the stationary point when μ is an even integer (2, 4, 6, …). This case which is shown schematically in Fig. 16b is the most common case. For example, see the zero-angle cusps obtained in the calculations of $H_2(1\sigma u)^2$ and $\mathrm{He}(2s)^2$ resonances [79,84].

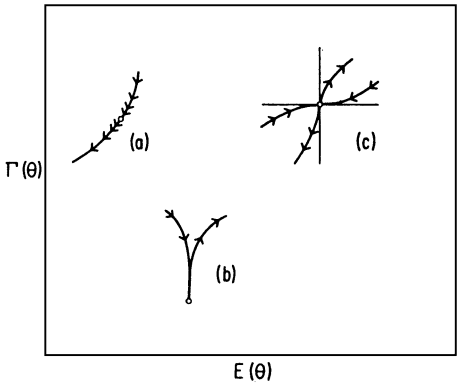

Fig. 16. θ_R trajectory when α is held fixed at $\alpha = \alpha_{opt}$. The arrows show the motion of complex "energies" as θ is varied. The open circles denote the stationary solutions that are obtained from $\eta = \theta_R = \theta_R^{(0)}$, (a) $\mu = 3, 5, 7, \ldots$ (b) $\mu = 2, 4, 6, \ldots$ (c) $\mu = 3/2, 7/2 \ldots$.

An interesting case occurs for rational $\mu = n/m > 1$, where n and m are coprime, since here the cusp angle is neither zero nor π. A fractional π is the result of the coalescence of at least m eigenvalues (and also the corresponding eigenvectors!) of the complex Hamiltonian *matrix* at the stationary point $\theta = \theta_{opt}$. As discussed in Section 2.5, $\bar{E}(\theta_{opt})$ in such a case is a defective eigenvalue. This case which is shown schematically in Fig. 16c, for $\mu = \frac{3}{2}$, apparently has not been observed so far in resonance calculations. Presumably, this is due to the very special conditions at which a defective eigenvalue is obtained.

This cusp conditions has been used also by Peskin and Moiseyev [85] for calculating the optimal scattering transition probability amplitude, $T_{scatt}(\theta)$. The optimal condition

$$\left|\frac{\partial T_{scatt}}{\partial \theta}\right|_{\theta_{opt}} = 0 \tag{2.8.16}$$

has been found to be the key point in the successful application of the complex-coordinate scattering theory (Section 3) to long-range potentials.

2.9. The hermitian representation of the complex coordinate method: Upper and lower bounds to the resonance positions and widths

The c-variational principle presented in Section 2.6 is a stationary principle rather than an upper or lower bound for either the real or imaginary part of the complex eigenvalue. On the basis of the hermitian representation of the complex coordinate method developed by Moiseyev [86], it has been proved that

$$|E(\text{exact}) - \bar{E}| \geq \lambda\,, \tag{2.9.1}$$

where λ^2 is the lowest real and positive eigenvalue of the complex, yet hermitian, operator $\hat{\mathscr{H}}^2$

$$\mathscr{H}^2(\bar{E}, \bar{E}^*)\phi = \lambda^2\phi \tag{2.9.2}$$

$$\mathscr{H}^2 \equiv (\hat{H}_\theta - \bar{E})^*(\hat{H}_\theta - \bar{E}) \tag{2.9.3}$$

and

$$\bar{E} \equiv \bar{\varepsilon} - (\mathrm{i}/2)\bar{\Gamma}\,. \tag{2.9.4}$$

If ϕ is a trial given function, then by using the Hellman–Feynman theorem, one can show that the minimal expectation value, $\langle\phi|\mathscr{H}^2|\phi\rangle/\langle\phi|\phi\rangle$, is obtained for

$$\bar{E} = \langle\phi|\hat{H}_\theta|\phi\rangle/\langle\phi|\phi\rangle\,. \tag{2.9.5}$$

By carrying out an iterative calculation, $\bar{E}$ as obtained from Eq. (2.9.5) is substituted in Eq. (2.9.2) to get a new estimate for ϕ. Here we assume that the ground state of the hermitian operator $\mathscr{H}^2$ can be accurately obtained from numerical computations (see, for example, Refs. [64–66,87–89]).

Eq. (2.9.1) can be used to obtain an error estimate of $\bar{E}$ obtained from c-variational calculations:

$$\bar{E} = \frac{(\phi|H_\theta|\phi)}{(\phi|\phi)} \equiv \frac{\langle\!\langle\phi|H_\theta|\phi\rangle\!\rangle}{\langle\!\langle\phi|\phi\rangle\!\rangle}\,. \tag{2.9.6}$$

Note that in Eq. (2.9.6) the c-product is used rather than the scaler product which has been used in Eq. (2.9.5). In such a case by combining Eq. (2.9.1) with the bounds to resonance eigenvalues evaluated by Davidson et al. [90] it is obtained *that E* (exact) *is embedded in an annular ring centered at* $\bar{E}$, *where the inner and outer radii are, respectively, the lowest eigenvalue of* $\mathscr{H}^2(\bar{E},\bar{E}^*)$ *and the complex-variance of* $\mathscr{H}^2(\bar{E},\bar{E}^*)$.

$$|\sigma_{\mathrm{C}}| \le |E(\text{exact}) - \bar{E}| \le \lambda \tag{2.9.7}$$

and

$$|\sigma_{\mathrm{C}}| \le \sigma_H |\langle\phi|\phi\rangle|^{1/2} \tag{2.9.8}$$

provided $|\langle\phi|\psi(\text{exact})\rangle|^2 > \frac{1}{2}$, and $\langle\phi|\phi\rangle = 1$. σ_{C} and σ_{H} are, respectively, the complex and Hilbert-space variances given by [90–92]

$$\sigma_{\mathrm{C}}^2 = \frac{(\phi|(H_\theta - \bar{E})^2|\phi)}{(\phi|\phi)}\,, \tag{2.9.9}$$

$$\sigma_H^2 = \frac{\langle\phi|\mathscr{H}^2(\bar{E},\bar{E}^*)|\phi\rangle}{\langle\phi|\phi\rangle}\,. \tag{2.9.10}$$

Note that ϕ is a complex normalized function $(\phi|\phi) = 1$, and therefore $\langle\phi|\phi\rangle > 1$.

An illustrative numerical example for the model Hamiltonian

$$H = -\tfrac{1}{2}\mathrm{d}^2/\mathrm{d}x^2 + (x^2/2 - 0.8)\mathrm{e}^{-0.1x^2} + 0.8 \tag{2.9.11}$$

is presented in Fig. 17.

Proof of Eq. (2.9.1): $|E(\text{exact}) - \bar{E}| \ge \lambda$

$$\hat{H}_\theta\psi = E(\text{exact})\psi \tag{2.9.12}$$

$\mathscr{H}^2(\bar{E},\bar{E}^*)$ is an hermitian operator and λ^2 is its lowest, real, and positive eigenvalue. Therefore, following the conventional variational principle:

$$\frac{\langle\psi|\mathscr{H}^2(\bar{E},\bar{E}^*)|\psi\rangle}{\langle\psi|\psi\rangle} \ge \lambda^2\,. \tag{2.9.13}$$

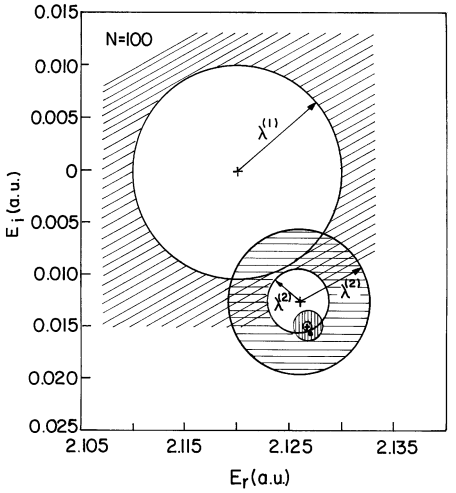

Fig. 17. Bounds of the estimate complex-coordinate resonance eigenvalues $\bar{E}$, obtained for N even-parity harmonic oscillator basis functions. $\bar{E}$ are indicated by the signs " + " and the exact value E by a dot. The dashed areas give an optimal estimate of the resonance location. The upper and lower bounds of the estimate shape-type complex-coordinate resonance eigenvalue, obtained for $N = 2, 3, 4$ even-parity harmonic oscillator basis functions [64].

Since,

$$\langle\psi|\mathscr{H}^2|\psi\rangle = \langle\chi|\chi\rangle\,, \tag{2.9.14}$$

where

$$\chi = (H_\theta - \bar{E})\psi = (E(\text{exact}) - \bar{E})\psi\,, \tag{2.9.15}$$

therefore,

$$\langle\psi|\mathscr{H}^2|\psi\rangle = |E(\text{exact}) - \bar{E}|^2\langle\psi|\psi\rangle\,. \tag{2.9.16}$$

By substituting Eq. (2.9.16) into Eq. (2.9.13), one gets that

$$|E(\text{exact}) - \bar{E}|^2 \geq \lambda^2\,. \tag{2.9.17}$$

Proof of Eq. (2.9.7): $|E(\text{exact}) - \bar{E}| \leq |\sigma_C|$

Here we shall use the Lanczos recursion procedure [93] to construct a three-diagonal complex-scaled Hamiltonian matrix,

$$\boldsymbol{H}_\theta = \begin{pmatrix} \alpha_0 & \beta_0 & & & \\ \beta_0 & \alpha_1 & \beta_1 & & \\ & \beta_1 & \alpha_2 & \beta_2 & \\ & & \ddots & \ddots & \ddots \end{pmatrix}, \tag{2.9.18}$$

where $\chi_0 \equiv \phi$ is a given wave function which describes well enough the exact eigenfunction $\psi(\text{exact})$, and

$$\alpha_0 \equiv \bar{E} = (\phi|\hat{H}_\theta|\phi)\,, \tag{2.9.19}$$

$$\beta_0 \equiv \sigma_C^2 = (\chi_1|\chi_1)^{1/2}\,, \tag{2.9.20}$$

$$\chi_1 = (\hat{H}_\theta - \alpha_0)\phi_0\,. \tag{2.9.21}$$

Similarly for $n \geq 1$,

$$\alpha_n = (\chi_n|\hat{H}_\theta|\chi_n)\,, \tag{2.9.22}$$

$$\chi_{n+1} = (\hat{H}_\theta - \alpha_n)\chi_n - \beta_{n-1}\chi_{n-1}\,, \tag{2.9.23}$$

$$\beta_n = (\chi_{n+1}|\chi_{n+1})^{1/2}\,. \tag{2.9.24}$$

By diagonalizing the three-diagonal Hamiltonian matrix $\boldsymbol{H}_\theta$ the exact eigenfunction is obtained

$$\psi(\text{exact}) = \sum_{n=0}^{\infty} C_n\chi_n(x) \tag{2.9.25}$$

where $\boldsymbol{C}$ is an eigenvector of $\boldsymbol{H}_\theta$,

$$\boldsymbol{H}_\theta\boldsymbol{C} = E(\text{exact})\boldsymbol{C} \tag{2.9.26}$$

and χ_n are the Lanczos recursive functions

$$(\chi_n|\chi_{n'}) = \delta_{n,\,n'} \tag{2.9.27}$$

as defined in Eq. (2.9.23).

By substituting Eq. (2.9.18) into Eq. (2.9.26), one gets

$$\alpha_0 C_0 + \beta_0 C_1 = \bar{E}(\text{exact})C_0\,. \tag{2.9.28}$$

Since $\alpha_0 = \bar{E}$ (see Eq. (2.9.19)) and $\beta_0 = \sigma_C^2$ (Eq. (2.9.20)) then from Eq. (2.9.28) one immediately obtains that

$$|E(\text{exact}) - \bar{E}|^2 = |\sigma_C|^2|C_1/C_0|^2\,. \tag{2.9.29}$$

If $\chi_0 = \phi$ is the dominant function in the Lanczos basis set expansion then $|C_0|^2 > \frac{1}{2}$,

$$|C_1/C_0|^2 < 1 \tag{2.9.30}$$

and, consequently,

$$|E(\text{exact}) - \bar{E}|^2 \leq |\sigma_C|^2\,. \tag{2.9.31}$$

3. Complex scaling of ab initio molecular potential surfaces

When the potential $V(x)$ is known analytically its analytic continuation, $V(x\exp(i\theta))$, is also known analytically. The problem is, however, that the molecular potentials are calculated on a finite grid in the conventional unscaled coordinate space. To overcome this difficulty several numerical procedures were proposed (see Section 2.2 in Ref. [94]). Moiseyev and Corcoran [95] studied the H_2^- and excited H_2 autoionization resonances by using an analytic continuation of the Hamiltonian matrix elements to the complex plane rather than of the Hamiltonian operator. Therefore, one can fit an ab initio potential to a given order polynomial, calculate analytically the potential matrix elements as function of the basis set parameters (such as box-size or scale

parameter), and finally carry out analytic continuation of the potential matrix elements into the complex plane. This approach was used by Lipkin and coworkers [96] in their study of resonances for piecewise potentials and more recently in the study of certain atmospheric conditions by which downwind at the mountains is formed [97]. A preferable method, however, is the one for which there is no need to fit the ab initio potential to any finite order polynomial or to any other analytic form in order to calculate the complex-scaled potential energy matrix elements. Lipkin et al. [98] suggested to carry out similarity transformation of the hermitian Hamiltonian matrix where the transformation matrix is an overlap between the complex scaled and the unsealed basis functions. More recently, Ryaboy and Moiseyev [94] used another approach. The *y* calculated the HCO and DCO predissociation resonances by carry out numerical integration along the real axis when the basis functions were scaled by $\exp(-\mathrm{i}\theta)$ whereas the ab initio potential remained unscaled. All the methods described above, use basis functions in the reaction coordinate which is scaled by a complex factor.

Starting from the theoretical work of Moiseyev and Hirschfelder [13] Mandelshtam and Moiseyev [99] developed a method which avoid the need of using the basis set approach along the reaction coordinate. Namely the complex-scaled potential can be generated on the same grid as

$$V(x_n \exp(\mathrm{i}\theta)) = \sum_k S_{n,k} V(x_k)\,, \tag{3.1}$$

where the matrix S represents the complex-scaling operator (conventional scaling or smooth exterior scaling) which is given by

$$\hat{S} = \mathrm{e}^{-\mathrm{i}\theta/2} \mathrm{e}^{\theta \hat{W}}\,, \tag{3.2}$$

where $\hat{W}$ is given by

$$\hat{W} \mathrm{e}^{[\mathrm{i} f^{1/2}(x)(\partial/\partial x) f^{1/2}(x)]}\,, \tag{3.3}$$

and $f(x)$ is a smooth function of x. When $f(x) = x$ the x coordinate is rotated by θ into the complex plane as in the conventional complex scaling [so-called the CCM (complex coordinate method)]. To illustrate how the complex-scaling operator $\hat{S}$ can be defined on a grid we shall consider here the case of $f(x) = x$. In such a case $\hat{W}$ is a hermitian unbounded operator,

$$\hat{W} = (x\hat{P}_x + \hat{P}_x x)/2\,, \tag{3.4}$$

where $P_x = \mathrm{i}\,\partial/\partial x$ is identical with the momentum operator.

The difficulty to carry out such a transformation can be illustrated by analyzing the Fourier transform of $V(x_n)$:

$$V(x) = \sum_n C_n \exp(2\pi n x \mathrm{i}/L)\,, \tag{3.5}$$

where L is the size of the grid. From the first glance the complex-scaled potential can simply be given by

$$V(x\mathrm{e}^{\mathrm{i}\theta}) = \sum_{n=-\infty}^{+\infty} C_n \exp(2\pi n x \exp(\mathrm{i}\theta)\mathrm{i}/L)\,, \tag{3.6}$$

However, this expansion will not be stable because of the exponentially diverging terms when $nx \to +\infty$.

The choice of basis functions is crucial when a finite basis set approach is taken to represent the complex scaling operator $\hat{S} = \exp(\theta\hat{W})$. It is easy to see it when $\hat{S}$ is introduced by using the spectral representation of $\hat{W}$. That is,

$$S_{n,k} = \mathrm{e}^{-\mathrm{i}\theta/2} \sum_{\mathrm{i}=1}^{N} \mathrm{e}^{\theta\lambda_i} C_i^{(n)*} C_i^{(k)}, \tag{3.7}$$

where $\boldsymbol{C}_i$ and λ_i are, respectively, the eigenvectors and eigenvalues of the matrix $\boldsymbol{W}$ which represent $\hat{W}$.

For example, if one uses $\sin(\pi nx/L)$ basis functions (i.e. particle-in-a-box basis functions) infinitely many terms should be taken to correctly describe eigenfunctions of $\hat{W}$ since the frequency of their oscillations is continuously changing from infinity (at small x) to zero (at large x). An alternative seemingly more stable expansion could be obtained if local basis functions are used.

Such local basis functions are the sinc-DVR basis functions (see Refs. [8–10,100–102]) defined as

$$\phi_n(x) = (1/\sqrt{\Delta})\,\mathrm{sinc}[\pi(x/\Delta - n)]\,. \tag{3.8}$$

In this basis the off-diagonal matrix elements of $\hat{W}$ can be approximated as

$$W_{n,m} = \langle\phi_n|\hat{W}|\phi_m\rangle \approx (-1)^{(n-m)}\frac{\mathrm{i}(n+m)}{(n-m)}, \tag{3.9}$$

and the diagonal matrix elements are

$$W_{n,n} = 0\,.$$

Even though the sinc-DVR basis functions are an approximation for the Dirac δ-functions,

$$\delta(x - n\Delta) \approx \phi_n(x)\,, \tag{3.10}$$

they are not quite localized in space leading to a very slow decay of the off-diagonal matrix elements of $\hat{W}$. On the other hand, the operator $\hat{W}$ is local and therefore its grid representation could be made local by damping the elements $W_{n,m}$ with large $|n-m|$,

$$W_{n,m} \approx (-1)^{(n-m)}\frac{\mathrm{i}(n+m)}{(n-m)}\mathrm{e}^{-\sigma(n-m)^2}\,. \tag{3.11}$$

Such an ansatz which has been checked numerically [99] can also be understood by analyzing the relation:

$$[\hat{W}f](x) = \int \mathrm{d}x' \langle x|\hat{W}|x'\rangle f(x') \approx \int \mathrm{d}x' \langle x|\hat{W}|x'\rangle \mathrm{e}^{-(\sigma/\Delta)(x-x')^2} f(x')\,. \tag{3.12}$$

For a sufficiently small σ this is a good approximation due to the local nature of the operator $\hat{W}$.

The Mandelshtam–Moiseyev method [99] has been used by Narevicius and Moiseyev [103] in the calculations of thousands of broad and overlapping ArHCl resonances for 3D potential energy

surface which has been calculated on a finite grid. In a very similar way, one can use the smooth-exterior scaling approach. It should be stressed that it is sufficient to scale the reaction coordinate and there is no need to scale by a complex factor all degrees of freedom. This method enables the study of the dynamics and resonance phenomena in polyatomic molecular systems for which the potential energy surface is available only on a grid.

4. The complex coordinate scattering theory: From complex-scaled Hamiltonians to partial-widths and cross sections

4.1. General discussion

The complex coordinate time-independent scattering theory [104–112] enables one to calculate cross sections, partial widths and state-to-state transition probabilities even for time-dependent Hamiltonians.

There are three key points in the derivation of the complex-coordinate scattering theory:

(1) The state-to-state, $\phi_i \to \phi_f$, transition probability amplitude matrix elements, $T = \langle \phi_f | V(1 + \hat{G}V) | \phi_i \rangle$, are calculated when the integration is carried out along a complex contour in the coordinate space. The complex spatial contour is obtained by scaling the cartesian coordinates by a complex factor $\exp(i\theta)$. Scaling the "reaction coordinate" only by a complex factor, where the other coordinates remain unscaled, has numerical advantages. The "reaction coordinate" may be considered as the distance between the center of mass of the scattered particle and the center of mass of the target.

(2) The Green operator, $\hat{G}$, is defined as $(E - H_\theta)^{-1}$ when H_θ is the complex-scaled Hamiltonian of the system. Consequently, the energy contour of integration becomes complex when $\hat{G}$ in the spectral representation is calculated. Since this is a crucial point in the derivation of the complex coordinate scattering method, we shall discuss it with some more details:

The Green operator $\hat{G}(E)$ provides the probability amplitude to get from $\boldsymbol{x}$ to $\boldsymbol{x}'$ at a given energy E. $\hat{G}$ in the spectral representation is given by

$$G_E(\boldsymbol{x}', \boldsymbol{x}) = \int dE' \rho(E') \frac{\psi_{E'}(\boldsymbol{x}')\psi_{E'}(\boldsymbol{x})}{E - E'}, \tag{4.1.1}$$

where $\psi_{E'}$ are the eigenfunctions of the full Hamiltonian and $\rho(E')$ is the density of states. As one can see from Eq. (4.1.1) G_E has a branch cut along the real energy axis. Consequently, large numerical errors are expected in a brute force application of Eq. (4.1.1), due to the vanishing of the energy denominator. This is a very serious technical problem, which can be avoided by rotating the energy contour of integration from the real axis into the complex plane. The energy contour of integration becomes complex when the relevant spatial contour is rotated into the complex plane, as discussed in Sections 1 and 2. The wave functions $\psi_{E'}$ and the energy E' in Eq. (4.1.1) are replaced by the eigenfunctions and eigenvalues of the complex-scaled Hamiltonian H_θ. The eigenfunctions of the complex-scaled Hamiltonian are associated with the discrete resonance spectrum, $E_n^{\text{res}} = \varepsilon_n - (i/2)\Gamma_n$, where ψ_n^{res}; $n = 1, 2, \ldots$ are square integrable functions, and with

the rotating continua, $\psi_{E_\theta^j}$ where $E_\theta^j = \varepsilon \exp(-2i\theta) + E_j^{\text{thres}}$, ε is varied from 0 to ∞ and E_j^{thres}; $j = 1, 2, \ldots$ are the (real) threshold energies. The complex-scaled Green operator in the spectral representation is given by (see Refs. [2–6,105–109], Rescigno and Reinhardt [113], Johnson and Reinhardt [117], Rescigno and McCurdy [118], and Froelich and coworkers [119]),

$$G_\theta(E) = \sum_{n(\text{res})} \frac{\psi_n^{\text{res}}(x')\psi_n^{\text{res}}(x)}{E - E_n^{\text{res}}} + \sum_{j(\text{thres})} \int dE_\theta^j \rho(E_\theta^{(j)}) \frac{\psi_{E_\theta^{(j)}}(x')\psi_{E_\theta^{(j)}}(x)}{E - E_\theta^{(j)}}. \tag{4.1.2}$$

Here we assume that the wave functions are complex only resulting from the complex scaling. When the eigenfunctions of the complex-scaled Hamiltonian are variationally obtained with complex basis functions one should use the left and the right eigenstates of H_θ as defined in Section 2. $\rho(E_\theta^{(j)})$ in Eq. (4.1.2) is the density of states. Due to the complex scaling the resonances are isolated and separated from the other states in the continuum. Consequently, $\rho(E_\theta^{(j)})$ does NOT depend on the potential interaction and depends ONLY on the dimension of the studied problem. For a d-dimensional continuum ρ is proportional to $\varepsilon^{(d/2-1)}$ where $\varepsilon \equiv |E_\theta^j - E_j^{\text{thres}}|$. When box normalization is used the integrals in Eq. (4.1.1) and in Eq. (4.1.2) are replaced by summations over the discrete quasi-continuum and, respectively, $\rho(E')$ and $\rho(E_\theta^{(j)})$ are replaced by 1.

(3) The transition probability amplitude, $T(E)$, gets complex values and is in principle θ-independent. In the numerical calculations when finite grid or finite basis set methods are used $T(E)$ is θ-dependent. The optimal values of T are associated with the stationary solutions for which $dT/d\theta = 0$. Since T is complex θ should be allowed to get complex values and to be optimized to satisfy the two Cauchy–Riemann conditions:

$$\left|\frac{\partial \text{Re}\, T(\theta)}{\partial \text{Re}\, \theta}\right|_{\theta_{\text{opt}}} = 0 \quad \text{and} \quad \left|\frac{\partial \text{Im}\, T(\theta)}{\partial \text{Re}\, \theta}\right|_{\theta_{\text{opt}}}$$

or

$$\left|\frac{\partial \text{Re}\, T(\theta)}{\partial \text{Im}\, (\theta)}\right|_{\theta_{\text{opt}}} = 0 \quad \text{and} \quad \left|\frac{\partial \text{Im}\, T(\theta)}{\partial \text{Im}\, \theta}\right|_{\theta_{\text{opt}}} = 0. \tag{4.1.3}$$

The fact that the optimal rotational angle θ_{opt} may get complex values can be introduced as the result of using a complex scaling factor

$$\eta = e^{i\theta} = \alpha e^{i\theta'}, \tag{4.1.4}$$

where α and θ' are real and α is not necessarily equal to one. The optimal values of α and θ' are those for which $\partial T/\partial \alpha = 0$ and $\partial T/\partial \theta' = 0$. Peskin and Moiseyev [111] have shown that the optimization of the complex scaling factor n (i.e. $\theta' = \theta_{\text{opt}}$, $\alpha = \alpha_{\text{opt}}$) enables the application of the complex coordinate scattering theory to long range potentials, and avoids the serious singularities and convergence problems due to the exponential divergence of the complex scaled "in"-asymptote $|\phi_i\rangle$ or "out"-asymptote $\langle\phi_f|$ which were explored by Rescigno and Reinhardt [111], Baumel et al. [114], Johnson and Reinhardt [115], by Rescigno and McCurdy [116], and by McCurdy et al. [120].

4.2. Time-independent Hamiltonians

The probability to get from the initial state ϕ_i to the final one ϕ_f is given by the S-matrix element,

$$P_{f\leftarrow i} = |S_{f,i}|^2 . \tag{4.2.1}$$

In the case of a one-dimensional "reaction coordinate" the scattering matrix is given by

$$S_{f,i} = 1 - T_{f,i} \tag{4.2.2}$$

if the scattering process is an elastic one and if the sign of the wave vector in the reaction coordinate is unchanged during the collision; i.e. $k_i = k_f$. In non-elastic scattering and in elastic scattering when $k_i = -k_f$ (as in the case of atom (molecule)/surface scattering),

$$S_{f,i} = T_{f,i} , \tag{4.2.3}$$

$T_{f,i}$ is the energy normalized complex-scaled T matrix element

$$T_{f,i}(E) = (1/\hbar)\langle\!\langle \phi_f | V + V\hat{G}_E V | \phi_i \rangle\!\rangle , \tag{4.2.4}$$

where $\hat{V}(\boldsymbol{x}', r) = V$ describes the interaction potential of the scattered particle and the target; $\{x\}$ are the internal (or target) coordinates; r is the reaction coordinate and $\hat{G}_E = (E - H)^{-1}$. The Hamiltonian is given by

$$\hat{H} = \hat{H}_0 + \hat{V} \tag{4.2.5}$$

where

$$\hat{H}_0 = -(\hbar^2/2\mu)\Delta_r + \hat{h}(\boldsymbol{x}) , \tag{4.2.6}$$

Δ_r stands for the Laplacian operator with respect to the coordinates of the scattered particle and $\hat{h}(\boldsymbol{x})$ is the Hamiltonian of the target. In this step of the representation we will carry out an analytical continuation of H, V, ϕ_i, ϕ_f and H_0 and $\hat{G}$ by scaling the reaction coordinate by a complex factor. That is,

$$r = r' e^{i\theta} \tag{4.2.9}$$

where r' gets real values only and,

$$\begin{aligned} V_\theta &= V(r' e^{i\theta}, \boldsymbol{x}) , \\ H_\theta &= \hat{H}(r' e^{i\theta}, \boldsymbol{x}) , \\ \hat{G}_\theta &= 1/(E - \hat{H}_\theta) . \end{aligned} \tag{4.2.10}$$

The energy normalized initial and final states are eigenfunctions of the complex-scaled H_0 Hamiltonian

$$|\phi_i\rangle\!\rangle = \sqrt{\frac{\mu}{\hbar^2 |k_i| e^{i\theta}}}\, e^{-ik_i e^{i\theta} r'} \cdot \chi_{m_i}(\boldsymbol{x}) \tag{4.2.11}$$

and

$$\langle\langle\phi_f| = \sqrt{\frac{\mu}{\hbar^2|k_f|e^{-i\theta}}}\, e^{ik_f e^{i\theta}r'} \cdot \chi^*_{m_f}(\boldsymbol{x})\,, \tag{4.2.12}$$

where χ_m are given by

$$\begin{aligned}\hat{h}(\boldsymbol{x})\chi_{m_i}(\boldsymbol{x}) &= E^{\text{thres}}_{m_i}\chi_{m_i}(\boldsymbol{x})\,,\\ \hat{h}(\boldsymbol{x})\chi_{m_f}(\boldsymbol{x}) &= E^{\text{thres}}_{m_f}\chi_{m_f}(\boldsymbol{x})\,.\end{aligned} \tag{4.2.13}$$

If the reaction coordinate is radial, $-2i\sin(ke^{\theta}r')$ replace the $\exp(-ike^{i\theta}r')$ in Eqs. (4.2.11) and (4.2.12). The initial and final wave vectors are defined such that the total energy of the "particle–target" systems is conserved:

$$E = \frac{(\hbar k_i)^2}{2\mu} + E^{\text{thres}}_{m_i} = \frac{(\hbar k_f)^2}{2\mu} + E^{\text{thres}}_{m_f}\,. \tag{4.2.14}$$

The right and left eigenfunctions of the complex scaled Hamiltonian can be obtained by the diagonalization of the Hamiltonian matrix $\boldsymbol{H}_\theta$ when $\{\chi_m\}$ are used as a basis function:

$$\begin{aligned}\Psi^{R,\theta}_n &= \sum_m \phi^{R,\theta}_{m,n}(r')\chi_m(\boldsymbol{x})\,,\\ \Psi^{L,\theta}_n &= \sum_m \phi^{L,\theta}_{m,n}(r')\chi_m(\boldsymbol{x})\end{aligned} \tag{4.2.15}$$

when

$$\begin{aligned}\boldsymbol{H}_\theta\phi^{R,\theta}_n &= E^\theta_n\phi^{R,\theta}_n\,,\\ \boldsymbol{H}^t_\theta\phi^{L,\theta}_n &= E^\theta_n\phi^{L,\theta}_n\,,\\ [\boldsymbol{H}_\theta]_{m',m} &= \langle\chi_{m'}|\hat{H}(\boldsymbol{x}, r'e^{i\theta})|\chi_m\rangle\,.\end{aligned} \tag{4.2.16}$$

By using the complex eigenvalues and eigenfunctions given in Eqs. (4.2.15) and (4.2.16) to construct the complex-scaled Green operator (see Eq. (4.1.2)), the complex coordinate T-matrix element is obtained (See Eq. (4.2.4))

$$\begin{aligned}T^\theta_{f,i}(E) = {}& \frac{\mu}{\hbar^2\sqrt{|k_i||k_f|}}\iint dr'd\{\boldsymbol{x}\}\chi^*_{m_f}(\boldsymbol{x})e^{-ik_f r'}V(r',\boldsymbol{x})\chi_{m_i}(\boldsymbol{x})e^{-ik_i r'}\\ &+ e^{i\theta}\sum_n (E-E^\theta_n)^{-1}\times\left[\iint dr'd\boldsymbol{x}\chi^*_{m_f}(\boldsymbol{x})e^{-ik_f e^{i\theta}r'}V(e^{i\theta}r',\boldsymbol{x})\psi^{R,\theta}_n(r',\boldsymbol{x})\right]\\ &\times\left[\iint dr'd\boldsymbol{x}\chi_{m_i}(\boldsymbol{x})e^{-ik_i e^{i\theta}r'}V(e^{i\theta}r',\boldsymbol{x})\psi^{L,\theta}_n(r',\boldsymbol{x})\right],\end{aligned} \tag{4.2.17}$$

where the summation $\sum_n$ is over all resonances and rotated continua solutions (which are associated with a discrete spectrum due to the use of finite number of basis functions).

Since the integral in the first term is unaffected by the value of θ (provided $V(r',x)$ is an analytical function) we choose here to carry this integral along the real $r = r'$-axis.

Note by passing that Eq. (4.2.17) can be simplified if the exterior scaling procedure rather than the commonly used complex scaling is used. If $r = r'$ when $r' \le r_0$; $r = (r' - r_0)e^{i\theta} + r_0$ when $r' > r_0$ and $V(r' > r_0, \boldsymbol{x}) = 0$, then the initial and final states and the interaction potential V remain unscaled. The only complex functions used in this case in Eq. (4.2.17) are the left and the right eigenfunctions of the exterior-complex-scaled Hamiltonian $\boldsymbol{H}_\theta$, and the only complex numbers in Eq. (4.2.17) are the corresponding complex eigenvalues of $\boldsymbol{H}_\theta$.

Eq. (4.2.17) provides an expression for the T-matrix element that does not suffer from the numerical disadvantages of $T(\theta = 0)$: The continuous spectrum of $\hat{H}$ is discretizised and the complex eigenvalues, E_n^θ, avoid the vanishing of the energy denominators in the Green operator (see Eq. (4.1.1)), such that the energy integral in Eq. (4.1.2) for summation in Eq. (4.2.17) converges. Another benefit is the inclusion of the resonance states (poles of the S-matrix) into the spectrum of $\hat{H}$, where one resonance eigenstate represents a large number of scattering eigenstates of the non-scaled Hamiltonian. The price we pay for these benefits is the need to confirm the stability of the calculated complex T-matrix in terms of the size of the basis set and the need to look for the optimal value of the scaling parameter $\eta = \exp(i\theta)$, for which

$$\left|\frac{\partial T_{f,i}^\theta}{\partial \mathrm{Re}(\theta)}\right|_{\theta_{\mathrm{opt}}} = 0 \quad \text{and} \quad \left|\frac{\partial T_{f,i}^\theta}{\partial \mathrm{Im}(\theta)}\right|_{\theta_{\mathrm{opt}}} = 0\,. \tag{4.2.18}$$

The complex coordinate method for time-independent Hamiltonians has been successfully used to calculate the specular and non-specular intensities of gas atom and molecules scattered from corrugated and smooth solid surfaces. See the remarkable agreement between the experimental results obtained for helium diffraction from Cu(115) which is shown in Fig. 18a and the theoretical (no fitting parameters) results presented in Fig. 18b which we obtained by using Eq. (4.2.30) for calculating the cross sections. The method is suitable also for the calculations of state-to-state transition probabilities in chemical reactions resulting from reactive scattering experiments.

4.2.1. The complex coordinate scattering theory and the Kohn variational principle

On the basis of the c-variational principle as proved in Section 2, the eigenfunctions of the complex-scaled Hamiltonian can be expanded in terms of N square integrable basis functions, ϕ_n,

$$|\psi_\alpha^\theta\rangle\!\rangle = \sum_{n=1}^{N} C_{n,\alpha}^\theta \Phi_n, \qquad \langle\!\langle\psi_\alpha^\theta| = \sum_{n=1}^{N} D_{n,\alpha}^\theta \Phi_n \tag{4.2.19}$$

The linear variational parameters C and D are, respectively, the right and left eigenvectors of the complex-scaled Hamiltonian matrix H_θ,

$$\begin{aligned} \boldsymbol{H}_\theta \boldsymbol{C}_\alpha^\theta &= E_\alpha^\theta \boldsymbol{C}_\alpha^\theta\,, \\ \boldsymbol{H}_\theta^{\mathrm{t}} \boldsymbol{D}_\alpha^\theta &= E_\alpha^\theta \boldsymbol{D}_\alpha^\theta\,, \end{aligned} \tag{4.2.20}$$

where

$$[H_\theta^\theta]_{n',n} = \langle \Phi_{n'} | \hat{H}(r' e^{i\theta}) | \Phi_n \rangle\,.$$

Since the Hamiltonian is non-hermitian (due to the complex scaling) the c-product should be used as an inner product rather than the usual scalar product. Consequently,

$$D^{\mathrm{t}} C = 1\,. \tag{4.2.21}$$

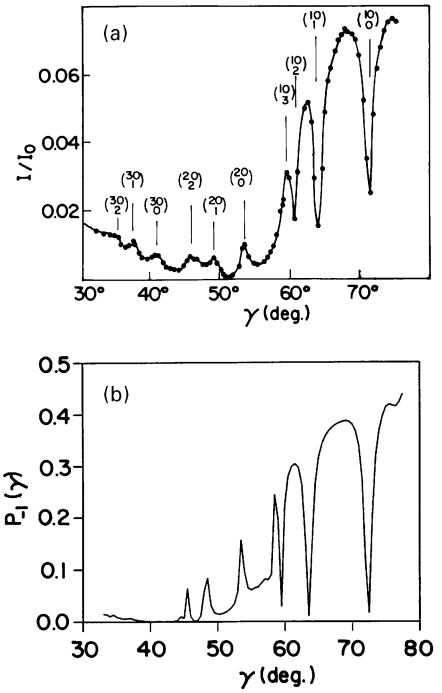

Fig. 18. (a) The experimental non-specular intensity as measured by Perreau and Lapujoulade [140], in scattering of He from Cu(115) corrugated non-symmetrical surface. (b) The theoretical transition probabilities as a function of the incident angle γ as calculated by Peskin and Moiseyev [109] from Eq. (4.2.30) in the text.

The spectral representation of the Green operator in terms of the variational eigenfunctions of the complex-scaled Hamiltonian matrix

$$G_E = \sum_{\alpha} \frac{|\psi_\alpha^\theta\rangle\!\rangle \langle\!\langle \psi_\alpha^\theta|}{(E - E_\alpha^\theta)} \tag{4.2.22}$$

is valid if and only if the eigenfunctions of $\hat{H}_\theta$ form a complete set. As discussed in Section 2, for any given finite number of basis functions, N, one can always find well-defined complex values of θ for which the spectrum is incomplete. In such cases, the number of the non-linear dependent (i.e. "orthogonal") eigenvectors of H_θ is smaller than N. Since under very small variation of θ the spectrum becomes complete this possibility can be ignored (see the relevant discussion on the generalized inner product in Section 2).

By substituting Eqs. (4.2.19), (4.2.20), (4.2.21) and (4.2.22) into Eq. (4.2.4), one can get

$$T = \langle \phi_f | \hat{V} | \phi_i \rangle + \mathrm{e}^{+2i\theta} (\boldsymbol{v}_f)^{\mathrm{t}} (\boldsymbol{C}\boldsymbol{A}^{-1}\boldsymbol{D}^{\mathrm{t}}) \boldsymbol{v}_i \,, \tag{4.2.23}$$

where $\boldsymbol{A}$ is defined as

$$A_{\alpha,\alpha'} = (E - E_\alpha^\theta)\delta_{\alpha,\alpha'} \tag{4.2.24}$$

and

$$[\boldsymbol{v}_f]_n = \langle\!\langle \phi_f^\theta | \hat{V}(r'\mathrm{e}^{\mathrm{i}\theta}) | \Phi_n \rangle\!\rangle ,$$
$$[\boldsymbol{v}_i]_n = \langle\!\langle \Phi_n | \hat{V}(r'\mathrm{e}^{\mathrm{i}\theta}) | \phi_i^\theta \rangle\!\rangle . \tag{4.2.25}$$

Since

$$\boldsymbol{A} = \boldsymbol{D}^{\mathrm{t}}[E\mathbf{1} - \boldsymbol{H}(\theta)]\boldsymbol{C} \tag{4.2.26}$$

then, by using Eqs. (4.2.22), (4.2.23) and (4.2.26), we get

$$T = \langle \phi_f | \hat{V} | \phi_i \rangle + \mathrm{e}^{+2\mathrm{i}\theta} (\boldsymbol{v}_f)^{\mathrm{t}} [E\mathbf{1} - \boldsymbol{H}(\theta)]^{-1} \boldsymbol{v}_i . \tag{4.2.27}$$

Let us denote the matrix elements of

$$[E\mathbf{1} - \boldsymbol{H}(\theta)]^{-1} \tag{4.2.28}$$

by

$$\{[E\mathbf{1} - \boldsymbol{H}(\theta)]^{-1}\}_{n,n'} = [\langle\!\langle \Phi_n | E - \hat{H}(r'\mathrm{e}^{\mathrm{i}\theta}) | \Phi_{n'} \rangle\!\rangle]^{-1} . \tag{4.2.29}$$

Then, by substituting Eq. (4.2.29) into Eq. (4.2.28) we obtain

$$T = \langle \phi_f | \hat{V} | \phi_i \rangle + \mathrm{e}^{2\mathrm{i}\theta} \sum_{n,n'} \langle\!\langle \phi_f^\theta | \hat{V}(r'\mathrm{e}^{\mathrm{i}\theta}) | \Phi_n \rangle\!\rangle [\langle\!\langle \Phi_n | E - \hat{H}(r'\mathrm{e}^{\mathrm{i}\theta}) | \Phi_{n'} \rangle\!\rangle]^{-1} \langle\!\langle \Phi_{n'} | \hat{V}(r'\mathrm{e}^{\mathrm{i}\theta}) | \phi_i^\theta \rangle\!\rangle . \tag{4.2.30}$$

This is exactly the result obtained from the Kohn T-matrix variational principle by Nuttall and Cohen [104]. Here we followed Peskin and Moiseyev's [110] proof that the complex coordinate scattering theory gives the Kohn variational solution for the T matrix when the "reaction" coordinate is analytically continued into the complex plane. Eq. (4.2.30) can be obtained from the following expression:

$$T = \langle \phi_f | \hat{V} | \phi_i \rangle + \mathrm{e}^{2\mathrm{i}\theta} [\langle\!\langle \phi_f^\theta | \hat{V}(r'\mathrm{e}^{\mathrm{i}\theta}) | \chi \rangle\!\rangle + \langle\!\langle \chi' | \hat{V}(r'\mathrm{e}^{\mathrm{i}\theta}) | \phi_i^\theta \rangle\!\rangle - \langle\!\langle \chi' | E - \hat{H}(r'\mathrm{e}^{\mathrm{i}\theta}) | \chi \rangle\!\rangle] , \tag{4.2.31}$$

where χ and χ' are square integrable functions (note that the c-product is used rather than the "usual" inner product, as discussed in Section 2) in the space spanned by the $\{\Phi_n;\ n = 1, \ldots N\}$ basis functions and are written as

$$\chi = \sum_{n=1}^{N} a_n \Phi_n, \qquad \chi' = \sum_{n=1}^{N} b_n \Phi_n . \tag{4.2.32}$$

By substituting χ and χ' in Eq. (4.2.31) and by the requirement of

$$\partial T/\partial a_n = 0, \quad \partial T/\partial b_n = 0; \quad n = 1, \ldots, N , \tag{4.2.33}$$

one can get that

$$a_n = \sum_{j=1}^{N} [\langle\!\langle \Phi_n | E - \hat{H}_\theta | \Phi_j \rangle\!\rangle]^{-1} \langle\!\langle \Phi_j | \hat{V}_\theta | \phi_i^\theta \rangle\!\rangle ,$$
$$b_n = \sum_{j=1}^{N} [\langle\!\langle \Phi_n | E - \hat{H}_\theta | \Phi_j \rangle\!\rangle]^{-1} \langle\!\langle \phi_f^\theta | \hat{V}_\theta | \Phi_j \rangle\!\rangle . \tag{4.2.34}$$

By substituting Eqs. (4.2.32) and (4.2.34) into Eq. (4.2.33) the complex transition probability amplitude given in Eq. (4.2.30) is obtained.

Another variational basis set method which satisfies the Kohn variational principle was developed by Miller and coworkers [121,122].

4.3. Resonance scattering: Partial widths

Partial widths represent the probability per unit time of getting a specific reaction product in a well-defined quantum state in a full scattering or half-collision experiments. The resonance-scattering-theory enables the calculations of partial widths from the "tail" (i.e. asymptote) of a single, time-independent, square integrable resonance wave function. This method has been used, so far, in the calculations of the rotational distribution of a diatom in a specular and non-specular scattering of the diatom from a solid surface; the rotational distribution of a diatom obtained in a photodissociation of a van der Waals complex; and of the probability for ionizing an atom or dissociate a diatom resulting from the absorption of n-photons in the presence of very strong electromagnetic fields.

Within the framework of the resonance-scattering-theory, as developed by Moiseyev and Peskin [105], one assumes that the dynamics of the studied system is controlled by a single intermediate narrow resonance state, and

$$\Gamma_{f\leftarrow i} = |T^{\theta}_{f,\,i}(E)|^2 \,, \tag{4.3.1}$$

where the complex scaled T-matrix element is approximately given by

$$\begin{aligned} T^{\theta}_{f,\,i}(E) &= \langle\!\langle \phi^{\theta}_f | V_\theta + V_\theta G_\theta(E) V_\theta | \phi^{\theta}_i \rangle\!\rangle \\ &\simeq \frac{\langle\!\langle \phi^{\theta}_f | V_\theta | \psi^{\theta}_{\mathrm{Res}} \rangle\!\rangle \langle\!\langle \psi^{\theta}_{\mathrm{res}} | V_\theta | \phi^{\theta}_i \rangle\!\rangle}{E - E_{\mathrm{res}}} \,, \end{aligned} \tag{4.3.2}$$

where

$$\begin{aligned} &H_\theta \psi^{\theta}_{\mathrm{res}} = E_{\mathrm{res}} \psi^{\theta}_{\mathrm{res}} \,, \\ &E_{\mathrm{res}} = E_r - (\mathrm{i}/2)\Gamma \,. \end{aligned} \tag{4.3.3}$$

This approximation holds provided that the contribution of the direct scattering event to the cross section is small relative to the contribution of the multipole-scattering events (i.e. the VG_EV terms), provided that $E \simeq E_r$ and provided that the resonance is narrow and is located in the complex energy plane much closer to the real energy axis than the rotating continuum, that is,

$$2(E_r - E^{\mathrm{thres}}_m)\tan(2\theta) \gg \Gamma \,, \tag{4.3.4}$$

where E^{thres}_m is the mth threshold energy which is defined as the discrete mth bound state energy of the $\hat{H}_0$ Hamiltonian given in Eq. (4.2.6).

The assumption made above that the complex-scaled resonance state is the single intermediate state in the scattering process, implies that here we assume that

$$\phi^{\theta}_i \overset{-\infty \leftarrow t}{\leftarrow} \psi^{\theta}_{\mathrm{res}} \overset{t \to \infty}{\rightarrow} \phi^{\theta}_f \tag{4.3.5}$$

or

$$\begin{aligned} \langle\!\langle \psi^{\theta}_{\mathrm{res}} \rangle\!\rangle &= (1 + G_{\theta}(E)V_{\theta})|\phi^{\theta}_{i}\rangle\!\rangle\,, \\ \langle\!\langle \psi^{\theta}_{\mathrm{res}}| &= \langle\!\langle \phi^{\theta}_{f}|(V_{\theta}G_{\theta}(E) + 1)\,. \end{aligned} \tag{4.3.6}$$

Eqs. (4.3.5) and (4.3.6), however, cannot be satisfied since ϕ_i and ϕ_f are associated with "in" and "out" going plane wave with a real momentum ($\hbar k_i$) and real ($\hbar k_f$). From the asymptotic behavior of the resonance wave function given in Eq. (1.5.2) one can see that Eqs. (4.3.5) and (4.3.6) can be satisfied if, and only if, ($\hbar k_i$) and ($\hbar k_f$) will be complex as required in Eq. (1.4.9). Consequently, the assumption that the dynamics is controlled by a single complex-scaled resonance state lead us to postulate that *in the complex-coordinate resonance scattering theory the complex energy is conserved and we introduce the complex momentum for the final state which is determined by* [105]

$$(\hbar k_f^{(m)})^2/2\mu = E_r - (\mathrm{i}/2)\Gamma - E_m^{\mathrm{thres}}\,. \tag{4.3.7}$$

From the same initial state several different final states can be obtained. That is,

$$|\phi_i\rangle \rightarrow \begin{cases} |\phi_f(k_f^{(m)})\rangle \equiv |\phi_m\rangle\,, \\ |\phi_f(k_f^{(m')})\rangle \equiv |\phi_{m'}\rangle\,, \\ |\phi_f(k_f^{(m'')})\rangle \equiv |\phi_{m''}\rangle\,. \end{cases} \tag{4.3.8}$$

From Eqs. (4.3.8), (4.3.1) and (4.3.2) one gets the branching ratio

$$\frac{\Gamma_m}{\Gamma_{m'}} = \left| \frac{\langle\!\langle \phi^{\theta}_{m}|V(r'\mathrm{e}^{\mathrm{i}\theta})|\psi^{\theta}_{\mathrm{res}}\rangle\!\rangle}{\langle\!\langle \phi^{\theta}_{m'}|V(r'\mathrm{e}^{\mathrm{i}\theta})|\psi^{\theta}_{\mathrm{res}}\rangle\!\rangle} \right|^2 . \tag{4.3.9}$$

Eq. (4.3.9) is the expression proposed by Noro and Taylor [123] for the calculation of branching ratios. We omit here the label "i" from $\Gamma_{f\leftarrow i}$ which is defined in Eq. (4.3.1) ("f" is associated with the final complex momentum ($\hbar k_f^{(m)}$)) since the derivation of Eq. (4.3.9) from Eq. (4.3.2) shows that during the scattering process the initial state has been "forgotten". This is probably true in a half-collision process when the system is initially prepared in a resonance state.

In the radial case $r' \in [0, \infty]$, $\langle\!\langle \phi^{\theta}(m)| = 0$ for $r' = 0$ and yet

$$\langle\!\langle \phi^{\theta}_{m}| \rightarrow \sqrt{\frac{\mu}{\hbar^2 k_f^{(m)}}}\,\mathrm{e}^{-\mathrm{i}k_f^{(m)}r'\mathrm{e}^{\mathrm{i}\theta}} \quad \text{as } r \rightarrow \infty\ . \tag{4.3.10}$$

Therefore, in the radial case

$$\langle\!\langle \phi^{\theta}_{m}| \equiv \phi^{\mathrm{L}}_{m}(r\mathrm{e}^{\mathrm{i}\theta}) = -2i\sqrt{\frac{\mu}{\hbar^2 k_f^{(m)}}}\sin(k_f^{(m)}r'\mathrm{e}^{\mathrm{i}\theta}) \tag{4.3.11}$$

and $k_f^{(m)}$ is defined as in Eq. (4.3.7). Eq. (4.3.9) can be rewritten by carrying out integration by parts as described by Moiseyev and Peskin in Ref. [105] to provide another formula for the branching ratio,

$$\frac{\Gamma_m}{\Gamma_{m'}} = \lim_{r'\rightarrow\infty} \left| \frac{\phi^{\mathrm{L}}_{m}(r'\mathrm{e}^{\mathrm{i}\theta})\dfrac{\mathrm{d}\Phi^{\theta}_{m}(r')}{\mathrm{d}r} - \Phi^{\theta}_{m}(r')\dfrac{\mathrm{d}\phi^{\mathrm{L}}_{m}(r'\mathrm{e}^{\mathrm{i}\theta})}{\mathrm{d}r}}{\phi^{\mathrm{L}}_{m'}(r'\mathrm{e}^{\mathrm{i}\theta})\dfrac{\mathrm{d}\Phi^{\theta}_{m'}(r')}{\mathrm{d}r} - \Phi^{\theta}_{m'}(r')\dfrac{\mathrm{d}\phi^{\mathrm{L}}_{m'}(r'\mathrm{e}^{\mathrm{i}\theta})}{\mathrm{d}r}} \right|^2 \tag{4.3.12}$$

ϕ_m^{L} and $\phi_{m'}^{\mathrm{L}}$ are the divergent complex-scaled incoming plane waves (defined in Eq. (4.3.11)) with a complex momentum defined in Eq. (4.3.7). Φ_m^θ and $\Phi_{m'}^\theta$ are the right square integrable functions obtained from the variational solution of the complex-scaled Schrödinger equation and are associated with resonance complex eigenvalue $E_r - (\mathrm{i}/2)\Gamma$. See Eq. (4.3.3). That is,

$$\psi_{\mathrm{res}}^\theta = \sum_m \chi_m(x)\Phi_m^\theta(r')\,, \tag{4.3.13}$$

where $\{\chi_m\}$ are the bound state eigenfunctions (associated with the eigenvalues E_m^{thres}) of the $\hat{H}_0(x)$ Hamiltonian given in Eq. (4.2.6). The Moiseyev–Peskin expression [105] for the partial widths given in Eq. (4.3.12) appears to be more compact (in dimensionality) than the first one [Noro–Taylor expression [123] given in Eq. (4.3.9)] and thus avoids the need to integrate over the target coordinates. By noticing that as $r' \to \infty$

$$\begin{aligned} &\langle\!\langle \Phi_m^\theta(r)| \to a_m \phi_m^{\mathrm{L}}(r'\mathrm{e}^{\mathrm{i}\theta})\,, \\ &|\Phi_m^\theta(r)\rangle\!\rangle \to a_m \phi_m^{\mathrm{R}}(r'\mathrm{e}^{\mathrm{i}\theta})\,, \end{aligned} \tag{4.3.14}$$

where ϕ_m^{L} is defined in Eq. (4.3.10) and ϕ_m^{R} is defined as

$$\phi_m^{\mathrm{R}}(r\mathrm{e}^{\mathrm{i}\theta}) \to \sqrt{\frac{\mu}{\hbar^2 k_f^{(m)}}}\,\mathrm{e}^{+\mathrm{i}k_f^{(m)}r'\mathrm{e}^{\mathrm{i}\theta}} \quad \text{as } r' \to \infty\,, \tag{4.3.15}$$

such that

$$\phi_m^{\mathrm{L}} \cdot \phi_m^{\mathrm{R}} = \frac{\mu}{\hbar^2 k_f^{(m)}}\,.$$

Eq. (4.3.12) is reduced to Peskin–Moiseyev–Lefebvre formula for the branching ratios [124]:

$$\Gamma_m/\Gamma_{m'} = |a_m/a_{m'}|^2\,, \tag{4.3.16}$$

where $|a_m|^2$ provides the probability to decay into the open channel m. By taking into consideration Eq. (4.3.14) and the fact that Φ_m^θ are energy normalized functions, one can see that $|a_m|^2$ is the probability flux of $\Phi_m^\theta(r')$ as $r' \to \infty$ and provides the number of particles at the quantum state m detected at $r = \infty$ per unit time per unit area. a_m can be easily obtained by carrying out an asymptotic analysis of the resonance wave function,

$$a_m = \lim_{r\to\infty}\left(\frac{\Phi_m^\theta(r')}{\phi_m^{\mathrm{R}}(r'\mathrm{e}^{\mathrm{i}\theta})}\right). \tag{4.3.17}$$

By substituting Eq. (4.3.16), Eq. (4.3.17) into Eq. (4.3.15) the branching ratio as proposed by Peskin et al. [124] is obtained

$$\frac{\Gamma_m}{\Gamma_{(m')}} = \lim_{r\to\infty}\left|\frac{(k_f^{(m')})^{1/2}\Phi_m^\theta(r)}{(k_f^{(m)})^{1/2}\Phi_{m'}^\theta(r)}\mathrm{e}^{\mathrm{i}(k^{m'}{}_f - k^{(m)}{}_f)r\mathrm{e}^{\mathrm{i}\theta}}\right|^2 \tag{4.3.18}$$

In this section three different formulas for the branching ratio are given in Eqs. (4.3.9), (4.3.12) and (4.3.18). As shown here, following Moiseyev and Peskin proof [105], the three formulas are related to one another in a simple manner. Consequently, in the limit of infinite-basis-set variational calculations the three formulas should provide the same results for the partial widths. The

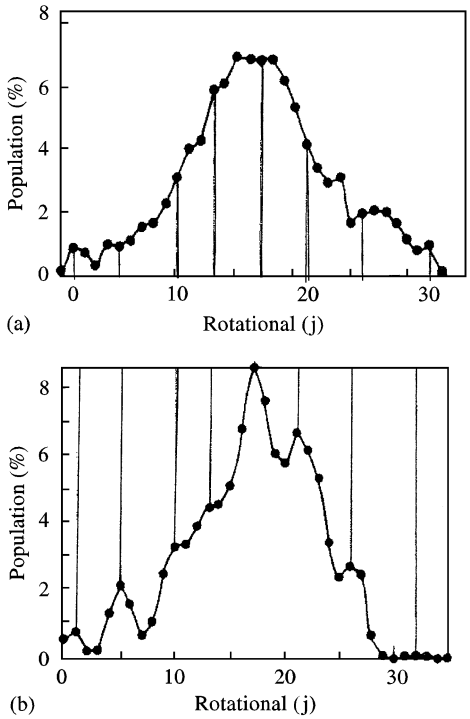

Fig. 19. (a) The experimental rotational distribution of ICL as measured by Lester and co-workers [141], in photodissociation of NeICl. (b) The theoretical rotational distribution of ICL as calculated from the tail of the complex-scaled square integrable NeICl resonance wave function by Lipkin et al. [19,139], in photodissociation of NeICl.

complex-coordinate-resonance-scattering approach has been successfully used in the calculation of partial widths in photodissociation of van der Waals molecules. In such experiments the partial widths provide the rotational distribution of the diatomic molecule obtained by exciting the vibrational mode of the diatom in the atomic van der Waals complex. In Fig. 19 we show a comparison between the experimental and the theoretical (obtained by calculating the partial widths from the asymptotic analysis of a single square integrable complex-scaled resonance wave function) rotational distribution of ICl which is obtained when NeICl complex is vibrationaly excited.

4.4. Time-dependent Hamiltonians by the (t,t') method

Before describing the (t,t') method and the complex coordinate time-independent scattering theory for time-dependent Hamiltonians, we should mention the fact that quasi-energy resonance positions and widths have been calculated by complex-scaling long time before the development of the (t,t') method. Reinhardt and coworkers [125], and Howland [126] studied the ac Stark Hamiltonians in the dipole approximation, $\mu_0 x\cos(\omega t)$. Chu [127] has extended it to molecular time-dependent Hamiltonians in the dipole approximation. Moiseyev and Korsch [128] extended

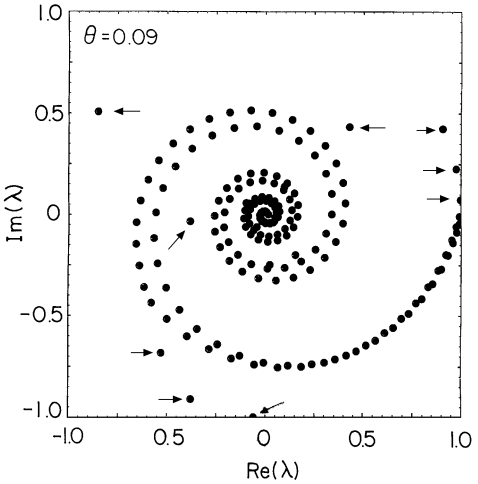

Fig. 20. The complex eigenvalues of the complex scaled time evolution operator of H_2^+ in time periodic field (wavelength of 329.7 nm and laser intensity of 2.5×10^{13} W cm^{-2}) as calculated by Moiseyev et al. [142]. The almost degenerated spirals are the two rotating continua and their 'rate' of convergence to the unit circle is θ-dependent. The 9 isolated circles are associated with the multiphoton quasi-energy resonances and are stable to small variation of the scaling angle θ.

the work of Chu and Reinhardt to any periodic field. Since the real part of the quasi-energies (eigen values of the complex-scaled Floquet operator which will be defined later in Eq. (4.4.1)) are defined modulo of $\hbar\omega$, it is more natural to represent them as the eigenvalues of the complex-scaled time evolution operator, $\lambda = \exp(-iE_{QE}t/\hbar)$. See, for example, Fig. 20 where the complex eigenvalues of the time evolution operator are shown for the case where the bound ground electronic H_2^+ potential energy curve is coupled to the repulsive first excited electronic curve via cw laser.

The time-independent scattering theory has been developed for time periodic Hamiltonians by Peskin and Moiseyev [111]. As they have shown [112], it is possible to extend the time-independent scattering theory to general time-dependent cases where the Hamiltonians are not necessarily time periodic. This scattering theory enables the derivation of time-independent expression for state-to-state transition probabilities.

The time-independent scattering theory for time-dependent Hamiltonians enables one to propagate analytically a given initial state to $t = \infty$. For example, the above-threshold-ionization (ATI), the "breathing" above-threshold-dissociation of Cl_2^-, and the high harmonic generation spectra of Xe model Hamiltonian were accurately obtained by the time-independent scattering theory which will be described below [112,129].

The time-independent scattering theory for time-dependent Hamiltonians is based on the assumption that as time passes a free particle (e.g. an electron or a molecular species) is obtained [112]. This assumption provides two kinds of limitations on the time-dependent Hamiltonians:

(1) The "bare" (i.e. field-free) atomic or molecular potential should be a non-coulombic potential. It can be a finite, short- or long-range potential. This is definitely not a serious restriction in the study of dissociation of molecules where the atom–atom potential interaction decays as R^{-3} when R is the distance between the two atoms. Moreover, due to the correlation effect of the inner shell electrons, the effective potential which describes the interaction of the ionizing electron and the ion

is often taken as a short-range potential. In the study of multiphoton ionization phenomena in hydrogenic like atoms the time-independent scattering theory can be used only within the framework of the cut-off approximation where the potential is finite and $V(x > x_0) = 0$.

(2) The interaction of the atom/molecule with the time-dependent field, $V(x,t)$, should vanish as $x \to \infty$. This condition is satisfied if the acceleration gauge is used rather than the length gauge (see the discussion in Section 1.7).

4.4.1. State-to-state transition probabilities and time evolution operator by the complex scaled (t,t') method

Let us define $\mathscr{H}(x,t')$ as

$$\mathscr{H}(x,t') = -i\hbar\partial/\partial t' + H(x,t'), \tag{4.4.1}$$

where $H(x,t')$ is the given time-dependent Hamiltonian and $-i\hbar\partial/\partial t'$ can be described as the momentum operator of the "photon" particle. Here t' acts as an additional coordinate. Using box normalization condition $t'\varepsilon[0,T]$, the inner product of the functions $f(x,t')$ and $g(x,t')$ in the generalized Hilbert space is defined by

$$\langle\langle f|g\rangle\rangle = \frac{1}{T}\int_0^T dt' \int_{-\infty}^{\infty} dx f^*(x,t')g(x,t'). \tag{4.4.2}$$

For ionizing or dissociative systems complex scaling is used and $f^*(x,t')$ is replaced by $f(x'e^{+i\theta}, -t')$ and $g(x,t')$ by $g(x'e^{+i\theta},t')$ assuming $g(x',0)$ and $f(x',0)$ as real functions. The reason for replacing the complex conjugate by $t' \to -t'$ is due to the fact that we wish to take the complex conjugate of the terms in the function which are complex NOT resulting from the use of complex scaling. Upon complex scaling $x = x'e^{i\theta}$ is substituted in the Hamiltonian when x' is varied along the real axis.

The solutions of the time-dependent Schrödinger equation

$$H(x,t)\Psi(x,t) = i\hbar\frac{\partial\Psi(x,t)}{\partial t} \tag{4.4.3}$$

for the initial state $\psi(x,t_0)$ is given by

$$\Psi(x,t) = \phi(x,t',t)|_{t'=t} = \frac{1}{T}\int_0^T dt'\phi(x,t',t)\delta(t'-t), \tag{4.4.4}$$

where $\phi(x,t',t)$ is obtained by solving the following equation

$$\hat{\mathscr{H}}(x,t')\phi(x,t',t) = i\hbar\frac{\partial\phi(x,t',t)}{\partial t} \tag{4.4.5}$$

or

$$\phi(x,t',t) = e^{-i\hat{\mathscr{H}}(x,t')(t-t_0)/\hbar}\phi(x,t',t_0). \tag{4.4.6}$$

For time periodic Hamiltonians we use the periodic boundary condition

$$\Psi(x,t) = \Psi(x,t,+T),$$
$$t' = t \bmod T.$$

It is an excellent approach when, for example, the time-dependent Hamiltonian describes the interaction of an atom or molecule with a pulse laser whose pulse envelope evolves oscillates over 50–100 optical cycles [129]. This periodic boundary condition can be used, however, even for non-periodic Hamiltonians.

By substituting Eq. (4.4.6) into Eq. (4.4.4) and by noticing that at $t = t_0$, $\phi(x, t', t_0) = \psi(x, t_0)$, the time evolution wave function is given by

$$\psi(x,t) = [\mathrm{e}^{-\mathrm{i}\hat{\mathscr{H}}(x,t')(t-t_0)/\hbar}\psi(x,t_0)]_{t'=t}$$

$$= \frac{1}{T}\int_0^T \mathrm{d}t'\delta(t'-t)[\mathrm{e}^{-\mathrm{i}\mathscr{H}(x,t')(t-t_0)/\hbar\psi(x,t_0)}]\,. \tag{4.4.7}$$

The solution of the time-dependent Schrödinger equation for a general time-dependent Hamiltonian is obtained from Eq. (4.4.7) by calculating the time evolution operator $\exp(-\mathrm{i}\hat{\mathscr{H}}t)$ where $\hat{\mathscr{H}}(x,t')$ is a Floquet-*type* operator and $0 \le t' \le T$ acts like an *additional* coordinate. Since $\hat{\mathscr{H}}$ is t-independent, the need to calculate time-ordering operators (such as first-, second- or high-order terms in the Magnus series expansion) is avoided.

From Eq. (4.4.7), one can see that the time evolution operator is given by

$$\hat{\mathscr{U}}(t|t_0) = \frac{1}{T}\int_0^T \mathrm{d}t'\delta(t'-t)\mathrm{e}^{-\mathrm{i}\hat{\mathscr{H}}(x,t')(t-t_0)/\hbar} \tag{4.4.8}$$

and

$$\hat{\mathscr{U}}(t_0|t) = \frac{1}{T}\int_0^T \mathrm{d}t'\delta(t'-t_0)\,\mathrm{e}^{-\mathrm{i}\hat{\mathscr{H}}(x,t')(t_0-t)/\hbar}\,. \tag{4.4.9}$$

Since

$$\lim_{t\to\infty}\hat{\mathscr{U}}(t|t_0)\Psi(x,t_0) = \lim_{t\to\infty}\hat{\mathscr{U}}_0(t|t_0)\psi_f(x,t_0)\,, \tag{4.4.10}$$

where $\psi(x,t_0)$ is the solution of the time-dependent Schrödinger equation given in Eq. (4.4.3) and the final energy normalized state is given by

$$\psi_f(x,t) = \hat{\mathscr{U}}_0(t|t_0)\chi_f(x,t_0)$$

$$= \mathrm{e}^{-\mathrm{i}\hat{\mathscr{H}}_0(x,t')(t-t_0)/\hbar}\sqrt{\frac{\mu}{\hbar^2 k_f}}\mathrm{e}^{\mathrm{i}k_f x} = \mathrm{e}^{-\mathrm{i}E_f(t-t_0)/\hbar}\sqrt{\frac{\mu}{\hbar^2 k_f}}\mathrm{e}^{\mathrm{i}k_f x}\,, \tag{4.4.11}$$

where $\hat{\mathscr{H}}_0$ is the free particle Hamiltonian which consists of the kinetic operator $(\hat{p}_x)^2/2\mu$ of the free ionized/dissociated particle and the operator $\hat{p}_{t'}$ of the momentum of the "photon".

$$\hat{\mathscr{H}}_0(x,t') = -\hbar^2/2\mu\,\partial^2/\partial x^2 - \mathrm{i}\hbar\,\partial/\partial t'\,, \tag{4.4.12}$$

$$E_f = (\hbar k_f)^2/(2\mu)\,. \tag{4.4.13}$$

By substituting Eq. (4.4.11) into Eq. (4.4.10) the solution of the time-dependent Schrödinger equation which provides as $t \to \infty$ the final state $\psi_f(x,t)$ is obtained:

$$\Psi(x,0) = \lim_{t\to\infty} \hat{\mathscr{U}}(0|t)\hat{\mathscr{U}}_0(t|0)\psi_f(x,0)$$

$$= \lim_{t\to\infty} \frac{1}{T}\int_0^T \mathrm{d}t'\delta(t')\mathrm{e}^{\mathrm{i}\mathscr{H}(x,t')t/\hbar}\mathrm{e}^{-\mathrm{i}\hat{\mathscr{H}}_0(x,t')t/\hbar}\psi_f(x,0) \tag{4.4.14}$$

$$= \frac{1}{T}\int_0^T \mathrm{d}t'\delta(t')\left(1 + \int_0^\infty \mathrm{d}t\frac{\partial}{\partial t}\mathrm{e}^{\mathrm{i}\mathscr{H}(x,t')t/\hbar}\mathrm{e}^{-\mathrm{i}\mathscr{H}_0(x,t')t/\hbar}\right)\psi_f(x,0)\,, \tag{4.4.15}$$

$t_0 = t = 0$ is taken as the time the atomic/molecular system interacts with the time-dependent field. Illustrative schematic representation is given by

$$\left(\begin{array}{l} t = t_0 \\ \psi_i(x,t) \text{ describes} \\ \text{the initial state of} \\ \text{the system before the} \\ \text{interaction with the} \\ \text{time-dependent field} \end{array}\right) \xrightarrow{t_0 \to t} \left(\begin{array}{l} t = 0 \\ \Psi(x,0) \text{ describes} \\ \text{the "particles" (e.g.} \\ \text{electrons/atoms/molecules)} \\ \text{interacting with the} \\ \text{electromagnetic field (laser)} \end{array}\right) \xrightarrow{t\to\infty} \left(\begin{array}{l} t = +\infty \\ \psi_f(x,t) \text{ describes} \\ \text{free "particles"} \end{array}\right).$$

When a sudden interaction of the system with the fields occurs we may assume that $t_0 = 0$. Following a similar derivation made by Taylor for time-independent Hamiltonians, one can get that [112]

$$\Psi(x,0) = \frac{1}{T}\int_0^T \mathrm{d}t'\delta(t')(1 + G_{E_f}(x,t')V(x,t'))\psi_f(x,0)\,, \tag{4.4.16}$$

where

$$V(x,t') = \hat{\mathscr{H}}(x,t') - \hat{\mathscr{H}}_0(x,t')\,, \tag{4.4.17}$$

$$G_{E_f}(x,t') = \frac{1}{E_f - \hat{\mathscr{H}}(x,t')}\,. \tag{4.4.18}$$

The state-to-state $[\psi_i(x,t_0) \to \psi_f(x,t)$ as $t \to \infty]$ transition probability, $P(E_f)$, is given by the overlap integral between the initial time-independent scattering state $\psi_i(x,t_0 = 0)$ and the solution of the full time-dependent problem, $\psi(x,0)$, which provides as $t \to \infty$ the final state $\psi_f(x,t)$:

$$P(E_f) = |\langle\psi_i(0)|\Psi(0)\rangle|^2\,. \tag{4.4.19}$$

4.4.2. Above-threshold-ionization (ATI) or above-threshold-dissociation (ATD) spectra

In multiphoton ionization/dissociation experiments the initial scattering state, $\psi_i(x,0)$, is the bound state of the field-free atomic/molecular Hamiltonian,

$$\psi_i(x,0) = \Psi_b(x)\,. \tag{4.4.20}$$

By substituting Eq. (4.4.11) and Eqs. (4.4.16) and (4.4.17) into Eq. (4.4.19) one gets the time-independent expression for the state-to-state transition probability

$$P(E_f) = |\langle\!\langle \Phi_i(t=0)|1 + G_{E_f}(x,t')V(x,t')|\Phi_f(t=0)\rangle\!\rangle|^2 , \tag{4.4.21}$$

where

$$\langle\!\langle \Phi_i(t=0)| = \Psi_b(x)\delta(t') = \sum_{n=-\infty}^{\infty} e^{iwnt'}\psi_b(x) , \tag{4.4.22}$$

$$|\Phi_f(t=0)\rangle\!\rangle = \sqrt{\frac{\mu}{\hbar^2 k_f}}\, e^{ik_f x} \tag{4.4.23}$$

and

$$w = 2\pi/T . \tag{4.4.24}$$

Eq. (4.4.21) provides the probability to detect a free electron (in ATI experiment) or a free atom/molecules (in ATD experiment) with a kinetic every $(\hbar k_f)^2/2\mu$. As it was observed in experiments and also in theoretical calculations (see Ref. [111] and references therein) the ATI spectra of atoms consists of a sequence of isolated peaks, separated by one photon energy.

4.4.3. Harmonic generation spectra by the complex-scaled (t,t') method

Kulander [131] associated the harmonic generation spectra with the Fourier transform of the time-dependent dipole moment,

$$\sigma_{HG}(\Omega) = \int_0^{\infty} dt e^{-i\Omega t}\langle\psi_b(t)|x|\psi_b(t)\rangle \tag{4.4.25}$$

where $\psi_b(t)$ is the time-dependent solution obtained from Eq. (4.4.7) which stands for the initial bound state of the field-free Hamiltonian, $\psi(x,t_0) = \Psi_b(x)$. By substituting Eq. (4.4.7) into Eq. (4.4.25) when the eigenfunctions of $\mathscr{H}(x,t')$ are used as basis functions, the time-independent formula for the harmonic generation (HG) spectra has been derived:

$$\sigma_{HG}(\Omega) = \left| \sum_{m=0}^{\infty} \sum_{\alpha,\,\alpha'} \delta_{\Omega,[(\varepsilon_{\alpha'}-\varepsilon_{\alpha})/\hbar + mw]} \sum_{n=-\infty}^{\infty} (\Psi_b|\chi_{\alpha'}(t=0))\cdot(\chi_{\alpha}(t=0)|\Psi_b) \right| \times |(\varphi_{\alpha',\,n-m}|x|\varphi_{\alpha,\,n})|^2 , \tag{4.4.26}$$

where w is defined as in Eq. (4.4.24); $\{\chi_\alpha(x,t')\}$ and $\{\varepsilon_\alpha\}$ are, respectively, the eigenfunctions and eigenvalues of the complex-scaled Floquet-type operator $\mathscr{H}(x,t')$; $\{\varphi_{\alpha,\,n}\}$ are the Fourier components of $\chi_\alpha(x,t')$; and $(\ldots|\ldots)$ stands for the c-product. α and α' get discrete values when box normalization is used for x. The high harmonics for which $\Omega = mw$; $m = 1,3,5,\ldots$ (for the conditions at which only odd harmonics are obtained see Ref. [127]) Eq. (4.4.26) is reduced to

$$\sigma_{HG}(\Omega = mw) = \left| \sum_{m=0}^{\infty} \sum_{\alpha} \delta_{\Omega,\,mw} \sum_{n=-\infty}^{\infty} (\psi_b|\chi_\alpha(t=0))^2(\varphi_{\alpha,\,n-m}|x|\varphi_{\alpha,\,n}) \right|^2 . \tag{4.4.27}$$

Here we assume that the ψ_b and χ_α are complex functions only due to the use of complex scaling, $x = x'\exp(i\theta)$, where x' is a real variable. Usually, ψ_b is a real function and therefore $(\psi_b|\chi_\alpha(t=0)) = \langle\psi_b|\chi_\alpha\rangle$.

4.4.4. The resonance approach

As in the resonance scattering theory described in Section 3 we assume here that the dynamics of the field-atom/molecule system is controlled by a single intermediate narrow resonance state. The use of complex scaling enables one to associate the metastable state of the time-periodic Hamiltonian (which describes the semiclassical interaction between radiation and matter) with a single square-integrable eigenfunction,

$$\Psi_{res}(x,t) = e^{-iE_{res}t}\chi_{res}(x,t), \quad x = x'e^{i\theta} \tag{4.4.28}$$

where χ_{res} and E_{res} are correspondingly the eigenfunction and the θ-independent complex eigenvalue of the complex scaled Floquet operator $\hat{\mathscr{H}}(x,t)$. Note by passing that usually we used different notation for the complex-scaled eigenfunction. That is, $\psi^\theta_{res}(x',t)$ instead of $\psi_{res}(x,t)$ or $\chi^\theta_{res}(x',t)$ instead of $\chi_{res}(x,t)$. Since $\chi_{res}(x,t)$ is time periodic χ_{res} can be written as

$$\chi_{res}(x,t) = \sum_{n=-\infty}^{\infty} e^{iwnt}\varphi^{res}_n(x) \tag{4.4.29}$$

when for the open channels, $n < 0$, (here we assume that the resonance is located at the $n = 0$ Brillouin zone and $-\hbar w < \mathrm{Re}(E_{res}) < 0$ while the threshold of the field-free potential is taken as zero reference energy).

$$\varphi^{res}_n(x) \to a_n\sqrt{\frac{\mu}{\hbar^2 k_n}}e^{ik_n x} \quad \text{as } x \to \infty \tag{4.4.30}$$

and

$$\frac{(\hbar k_n)^2}{2\mu} = E_{res} + \hbar wn \tag{4.4.31}$$

4.4.4.1. Harmonic generation spectra within the framework of the resonance approximation. Within the framework of the resonance approximation Eq. (4.4.27) can be simplified by assuming that the dynamics is controlled by a single intermediate narrow resonance state. When α_0 is associated with the longest-lived resonance state, then Eq. (4.4.27) is reduced to Ben-Tal et al. [130] expression for HG, spectra

$$\sigma^{res}_{HG}(\Omega = m\omega) = \left|\sum_{n=-\infty}^{\infty}(\varphi_{\alpha_{0,\,n-m}}|x|\varphi_{\alpha_{0,\,n}})\right|^2, \tag{4.4.32}$$

where $(\ldots|\ldots)$ stands for the c-product. If real basis set are used then

$$(\varphi_{\alpha_{0,\,n-m}}|x|\varphi_{\alpha_{0,\,n}}) = \langle\varphi^*_{\alpha_{0,\,n}}|x|\varphi_{\alpha_{0,\,n}}\rangle, \tag{4.4.33}$$

where $\langle\ldots|\ldots\rangle$ stands as usual for the scalar product. Note that Eq. (4.4.27) is reduced to Eq. (4.4.32) when $\rangle\psi_b|\chi_{\alpha_0}(t=0)\rangle \simeq 1$.

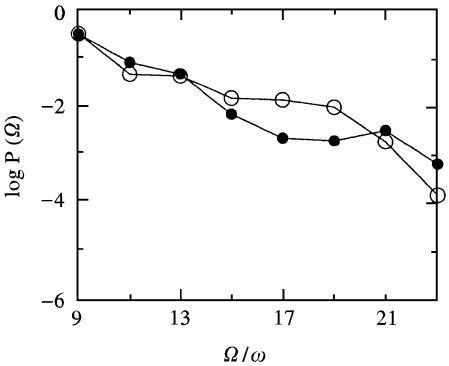

Fig. 21. The experimental harmonic generation spectra of helium in 5 eV KrF laser (full circles) as measured by Sarukura and co-workers [143], and the theoretical ab initio spectra as calculated by Moiseyev and Weinhold (Ref. [135]) from a single complex-scaled resonance Floquet state.

By analyzing the symmetry properties of $\sigma_{HG}^{res}(\Omega)$ Ben-Tal et al. [133] provided a non perturbative proof for field-free Hamiltonians which support discrete and continuum spectra, which shows that under specific well-defined symmetric conditions only odd harmonics are obtained. Moiseyev et al. [134] have shown that for mononuclear diatomic molecule only odd harmonics are obtained regardless of the symmetry properties of the electronic potential surfaces.

The fact that a *single* complex-scaled Floquet state describes the atom/molecule even in high intensity fields has been used by Moiseyev and Weinhold [135] in their calculations of the high harmonic generation spectra of He in KrF laser. The remarkable agreement of the theoretical HG spectra with the experimental results even for the very high harmonics first has been shown that high harmonics can be obtained by neutral atoms. See the experimental vs. the theoretical harmonic generation spectra of helium in Fig. 21. This is due to the dynamical electronic correlation which "push" apart the two electrons to the opposite sides of the nucleus, thus "decreasing" the nuclear charge and thereby avoid ionization.

4.4.4.2. The ATI/ATD spectra within the framework of the resonance approximation. As Moiseyev et al. [134,132] pointed out $|a_n|^2$ which are given in Eq. (4.4.30) are the partial widths, Γ_n, which provide the probability for ionization/dissociation resulting from absorbing n number of photons and, therefore,

$$\Gamma_n = \frac{\hbar^2|k_n|}{\mu}\lim_{x\to\infty}|\varphi_n^{res}(x'e^{i\theta})e^{-ik_n x' e^{i\theta}}|^2 . \tag{4.4.34}$$

Within the framework of the resonance scattering theory two assumptions can be made to simplify the expressions of the state-to-state transition probability (e.g. the expressions of the above-threshold-ionization (ATI), the above-threshold-dissociation (ATD) and the high harmonic generation spectra):

1. The Green operator in the spectral representation is given by

$$\hat{G}_{E_f} \simeq \frac{|\Psi_{\rm res}(t)\rangle\!\rangle\langle\!\langle \Psi_{\rm res}(t)|}{E_f - E_{\rm res}} = \frac{|\chi_{\rm res}(t)\rangle\!\rangle\langle\!\langle \chi_{\rm res}(t)|}{E_f - E_{\rm res}} . \tag{4.4.35}$$

2. The projection of the resonance state on the bound initial state is almost time-independent,

$$\langle\!\langle \Psi_{\rm b}|\chi_{\rm res}(t)\rangle\!\rangle = \langle\!\langle \Psi_{\rm b}|\varphi_0^{\rm res}\rangle\!\rangle \simeq 1 . \tag{4.4.36}$$

By substituting Eqs. (4.4.34), (4.4.35) and (4.4.36) into Eq. (4.4.21) Bensch, Korsch and Moiseyev received a simple expression for the isolation peaks in the ATI/ATD spectra [137]:

$$P(E_f) \simeq \sum_{n<0} \frac{\Gamma_n}{|E_f - (E_{\rm res} + \hbar w n)|^2} \tag{4.4.37}$$

which explains the experimental evidence that the isolated peaks in the ATI/ATD spectra (e.g. of Xe as shown in Ref. [136] are separated by $\hbar w$; all of them have the same width (i.e. $\Gamma = 2{\rm Im}(E_{\rm res})$); and their relative heights are the branching ratio $\Gamma_n/\Gamma_{n'}$, as obtained from Eq. (4.4.34) by carrying out calculations which combine Floquet theory and complex scaling. As an example we represent in Fig. 22 the ATI spectra for a driven Rosen–Morse model Hamiltonian as obtained by

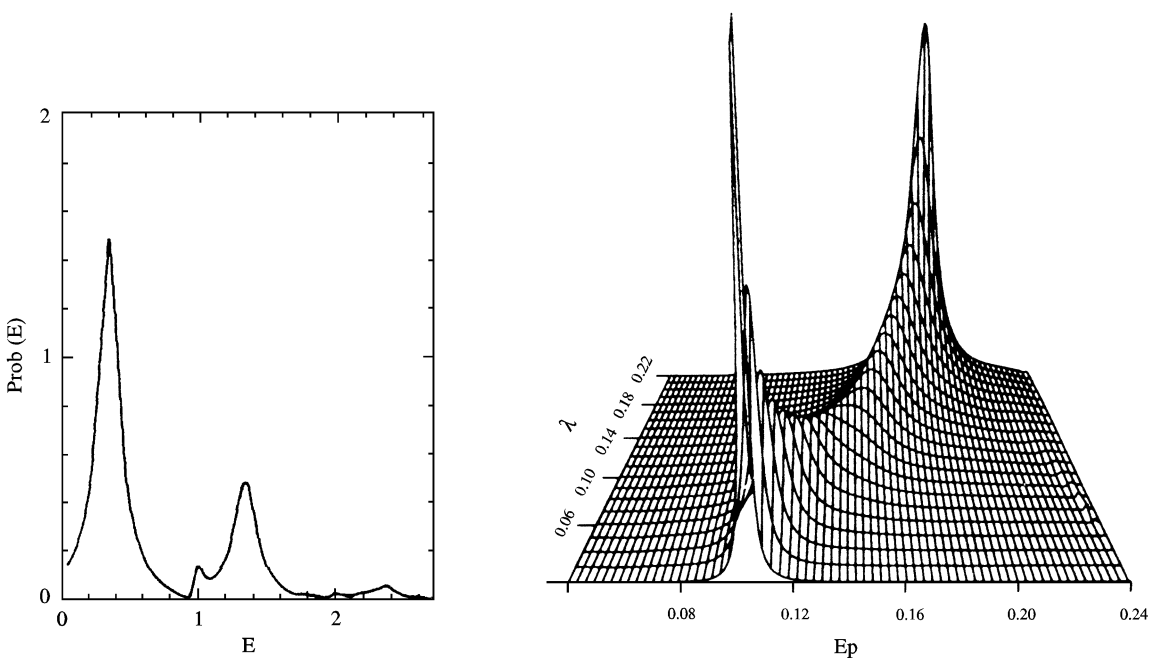

Fig. 22. The ATI spectra for a driven Rosen–Morse model Hamiltonian as obtained by Bench et al. [137] by using the complex scaling approach for calculating the quasi-energy resonance position, width and partial widths.

Fig. 23. The "breathing ATI spectra" of Cl^- in ArF excimer-laser as calculated by Peskin and Moiseyev [112] using the complex coordinate time-independent scattering theory for time-dependent Hamiltonians.

Bench et al. [137] by using the complex scaling approach for calculating the quasi-energy resonance position, width and partial widths.

In Fig. 23 The "breathing ATI spectra" of Cl^- in ArF excimer-laser field as calculated by Peskin and Moiseyev [112] using the complex coordinate time-independent scattering theory for time-dependent Hamiltonians they developed. The "breathing ATI spectra" describes a phenomenon where the atoms are stabilized (i.e. the quasi-energy resonance lifetime is increased) at high intensity fields.

Acknowledgements

My work on complex scaling started when I was still a graduate student and extended the virial theorem to resonance poles of the scattering matrix (complicated proof which is different from the simple proof given later with Weinhold and Certain from Wisconsin). Thanks to Prof. Gabi Kventzel with whom we shared an office at that time; he went through my derivation and encouraged me by citing Landau – the result looks simple enough to be true.

Special thanks are due to Prof. Frank Weinhold and Prof. Phillip Certain with whom we get together into the subject of complex scaling.

In particular, it is a pleasure to thank Phil Certain for twenty fruitful and most enjoyable years of closed collaboration. His wisdom, patience and friendship were always a source of support and encouragement.

It is also a great pleasure to thank the graduate students who participate in the development of the method and its application to many different subjects. Thanks to Dr. Nurit-Nuphar Lipkin, Dr. Nir Ben-Tal, Dr. Uri Peskin, Dr. Naomi Rom, Mr. Ofir Alon, Mr. Vitali Averbukh, Mr. Ilya Vorobechick and Mr. Edi Narievichus for the fun we had doing science together.

My colleagues and friends Prof. Roland Lefebvre and Dr. Victor Ryaboy should be acknowledged for many years of collaboration with applications of the complex-scaling method to many different problems in Physics and Chemistry.

The US–Israel Binational Science Foundation, The Israeli Academy of Sciences and the Foundation of Promotion Research at the Technion should be acknowledged for many years of support.

Last but not the least, I wish to thank Mrs. Charlotte Diament who not only shaped and typed this report and most of my papers, proposals and correspondence during the last decade but also took care of most of the administration work of the scientific meetings we organized.

References

[1] J.R. Taylor, Scattering Theory, Wiley, New York, 1972.
[2] G.A. Gamow, Zs. f. Phys. 51, 204; 52 (1928) 510; R.W. Gurney, E.U. Condon, Phys. Rev. 33 (1929) 127.
[3] See for example A. Schutte, D. Bassi, F. Tommasini, G. Scoles, W.C. Stawlley, A. Niehaus, D.R. Herschbach, J. Chem. Phys. 62 (1975) 600; J. Chem. Phys. 63 (1975) 3081.
[4] I. Eliezer, H.S. Taylor, J.K. Williams, J. Chem. Phys. 47 (1967) 2165. For a study by complex scaling see: N. Moiseyev, C.T. Corcoran, Phys. Rev. A 20 (1979) 814.

[5] O. Alon, M.Sc. Thesis, Technion – Israel Institute of Technology.
[6] For experimental and theoretical study of scattering of MD molecule from Ag(111) and Pt(111) surfaces see: J.P. Cowin, C.F. Yu, S.J. Siebener, J.E. Hurst, J. Chem. Phys. 75 (1981) 1033; C.F. Yu, C.S. Hogg, J.P. Cowin, K.B. Whaley, J.C. Light, S.J. Sibener, Isr. J. Chem. 22 (1982) 305; C.F. Yu, K.B. Whaley, C.S. Hogg, S.J. Sibener, P.R.L. 51 (1983) 2210; K.B. Whaley, J.C. Light, J. Chem. Phys. 81 (1984) 2144. C.F. Yu, K.B. Whaley, C.S. Hogg, S.J. Sibener, J. Chem. Phys. 83 (1985) 4217; K.B. Whaley, C.F. Yu, C.S. Hogg, J.C. Light, S.J. Sibener, ibid. 83 (1985) 4235; R. Schinke, Surf. Sci. 127 (1983) 283. For a study by Complex Scaling see: N. Moiseyev, T. Maniv, R. Elber, R.B. Gerber, Mol. Phys. 55 (1985) 1369; U. Peskin, N. Moiseyev, J. Chem. Phys. 96 (1992) 2347.
[7] U. Peskin, D.Sc. Thesis, Technion – Israel Institute of Technology (1993).
[8] O. Alon, N. Moiseyev, Phys. Rev. A. 46 (1992) 3807.
[9] H.J. Korsch, R. Möhlenkamp, H.-D. Meyer, J. Phys. B 17 (1984) 2955 and references therein.
[10] A.I. Baz', Ya.B. Zel'dovich, A.M. Perelomov, Scattering, Reactions and Decay in Nonrelativistic Quantum Mechanics; Israel Program for Scientific translation, Jerusalem, 1969.
[11] V.I. Kukulin, V.M. KrasrOpol'sky, J. Horácek, Theory of Resonances: Principles and Applications, Kluwer Academic Publishers, Prague, 1989.
[12] L.D. Landau, E.M. Lifshitz, Quantum Mechanics, Pergamon, New York, 1965.
[13] N. Moiseyev, J.O. Hirschfelder, J. Chem. Phys. 88 (1988) 1063.
[14] E. Balslev, J.M. Combes, Commun. Math. Phys. 22 (1971) 280.
[15] B. Simon, Commun. Math. Phys. 27 (1992) 1; Ann. Math. 97 (1973) 247.
[16] For the proof that upon complex scaling $|\langle\varphi_f|V|\phi_n^{\mathrm{res}}\rangle|^2 \propto \Gamma_n/2$ see N. Moiseyev, U. Peskin, Phys. Rev. A 42 (1990) 225.
[17] D.H. Levy, Adv. Chem. Phys. 47 (1981) 363; J.A. Beswick, J. Jortner, Adv. Chem. Phys. 47 (1981) 363; K.C. Janda, Adv. Chem. Phys. 60 (1985) 201.
[18] J.M. Skene, J.C. Drobits, M.I. Lester, J. Chem. Phys. 85 (1986) 2329.
[19] O. Roncero, J.A. Beswick, N. Halberstadt, P. Villarreal, G. Delgado-Barrico, J. Chem. Phys. 92 (1990) 3348; for a study by complex scaling see: N. Lipkin, N. Moiseyev, C. Leforestier, J. Chem. Phys. 98 (1993) 1888.
[20] A. Tempkin, Autoionization, Mono Book Corp., 1966.
[21] P. Auger, Compt. Rend. 180 (1925) 1935; J. Phys. Rad. 6 (1925) 205.
[22] N. Moiseyev, Isr. J. Chem. 31 (1991) 311.
[23] W.P. Reinhardt, Annu. Rev. Phys. Chem. 33 (1982) 223.
[24] B.R. Junker, Adv. At. Mol. Phys. 18 (1982) 107.
[25] Y.K. Ho, Phys. Rep. C 99 (1983) 1.
[26] Ref. [23]; S.-I. Chu, Adv. At. Mol. Phys. 21 (1985) 197; S.-I. Chu, Adv. Chem. Phys. 73 (1989) 739.
[27] W.C. Henneberger, Phys. Rev. Lett. 21 (1958) 838; H.A. Kramers, Collected Scientific Papers, North-Holland, Amsterdam, 1956, p. 272.
[28] U. Peskin, N. Moiseyev, J. Chem. Phys. 99 (1993) 4590.
[29] See J.N.L. Connor, J. Chem. Phys. 78 (1983) 6161 and references therein.
[30] B. Gyarmati, R.T. Vertse, Nucl. Phys. A 160 (1971) 523.
[31] C.A. Nicolaides, D.R. Beck, Phys. Lett. A 65 (1978) 11.
[32] B. Simon, Phys. Lett. A 71 (1979) 211.
[33] N. Rom, N. Moiseyev, J. Chem. Phys. 99 (1993) 7703.
[34] N. Rom, E. Engdahl, N. Moiseyev, J. Chem. Phys. 93 (1990) 3413.
[35] N. Moiseyev, J. Phys. B (1997).
[36] R.R. Johnson, Multiple Scattering Corrections to the Nuclear Optical Potentials, 1961.
[37] See for example, G. Jolicard, E.J. Austin, Chem. Phys. Lett. 121 (1985) 106; D. Neuhauser, M. Baer, J. Chem. Phys. 90 (1989) 4351; ibid. 91 (1989) 4651; G. Jolicard, G. Billing, J. Chem. Phys. 97 (1992) 997; J. Perie, G. Jolicard, J.P. Killingbeck, J. Chem. Phys. 98 (1993) 6344.
[38] U.V. Riss, H.-D. Meyer, J. Phys. B. 26 (1993) 4503.
[39] See for example: C. Leforestier, R.E. Wyatt, J. Chem. Phys. 78 (1983) 2334; D. Neuhauser, R.S. Judson, D.J. Kouri, D.A. Kliner, N. Schefer, O. Adelman, R.N. Zare, Science 257 (1992) 522.
[40] U. Manthe, T. Seideman, W.H. Miller, J. Chem. Phys. 99 (1993) 10 078; D. Neuhauser, ibid. 100 (1994) 9272; D.H. Zhang, J.Z.H. Zhang, ibid. 101 (1994) 1146.

[41] R. Mittra, H.M. Ramahi, A. Khebir, A. Kouki, IEEE Transact. Magnetics, 25 (1989) 3034; J.A. Kong, M.A. Morgan (Eds.), in Differential Methods in Electromagnetic Scattering, Elsevier, New York, 1989, ch. 4, pp. 133–173.
[42] D. Neuhauser, J. Chem. Phys. 103 (1995) 8513.
[43] N. Rom, N. Lipkin, N. Moiseyev, Chem. Phys. Lett. 151 (1991) 199.
[44] U.V. Riss, H.-D. Meyer, J. Phys. B 28 (1995) 1475.
[45] A. Jaeckle, H.-D. Meyer, J. Chem. Phys. 105 (1996) 6778.
[46] N. Lipkin, E. Brandas, N. Moiseyev, Phys. Rev. A 40 (1989) 549.
[47] O. Atabek, R. Lefebvre, M. Garcia Sucre, J. Gomez-Llorente, H. Taylor, Int. J. Quantum Chem. 15 (1991) 211.
[48] L.D. Landau, E.M. Lifshitz, Quantum Mechanics, Pergamon, Oxford 1965. Problem 3 in Section 36.
[49] G. Doolen, Int. J. Quantum Chem. 14 (1978) 523.
[50] W.H. Miller, Fraday Discuss. Chem. Soc. 62 (1977) 40.
[51] T. Seideman, W.H. Miller, J. Chem. Phys. 95 (1991) 1768.
[52] V. Ryaboy, N. Moiseyev, J. Chem. Phys. 98 (1993) 9618.
[53] Ref. [126], Problem 4 in Section 23.
[54] N. Rosen, P.N. Morse, Phys. Rev. 42 (1932) 210.
[55] P.M. Morse, H. Feshbach, Methods of Theoretical Physics, McGraw-Hill, New York, 1983.
[56] G.A. Natanzon, Vestn. Lening. Univ. 10 (1971) 22; Teor. Mat. Fiz. 38 (1979) 146.
[57] D.T. Colbert, R. Mayrhofer, P.R. Certain, Phys. Rev. A 33 (1986) 3560.
[58] J.N. Ginocchio, Ann. Phys. 152 (1984) 203.
[59] N. Lipkin, N. Moiseyev, Phys. Rev. A 36 (1987) 4076.
[60] Y. Alhassid, F. Iachello, R.D. Levine, Phys. Rev. Lett. 54 (1985) 1746.
[61] N. Moiseyev, J. Katriel, Chem. Phys. Lett. 105 (1984) 194.
[62] O. Atabek, R. Lefebvre, Nuovo Cimento 76B (1983) 176; Chem. Phys. Lett. 84 (1981) 233.
[63] N. Moiseyev, P.R. Certain, F. Weinhold 36 (1978) 1613.
[64] E. Brändas, N. Elander (Eds), The Letropet Symposium View on a Generalized Inner Product, Lecture Notes in Physics, vol. 325, Springer, Berlin, 1989.
[65] N. Ben-Tal, N. Moiseyev, R. Kosloff, C. Cerjan, J. Phys. B 26 (1993) 1445.
[66] See for example: N. Moiseyev, J.H. Korsch, Isr. J. Chem. 30 (1990) 107.
[67] K.C. Kulander, Phys. Rev. A 35 (1987) 445.
[68] U. Peskin, N. Moiseyev, J. Chem. Phys. (1993).
[69] J.S. Howland, Math. Ann. 207 (1974) 315; Indiana Univ. Math. J. 28 (1971) 471.
[70] H.L. Cycon, R.G. Forese, W. Kirsch, B. Simon, Schrödinger Operators, Springer, Berlin, 1987, p. 144.
[71] S.T. Motzkin, O. Taussky, Trans. Ann. Math. Soc. 73 (1952) 108.
[72] N. Moiseyev, S. Friedland, J. Chem. Phys. 22 (1980) 618.
[73] N. Moiseyev, P.R. Certain, Mol. Phys. 37 (1979) 1621.
[74] N. Moiseyev, Mol. Phys. 47 (1982) 585.
[75] E. Brändas, P. Froelich, Phys. Rev. A 16 (1977) 2207.
[76] P. Winkler, R. Yaris, J. Phys. B 11 (1978) 1475.
[77] N. Moiseyev, Phys. Rev. A 24 (1981) 2824.
[78] H. Hellmann, Einführung in die Quantumchemie (F. Deutsche), 1937; R.P. Feynman, Phys. Rev. 56 (1939) 340.
[79] N. Moiseyev, C.T. Corcoran, Phys. Rev. A 20 (1979) 814.
[80] G.D. Doulen, J. Nuttal, R.W. Stagat, Phys. Rev. A 10 (1974) 1612.
[81] See for example Int. J. Quantum Chem. 14 (1978).
[82] N. Moiseyev, S. Friedland, P.R. Certain, 74 (1981) 4739.
[83] C.W. McCurdy (private communication). See also footnote 7 in Ref. [80].
[84] N. Moiseyev, P.R. Certain, F. Weinhold, Int. J. Quantum Chem. 14 (1978) 727.
[85] U. Peskin, N. Moiseyev, J. Chem. Phys. 97 (1992) 6443.
[86] N. Moiseyev, Chem. Phys. Lett. 99 (1983) 364.
[87] N. Moiseyev, P. Froelich, E. Watkins, J. Chem. Phys. 80 (1985) 3623.
[88] P. Froelich, N. Moiseyev, J. Chem. Phys. 81 (1988) 1352.
[89] E. Engdahl, N. Moiseyev, J. Chem. Phys. 84 (1986) 1379.

[90] E.R. Davidson, E. Engdahl, N. Moiseyev, Phys. Rev. A 33 (1986) 2436.
[91] P. Froelich, E.R. Davidson, E. Brändas, Phys. Rev. A 28 (1983) 2641.
[92] N. Moiseyev, F. Weinhold, Int. J. Quantum Chem. 17 (1980) 1201.
[93] C. Lanczos, J. Res. Natl. Bur. Std. 45 (1950) 255. On the complex resonance eigenvalues by the Lanczos recursion method see K.F. Milfeld, N. Moiseyev, Chem. Phys. Lett. 130 (1986) 145.
[94] V. Ryaboy, N. Moiseyev, J. Chem. Phys. 103 (1995) 4061.
[95] N. Moiseyev, C.T. Corcoran, Phys. Rev. A 20 (1979) 814.
[96] N. Lipkin, N. Moiseyev, J. Katriel, Chem. Phys. Lett. 147 (1988) 603.
[97] D.S. Tannhauser, N. Moiseyev, Meteorol. Zeitschrift 4 (1995) 257.
[98] N. Lipkin, N. Moiseyev, C. Leforestier, J. Chem. Phys. 98 (1993) 1888.
[99] V. Mandelshtam, N. Moiseyev, J. Chem. Phys. 104 (1996) 6192.
[100] D.T. Colbert, W.H. Miller, J. Chem. Phys. 96 (1992) 1982.
[101] G.C. Groenenboom, D.T. Colbert, J. Chem. Phys. 99 (1993) 9681.
[102] C. Schwartz, J. Math. Phys. 26 (1985) 411.
[103] E. Narevicius, N. Moiseyev, Chem. Phys. Lett. 287 (1998) 250; Mol. Phys. (1998), in press.
[104] J. Nuttal, H.L. Cohen, Phys. Rev. 188 (1969) 1542.
[105] N. Moiseyev, U. Peskin, Phys. Rev. A 42 (1990) 255.
[106] E. Engdahl, N. Moiseyev, T. Maniv, J. Chem. Phys. 94 (1991) 1636.
[107] E. Engdahl, T. Maniv, N. Moiseyev, J. Chem. Phys. 94 (1991) 6330.
[108] U. Peskin, N. Moiseyev, J. Chem. Phys. 96 (1992) 2347.
[109] U. Peskin, N. Moiseyev, J. Chem. Phys. 97 (1992) 2804.
[110] U. Peskin, N. Moiseyev, J. Chem. Phys. 97 (1992) 6443.
[111] U. Peskin, N. Moiseyev, Phys. Rev. A 49 (1994) 3712.
[112] U. Peskin, N. Moiseyev, J. Chem. Phys. 99 (1993) 4590; see also Comments At. Mol. Phys. 31 (1995) 87.
[113] T.N. Rescigno, W.P. Reinhardt, Phys. Rev. A 8 (1973) 2828; 10 (1974) 158.
[114] R.T. Baumel, M.C. Crocker, J. Nuttall, Phys. Rev. A 12 (1975) 486.
[115] B.R. Johnson, W.P. Reinhardt, Phys. Rev. A 29 (1984) 2933.
[116] T.N. Rescigno, C.W. McCurdy, Phys. Rev. A 31 (1985) 624.
[117] B.R. Johnson, W.P. Reinhardt, Phys. Rev. A 28 (1983) 1930.
[118] T.N. Rescigno, C.W. McCurdy, Phys. Rev. A 37 (1985) 624.
[119] P. Froelich, A. Flores-Riveros, W. Wegric, J. Chem. Phys. 82 (1985) 2305.
[120] C.W. McCurdy, T.N. Rescigno, B.I. Schneider, Phys. Rev. A 36 (1987) 2061.
[121] W.H. Miller, J. Op de Haar, J. Chem. Phys. 86 (1988) 6233.
[122] J.Z.H. Zhang, S.-I. Chu, W.H. Miller, J. Chem. Phys. 88 (1988) 6233.
[123] T. Noro, H.S. Taylor, J. Phys. B 13 (1990) L377.
[124] U. Peskin, N. Moiseyev, R. Lefebvre, J. Chem. Phys. 92 (1990) 2902.
[125] W.P. Reinhardt, Int. J. Quantum Chem. S 10 (1976) 359; S.-I. Chu, W.P. Reinhardt, Phys. Rev. Lett. 39 (1977) 1195; C. Cerjan, W.P. Reinhardt, J. Avron, J. Phys. B 11 (1978) 2201; C. Cerjan, R. Hedges, C. Holt, W.P. Reinhardt, K. Scheibner, J. Wendoloski, Int. J. Quantum Chem. 14 (1978) 393; C.R. Holt, M.G. Raymer, W.P. Reinhardt, ibid. 27 (1983) 2971.
[126] J.S. Howland, J. Math. Phys. 24 (1985) 1240.
[127] S.-I. Chu, J. Chem. Phys. 75 (1981) 2215; T.-S. Ho, S.-I. Chu, O. Laughlin, ibid. 81 (1984) 788; S.-I. Chu, J. Cooper, Phys. Rev. A 32 (1985) 2769.
[128] N. Moiseyev, H.J. Korsch, Phys. Rev. A 41 (1990) 498.
[129] N. Moiseyev, M. Chrysos, O. Atabek, R. Lefebvre, J. Phys. B 28 (1995) 2007; N. Moiseyev, M. Chrysos, R. Lefebvre, J. Phys. B 28 (1995) 2599.
[130] N. Ben-Tal, N. Moiseyev, R. Kosloff, C. Cerjan, J. Phys. B 26 (1993) 1445.
[131] K.C. Kulander, Phys. Rev. A 35 (1987) 445.
[132] F. Bensch, H.J. Korsch, N. Moiseyev, J. Phys. B 24 (1991) 1321.
[133] N. Ben-Tal, N. Moiseyev, A. Beswick, J. Phys. B 26 (1993) 3017.
[134] N. Moiseyev, F. Bensch, H.J. Korsch, Phys. Rev. A 42 (1990) 4045.
[135] N. Moiseyev, F. Weinhold, Phys. Rev. Lett. 78 (1997) 2100.

[136] P. Agostini, F. Fabre, G. Mainfray, G. Petite, N.K. Raham, Phys. Rev. Lett. 42 (1979) 1127; R.R. Freeman, P.H. Bucksbaum, H. Milchberg, S. Darak, P. Schumacher, M.E. Gensic, Phys. Rev. Lett. 59 (1987) 1092.
[137] F. Bensch, H.J. Korsch, N. Moiseyev, Phys. Rev. A 43 (1991) 5145.
[138] E. Engdahl, T. Maniv, N. Moiseyev, J. Chem. Phys. 88 (1988) 5864.
[139] N. Lipkin, N. Moiseyev, C. Leforestier, J. Chem. Phys. 98 (1993) 1888.
[140] J. Perreau, J. Lapujoulade, Surf. Sci. 122 (1982) 341.
[141] J.M. Skene, J.C. Drobits, M.I. Lester, J. Chem. Phys. 85 (1986) 2329.
[142] N. Moiseyev, M. Chrysos, R. Lefebvre, J. Phys. B 28 (1995) 2599.
[143] N. Sarukura et al., Phys. Rev. A (1991) 1669.
[144] N. Moiseyev, J. Phys. B 32 (1998), in press.